JACOBS
UNIVERSITY

Dynamic modeling and simulation of biogas production based on anaerobic digestion of gelatine, sucrose and rapeseed oil

by

Anna Schneider

A Thesis submitted in partial fulfillment
of the requirements for the degree of

Doctor of Philosophy
in Biochemical Engineering

Approved Dissertation Committee

Supervisor:
Prof. Dr. h. c. Roland Benz

Supervisor:
Prof. Dr.-Ing. Volker C. Hass

Reviewer:
Dr. Florian Kuhnen

Reviewer:
Prof. Dr. Mathias Winterhalter

Date of Defense: 13.11.2015

To my Family

Acknowledgements

I am grateful to Jacobs University, department of Life Sciences and Chemistry, and University of Applied Sciences in Bremen for offering me a great opportunity to pursue the PhD program. I gratefully acknowledge the funding sources that made my PhD study possible. I was funded by Jacobs University Bremen and German Federal Ministry for Education and Research (BMBF) for the financial support through the FHProfUnt /Project Az/FkZ 17021*10 (Anaerobdetektiv).

I would like to express my sincere thanks to Prof. Dr. Roland Benz, my supervisor at Jacobs University, for giving me an opportunity to study under his supervision and for patiently guiding me through this study. I express my appreciation to my supervisor at University of Applied Sciences, Prof. Dr. - Ing. Volker C. Hass, who brought me into the subject, for his supervision and valuable comments. I am grateful to Prof. Dr. Winterhalter, my adviser at Jacobs University, who guided me through my Master studies and supported me a lot during PhD.

Particularly, I would like to thank Dr. Florian Kuhnen for his constant guidance and help in the modeling and simulation and all his contributions of time, ideas and support throughout the study.

Yann Barbot and Harry Falk are also gratefully acknowledged for introducing me in the analytical methods and assistance overall experimental period, for fruitful discussions and joint brainstorming. I wish to express my gratitude to those who have contributed to the completion of this thesis work for one way or another.

In closing, I am thankful to all my colleagues, friends and students in Germany for supporting, for always being friendly and helpful, for nice discussions and exchange of opinions, and for sharing the pleasant working atmosphere.

My gratitude is also sent to my families, my dad, my mother, my brother; my husband, my son, and my parents-in-law, for all their endless support and encouragement.

Summary

Biomass is seen to be one of the promising renewable energy resources in the future (Chynoweth et al., 2001). Rapidly growing application of anaerobic digestion (AD) for the treatment of organic waste, the development and improvement of AD process and optimization techniques has grown spectacularly. In spite of the AD technique has been well known for many years some aspects still remain unclear, basically due to complexity of microbial and physicochemical reaction. Thus, there is a need for understanding of the AD mechanisms which can improve stability and enhance the process performance for better efficiency of the biogas plants operation. The process stability and velocity are influenced by the chemical composition of the feedstock and the full supply of the microbial community with essential elements (Yen and Brune, 2007). Consequently, suitable feedstock combination requires a method to foresee the consequences when the new substrate is introduced into the system.

Modeling and simulation represents an appropriate analytical tool for studying and improving the biogas process generation and reduces the expenditure of time and cost for the laboratory experiments. A variety of biogas models contains unknown parameters and complex structure which makes the parameterization step difficult and requires many assumptions. In order to overcome this problem, in this study, a relatively simple model was formulated in order to represent accurately the dynamics of AD by adjusting three master substrates (proteins, carbohydrates and lipids). The model was calibrated using three sets of experimental data in batch: mono-fermentations of gelatine, sucrose and rapeseed oil. The parameterized model accurately predicts the AD of the substrates mixture of gelatine, sucrose and rapeseed oil for the following key process variables such as the volume of biogas and methane, the volumetric flow rate of biogas, the volumetric concentration dynamics of methane and the total chemical oxygen demand.

Furthermore, the model was cross-validated by experimental data where potato waste water (PWW) and starch were digested and tested for two ways of the substrates replacement in continuous laboratory-scale biogas fermenter. The substrates were exchanged in one step and step-wise ways. The model accurately predicts the dynamics of the CH_4 concentration and the volume of biogas by adjustment only two master

substrates: proteins and carbohydrates which were presented by PWW and starch, respectively.

The developed model was adopted for the tank cascade system with the biogas fermenter at the end with total capacity of 2500 m^3. We managed to generate the annual prognosis for continuous long-term the AD process only by arrangement of three components: proteins, carbohydrates and lipids. The volumetric concentration dynamics of methane and the volume of biogas were successfully foreseen by the modeling studies.

Statutory Declaration
(on Authorship of a Dissertation)

I, Anna Schneider, hereby declare that I have written this PhD thesis independently, unless where clearly stated otherwise. I have used only the sources, the data and the support that I have clearly mentioned. This PhD thesis has not been submitted for conferral of degree elsewhere.

I confirm that no rights of third parties will be infringed by the publication of this thesis.

Bremen, March 17, 2016

Signature _____

"The most important thing in sciences not so much to obtain new facts as to discover new ways of thinking about them."

Sir William Bragg

Table of Contents

List of Abbreviations and Symbols

AA:	amino acids	
AD:	anaerobic digestion	
ADM1:	Anaerobic Digestion Model no. 1	
ADSIM:	anaerobic digestion simulation model	
AM2:	Acidogenesis/Methanogenesis model	
C: N:	carbon/ nitrogen ratio	
CSTR:	continuous stirred tank reactor	
COD_{Tot}:	total chemical oxygen demand	[kg COD·m^{-3}]
HRT:	hydraulic retention time	
LCFA:	long - chain fatty acids	
ODE:	ordinary differential equation	
OLR:	organic loading rate	
pKa:	acid constant	
oTS:	organic total solids	[g·L^{-1}]
SCFA:	short-chain fatty acids	
SRT:	Solid retention time	
T:	temperature	
TAN:	Total ammonia nitrogen	
TS:	total solids	[g·L^{-1}]
UASB:	upflow anaerobic sludge blanket	
VS:	volatile solids	[g·L^{-1}]
FM:	fresh mass	
Cp:	*primary* carbohydrates	[kg·m^{-3}]
Pp:	*primary* proteins	[kg·m^{-3}]
Lp:	*primary* lipids	[kg·m^{-3}]
C_S*:*	accessible carbohydrates	[kg·m^{-3}]
P_S*:*	accessible proteins	[kg·m^{-3}]
L_S*:*	accessible lipids	[kg·m^{-3}]
Xaci:	acid forming bacteria	[kg·m^{-3}]
Xmeth:	methanogenic bacteria	[kg·m^{-3}]
TIC:	Total inorganic carbon	[mol·s^{-1}]
VFA:	volatile fatty acids	[mol·s^{-1}]
Me:	methane	[kg·m^{-3}]
Y_{XC} :	yield factor for primary carbohydrates degradation	[kg·kg^{-1}]
Y_{XP} :	yield factor for primary proteins degradation	[kg·kg^{-1}]
Y_{XL} :	yield factor primary lipids degradation	[kg·kg^{-1}]
Y_{XVFA} :	yield factor VFA degradation	[kg·kg^{-1}]
U_C:	yield factor for VFA production from carbohydrates	[kg·kg^{-1}]
U_P:	yield factor for VFA production from protein	[kg·kg^{-1}]
U_L:	yield factor VFA production from lipids	[kg·kg^{-1}]
v_{VFA}:	yield factor for CH_4 production from VFA	[mol·kg^{-1}]
$k_{hyd\,C}$:	hydrolysis constant for carbohydrates	[s^{-1}]
$k_{hyd\,P}$:	hydrolysis constant for proteins	[s^{-1}]

$k_{hyd\,L}$:	hydrolysis constant for lipids	[s^{-1}]
μ_C^{max}:	maximum uptake rate for carbohydrates	[s^{-1}]
μ_P^{max}:	maximum uptake rate for proteins	[s^{-1}]
μ_L^{max}:	maximum uptake rate for lipids	[s^{-1}]
μ_{VFA}^{max}:	maximum uptake rate for VFA	[s^{-1}]
μ_C:	rate of acidogens production on carbohydrates	[$kg \cdot m^{-3} \cdot s^{-1}$]
μ_P:	rate of acidogens production on proteins	[$kg \cdot m^{-3} \cdot s^{-1}$]
μ_L:	rate of acidogens production on lipids	[$kg \cdot m^{-3} \cdot s^{-1}$]
μ_P:	rate of methanogens production on VFA	[$kg \cdot m^{-3} \cdot s^{-1}$]
K_{C_s}:	half-saturation constant carbohydrates	[$kg \cdot m^{-3}$]
K_{P_s}:	half-saturation constant proteins	[$kg \cdot m^{-3}$]
K_{L_s}:	half-saturation constant lipids	[$kg \cdot m^{-3}$]
K_{VFA}:	half-saturation constant VFA	[$kg \cdot m^{-3}$]
IpL_S:	inhibition coefficient	[$mol \cdot kg^{-1}$]
V_{liq}:	volume of the reactor	[m^3]
TR:	temperature in the reactor	[K]
$MWCO2$:	molecular weight of carbon dioxide	[$kg \cdot mol^{-1}$]
R:	the ideal gas constant	[$Jmol^{-1} \cdot K^{-1}$]
$TGas$:	temperature of gas	[K]
P_{outGa}:	the pressure of the gas	[Pa]
ΔG_f :	Gibbs free energy	[kJ mol^{-1}]
V_{BG}:	molar flow rate of volume of biogas	[m^3]
V_{CH4}:	volume of methane	[m^3]
V_{liq}:	volume of the reactor	[m^3]
xCH_4:	volumetric concentration of methane	[Vol.-%]
xCO_2:	volumetric concentration of carbon dioxide	[Vol.-%]
$\dot{q}_{out}Ga$:	flow rate of biogas	[$m^3 \cdot s^{-1}$]
$\dot{q}_{out}CH_4$:	flow rate of methane	[$m^3 \cdot s^{-1}$]
C_p^0:	initial concentrations of carbohydrates	[$kg \cdot m^{-3}$]
P_p^0:	initial concentrations of proteins	[$kg \cdot m^{-3}$]
L_p^0:	initial concentrations of lipids	[$kg \cdot m^{-3}$]
$\dot{q}_C^0$:	inflow rate of carbohydrates	[$kg \cdot m^{-3} \cdot s^{-1}$]
$\dot{q}_P^0$:	inflow rate of proteins	[$kg \cdot m^{-3} \cdot s^{-1}$]
$\dot{q}_L^0$:	inflow rate of lipids	[$kg \cdot m^{-3} \cdot s^{-1}$]
$\dot{q}_{ino}^0$:	inflow of inoculum into the digester	[$kg \cdot m^{-3} \cdot s^{-1}$]
X_{Aci}^0:	initial concentrations of acidogenic bacteria	[$kg \cdot m^{-3}$]
X_{Meth}^0:	initial concentrations of methanogenic bacteria	[$kg \cdot m^{-3}$]
V_K:	volume in the head space of the biogas digester	[m^3]
$\dot{n}_{CH_4}$:	molar flow rate of methane	[$kg \cdot m^{-3} \cdot s^{-1}$]
$\dot{n}_{CO_2}$:	molar flow rate of carbon dioxide	[$kg \cdot m^{-3} \cdot s^{-1}$]
$\dot{q}_{out}Tot$:	effluent flow rate	[$kg \cdot m^{-3} \cdot s^{-1}$]
$\dot{q}_{tot}^0$:	total influent flow rate	[$kg \cdot m^{-3} \cdot s^{-1}$]
y_{CO2}:	molar fraction of carbon dioxide	
y_{CH4}:	molar fraction of methane	

V:	volume of tank with organic waste	[m^3]
VM:	volume of tank with manure	[m^3]
cs1:	concentration of proteins in receiving tank	[$kg \cdot m^{-3}$]
cs2:	concentration of carbohydrates proteins in receiving tank	[$kg \cdot m^{-3}$]
cs3:	concentration of lipids in receiving tank	[$kg \cdot m^{-3}$]
cM:	concentration of manure in receiving tank	[$kg \cdot m^{-3}$]
VS:	volume of sanitation tank	[m^3]
cs1s:	concentration of proteins in sanitation tank	[$kg \cdot m^{-3}$]
cs2s:	concentration of carbohydrates in sanitation tank	[$kg \cdot m^{-3}$]
cs3s:	concentration of lipids in sanitation tank	[$kg \cdot m^{-3}$]
VB:	volume of buffer tank	[m^3]
cs1sb:	concentration of proteins in buffer tank	[$kg \cdot m^{-3}$]
cs2sb:	concentration of carbohydrates in buffer tank	[$kg \cdot m^{-3}$]
cs3sb:	concentration of lipids in buffer tank	[$kg \cdot m^{-3}$]
VF:	volume of biogas plant	[m^3]
$V_{BG\,Tot,\ S}$:	produced biogas volume after the AD of sucrose	[L]
$V_{BG\,Tot,\ G}$:	produced biogas volume after the AD of gelatine	[L]
$V_{BG\,Tot,\ R}$:	produced biogas volume after the AD of rapeseed oil	[L]
$V_{CH4\,Tot,\ S}$:	produced methane volume after the AD of sucrose	[L]
$V_{CH4\,Tot,\ G}$:	produced methane volume after the AD of gelatine	[L]
$V_{CH4\,Tot,\ R}$:	produced methane volume after the AD of rapeseed oil	[L]
$V_{BG\,Tot,mix}$:	theoretical volume of biogas after the AD of mixture	[L]
$V_{CH4\,Tot,mix}$:	theoretical volume of methane after the AD of mixture	[L]
m_S:	mass of sucrose used for the AD sucrose	[gVS L^{-1}]
m_G:	mass of gelatine used for the AD gelatine	[gVS L^{-1}]
m_R:	mass of rapeseed oil used for the AD rapeseed oil	[gVS L^{-1}]
$m_{S,mix}$:	mass of sucrose used for the AD mixture	[gVS L^{-1}]
$m_{G,mix}$:	mass of gelatine used for the AD mixture	[gVS L^{-1}]
$m_{R,mix}$:	mass of rapeseed oil used for the AD mixture	[gVS L^{-1}]

INTRODUCTION

1.1 Renewable energy from biogas

The world´s fossil fuels reserves are getting depleted and, the environmental and economical concerns can be the prominent reasons for the alternative option for energy generation (Asam et al., 2011). For European countries considering the dependency on energy imports on the one side and the growing energy demand on the other side the development of renewable energy (RE) sources has become particularly important. In this context, among the existing RE sources anaerobic biomass digestion is considered to be one of the most promising and feasible alternatives. Biogas is a versatile renewable energy source, which is suitable for the simultaneous production of electricity and heat, as a fuel and as natural gas substitute. Alternatively, biogas can be upgraded and injected into the national gas grid. The other benefits of the anaerobic digestion are considered as waste recycling, production of high-quality fertilizer, reduction of greenhouse gases emission and environmental protection from the pollutants (Tafdrup, 1995; Divya et al., 2015; Weiland, 2010).). Boosting of the RE industry will encourage technological innovation and provide new jobs, for example, in Germany 41,000 people are employed in the biogas sector and in the European Union in total 500,000 people are involved in the RE branch (Agency for Renewable Resources, 2013).

In 2009, the member states of the European Union (EU) submitted their national targets which set the share of energy from RE consumed in transport, production of electricity and heating/ cooling, by 2020. These targets comprise the combination of all RE sectors including wind, solar, hydro-electric and tidal power as well as geothermal energy and biomass. The EU members have set the following goals for 2020:

- to decrease the emission of greenhouse gases by at least 20%;
- to replace 20% of energy demand by RE;
- to reduce the energy consumption by 20% by means of better energy efficiency (Agency for Renewable Resources, 2013; European parliament and council, 2009; European Parliament and Council, 2010).

Every member state apply different pathways, policy supports or other supporting instruments (feed-in tariffs and investing grants) for achieving the targets (Kitzing et al., 2012). In 2013, in the first RE progress report was reported that most member states experienced significant growth in RE consumption and the reported figures indicated that the EU as a whole is on its trajectory towards the 2020 targets with a renewable energy share of 12.7%. However, as the trajectory grows steeper towards the end, more efforts will still be needed, e.g. regarding the implementation of the biofuels scheme which is considered too slow (Report from the commission to the European parliament).

1.2 Biogas – potential and promotion within Germany

The generation of biogas is growing as never before – new strong markets emerge in Europe. Germany remains the driver of growth in the sector of biogas plants thanks to the legal framework provided by the EEG (Renewable Energy Source Act, 2004) which provides for a 20-year guarantee on remuneration rates and the prioritized feed-in of electricity from renewable sources, including biogas (Agency for Renewable Resources, 2013). The tariffs depend on the size and age of the biogas plants, on feedstock (e.g. energy crops, waste, and manure) and technology applied, and on whether the electricity is produced in combined heat and power units. At the end of 2012, about 7,515 biogas plants with an installed electrical capacity of 3,352 MW_{el} were operating in Germany (Weiland, 2010). Figure 1-1 shows the development of plants and installed electric power since 1992.

According to Agency for the Renewable Resources, biogas plant in Germany already replace more than five coal-fired power plants with an average electrical capacity of approximately 600 MW_{el} or two large nuclear power plants with a capacity of approximately 1,485 MW_{el} each. These numbers provide the proof that biogas small producers of biogas have high potential as energy generators with decentralized technologies while the fossil fuels are treated in the centralized power stations (Agency for Renewable Resources, 2013). Presently biogas production remains challenging technology in terms of energy concept and has great perspectives in the future once achieve more efforts in this field. Development of new strategies and techniques for

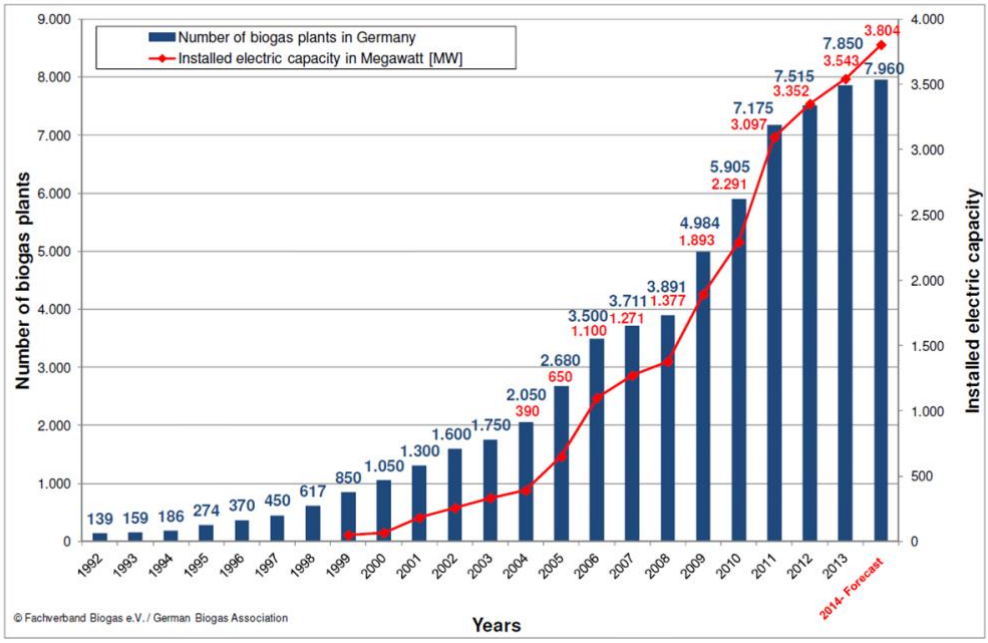

Figure 1-1: Development of the number of biogas plants in Germany over the last 20 years (Fachverband Biogas 2013)

biogas process monitoring, measurement, control and optimization are still actual issue. Different institutions have intensively promoted development in the area of AD. Various initiatives originate with agriculture, industry and the public sector. Research and development efforts are of particular importance here.

1.3 Biochemical mechanism of anaerobic fermentation process

Biogas production is a complex process of the organic biomass degradation into a gaseous mixture basically composed of methane and carbon dioxide by a consortium of various bacteria in an oxygen free environment (Ahring, 2003). In nature, AD occurs in the bottom of lakes, in swamps, paddy fields, landfills and in intestinal tracts of humans and animals (Issazadeh et al., 2013). Raw biogas typically consist of CH_4 (50-75%), CO_2 (25-45%), trace amounts of water vapor (2-7%), and trace amounts of O_2, N_2, H_2S (Kumar et al., 2013). The amount and composition of biogas depends on the amount and composition and the degradability of the organic matter, the presence of the toxic compounds, the process techniques and the operation of the plant. Physical, chemical and

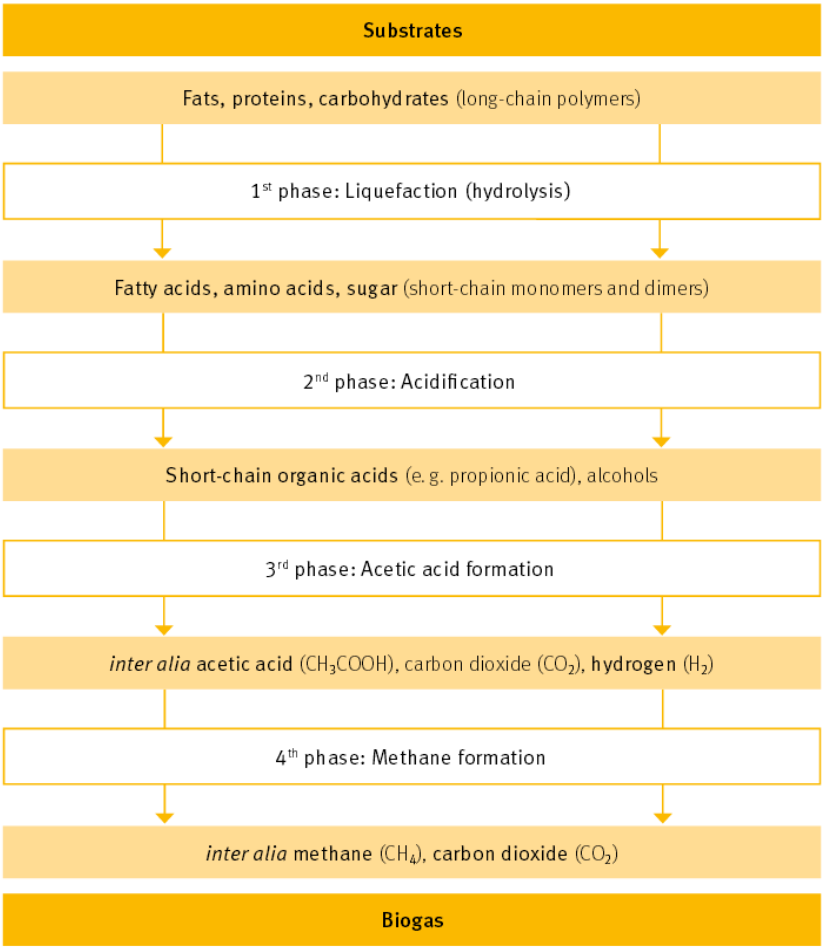

Figure 1-2: The simplified scheme of the degradation of organics during AD. There are four main phases of AD: hydrolysis, acidification, and formation of acetic acid and CH_4 formation (Agency for Renewable Resources, 2013)

biological processes run simultaneously and are affected by external influences (environmental changes and daily feed load). There are four main steps of anaerobic digestion: hydrolysis, acidogenesis, acetogenesis and methanogenesis (Merlin Christy et al., 2014). The simplified scheme of the AD process is presented in Figure 1-2.

1.3.1 Hydrolysis

Hydrolysis is the first step in the AD where facultative (*Streptococci* and *Enterobacteriaceae*) and obligatory (e.g. *Bacteriocides*, *Clostridia*, and *Bifidobacteria*) anaerobic bacteria use enzymes to decompose high molecular mass organic compounds such as proteins, carbohydrates and fats, into low molecular compounds, e.g. amino

acids, lipids and mono-saccharides (Figure 1-2) (Deublein and Steinhauser, 2008). Depending on the compounds content, the degradation takes place differently. Hydrolytic microorganisms excrete hydrolytic enzymes such as cellulases, amylases, xylanases, lipases, proteases and cellobiases (Parawira et al., 2004; Weiland, 2010). The hydrolysis phase includes several steps: enzyme production, diffusion, adsorption, reaction, and finally, enzyme deactivation. The overall hydrolysis success depends on organic material structure, size, shape, surface, concentration, enzyme production and adsorption (Batstone et al., 2002). The hydrolysis has been considered as a rate-limiting step in biogas process formation because some substrates can contain chemicals that inhibit the growth and activity of bacteria or have a poorly accessible structure for the microbes due to their low surface area or highly crystalline structure (Pavlostathis and Giraldo-Gomez, 1991). Therefore, various pretreatment techniques are applied to break down the polymer and enhance the biogas generation. There are physical (mechanical, thermal, ultrasound and electrochemical), chemical (alkali, acid, oxidative), biological (microbiological and enzymatic) and combined methods (Khalid et al., 2011; Montgomery and Bochmann, 2014).

1.3.1.1 Hydrolysis of polysaccharides

Polysaccharides contain chains of linked sugars, e. g. cellulose, hemicellulose, starch, pectin, and glycogen. Cellulose, hemicellulose, pectin and starch can be found in plant material (fruit, grains, vegetables, and crops) and glycogen can serve as a sugar reserve, primarily in animals. Polysaccharides can be linear (cellulose, amylose) or branched chains of sugars (hemicellulose, amylopectin, glycogen). Hydrolysis of cellulose is performed by a mixture of cellulolytic enzymes, e.g. exo-, endo- glucanases and cellobiases (Sanders, 2001). Starch (amylase and amylopectin) and glycogen are cleaved by amylases into glucose units, and several different sugars are formed from hemicellulose and pectin. Structural carbohydrates (cellulose and hemicellulose) are the most difficult to hydrolyze, and conversion of these molecules tends to be extremely slow and incomplete while hydrolysis of non-structural polysaccharides takes only short periods of time. Lignocelluloses are more difficult to degrade; therefore, some effective pretreatment techniques are necessary. The most active bacterial groups during the

hydrolysis of polysaccharides are presented by the genera *Bacteriodes*, *Clostridium*, and *Acetivibrio* (Schnürer and Jarvis, 2010).

1.3.1.2 Hydrolysis of proteins

Proteins are hydrolysed by two groups of extracellular enzymes: protease and peptidases, into their constituent polypeptides and amino acids. Proteins can be found in meat-derived substrates, in chicken and swine manure and dairy wastewater stream as well as in other processing industries such as whey, cheese, fish and casein (Ramsay and Pullammanappallil, 2001). Proteolytic organisms in the biogas process include, among others, the genera *Clostridium*, *Peptostreptococcus*, and *Bifidobacterium* (Schnürer and Jarvis, 2010).

1.3.1.3 Hydrolysis of lipids

Lipids are first hydrolyzed to glycerol and free long-chain-fatty acids (LCFAs). Lipid-rich waste is produced in huge amounts from the food processing industry, slaughterhouses, oil processing and dairy industry and grease-separation sludge. Enzymes that break down fats are called extracellular lipases. The further conversion takes place into the cells (Cirne et al., 2007). Lipid hydrolysis can be inhibited by products accumulation due to the particularity of enzymes which is based on the availability of an interface to become active. Due to amphiphilic structure physical and chemical properties of the interface may change. The lipases are more active towards insoluble than soluble substrates (Sanders, 2001). Methane production can result in reduction of the coagulation of the lipid spheres, therefore, maintaining a large lipid-water interface (Cirne et al., 2007). Most of the known lipases are produced by aerobic or facultative aerobic microorganisms. Strict anaerobes that secrete lipases include, among others, the genus *Clostridium* (Schnürer and Jarvis, 2010).

1.3.2 Acidogenesis

Acidogenesis is a robust and often the fastest stage in the whole anaerobic digestion process. The products of the hydrolysis phase are degraded by acid forming bacteria while long-chain fatty acids (LCFA) must be oxidized by an external electron acceptor with formation of short-chain fatty acids (SCFA) (e.g. acetic, propionic, valeric and

butyric acids). The other option of degradation is when one amino acid acts as an electron donor and another one as an acceptor (Ramsay and Pullammanappallil, 2001). Acetate, carbon dioxide, hydrogen sulfide and ammonia that are formed during this phase act as initial products for methane formation. Transition from organic material to organic acids causes the drop of the pH value which is beneficial for acidogenic and acetogenic bacteria as they prefer slightly acidic environment. Hydrolysis and acidogenesis can be enhanced by increasing the temperature however it can lead to accumulation of volatile acids in the broth, resulting in inhibition of acetogenic and methanogenic bacteria (Chang et al., 2004). The intermediate products cannot be utilized by the methanogens, and must be further consumed by acetogenic bacteria. The typical representatives of this step are *Clostridium*, *Streptococcus, Bacillus*, *Lactobacillus* and *Raminococcus* (Deublein and Steinhauser, 2008). In this phase glucose is metabolized through different pathways to acetic acid, propionic acid, butyrate, lactate and ethanol, respectively. The pathway selection depends on the substrate concentration, pH, and dissolved H_2. At low pH values, ethanol production is increased, while at higher pH more volatile fatty acids (VFA) are formed. H_2 partial pressure has the biggest influence on the pathway. When it is low the fermentation pathway to acetate and H_2 is favored (Schink, 1997).

1.3.3 Acetogenesis

The organic acids longer than two C - atoms and alcohols longer than one C - atom are broken down during the acetogenic process into acetate, CO_2 and H_2, which later on are used as the substrates for methanogens. Hydrogen plays an important intermediary role in this process, as the reaction will only occur if the hydrogen partial pressure is low enough to thermodynamically allow the conversion of all the acids. Acetogens make syntrophic associations with hydrogen scavenging bacteria which are lowering the partial pressure, thus the hydrogen concentration of a digester is an indicator of its health (Mata-Alvarez, 2003). The typical representatives of this step are *Desulfovibrio* (oxidizes organic acids and alcohols to acetate and transfer the electrons to sulfate), *Aminobacterium* (ferment amino acids and produce acetate) and *Acidamicoccus* (ferment amino acids, citrate to acetate, CO_2 and H_2) genus (Weiland, 2010; Deublein and Steinhauser, 2008). The typical reactions are shown in Table 1-1. The reactions in this phase are endothermic, e.g.

for degradation of propionic acid are needed $\Delta G_f' = 76.11$ kJ mol^{-1} or for ethanol degradation $\Delta G_f' = +9.6$ kJ mol^{-1} (Deublein and Steinhauser, 2008). Connection to microorganisms with exothermic metabolism results in energetically possible of the net reaction.

Table 1-1: Acetogenic degradation (Deublein and Steinhauser, 2008)

Substrate	Reaction
Propionic acid	$CH_3(CH_2)COOH + 2H_2O \rightarrow CH_3COOH + CO_2 + 3H_2$
Butyric acid	$CH_3(CH_2)2COO^- + 2H_2O \rightarrow 2CH_3COO^- + H^+ + 2H_2$
Valeric acid	$CH_3(CH_2)_3COOH + 2H_2O \rightarrow CH_3COO^- + CH_3CH_2COOH + H^+ + 2H_2$
Isovaleric acid	$(CH_3)_2CHCH_2COO^- + HCO^{3-} + H_2O \rightarrow 3CH_3COO^- + H_2 + H^+$
Capronic acid	$CH_3(CH_2)_4COOH + 4H_2O \rightarrow 3CH_3COO^- + H^+ + 5H_2$
Carbondioxid-hydrogen	$2CO_2 + 4H_2 \rightarrow CH_3COO^- + H^+ + 2H_2O$
Glycerine	$C_3H_8O_3 + H_2O \rightarrow CH_3COOH + 3H_2 + CO_2$
Lactic acid	$CH_3CHOHCOO^- + 2H_2O \rightarrow CH_3COO^- + HCO^{3-} + H^+ + 2H_2$
Ethanol	$CH_3(CH_2)OH + H_2O \rightarrow CH_3COOH + 2H_2$

1.3.4 Methanogenesis

During the final stage, the fermentation products (acetate, hydrogen and carbon dioxide however, formate, methanol, methylamines, and CO) are converted to CH_4 and CO_2 by strict anaerobes belonging to the *Archaea* family (*Methnobacterium, Methanospirillum hungatei* and *Methanosarcina*) (Miyamoto, 1997; Verma, 2002). There are two ways for the production of methane either by means of cleavage of acetic acid molecules to generate CO_2 and CH_4 - acetoclastic methanogenic pathway, or by reduction of CO_2 with H_2 - hydrogenotrophic methanogenic pathway (Ostrem, 2004). Some typical conversions in this phase, together with their free Gibbs energy changes, are shown in Table 1-2. The hydrogen consuming methanogens are fast growing bacteria with the maximum doubling time of 6 hours compared with slow growing aceticlastic methanogens with doubling time between 3-15 days (Merlin Christy et al., 2014). The first group of bacteria is most resistant to environmental changes than the second bacterial group. A significant quantity of the CH_4 production up to 70% is produced by acetoclastic methanogenic bacteria

while up to 30% of the total is produced by hydrogen-utilizing methanogenic bacteria (Duncan and Nigel, 2003). Generally, methanogenic bacteria prefer slightly alkaline environment and they are most active in the pH range of 6.5-8.0. Waste stabilization is accomplished when methane gas and carbon dioxide are produced. The remaining compounds like alcohols, organic-nitrogen compounds are accumulated in the fermenter (Deublein and Steinhauser, 2008).

Table 1-2: Methanogenic degradations and the energy changes of reaction (Deublein and Steinhauser, 2008)

Substrate type	Chemical reaction	$\Delta G_f'$ [kJ mol^{-1}]
CO_2 − Type	$4H_2 + HCO_3^- + H^+ \rightarrow CH_4 + 3H_2O$	− 135.4
	$CO_2 + 4H_2 \rightarrow CH_4 + 2H_2O$	− 131.0
CO_2 − Type	$4HCOO^- + H_2O + H^+ \rightarrow CH_4 + 3HCO^{3-}$	− 130.4
Acetate	$CH_3COO^- + H_2O \rightarrow CH_4 + HCO_3$	− 30.9
Methyl type	$4CH_3OH \rightarrow 3CH_4 + HCO^{3-} + H^+ + H_2O$	− 314.3
Methyl type	$CH_3OH + H_2 \rightarrow CH_4 + H_2O$	− 113.0
e.g. Methyl type: ethanol	$2CH_3CH_2OH + CO_2 \rightarrow CH_4 + 2CH_3COOH$	− 116.3

1.4 The environmental conditions and factors affecting anaerobic digestion process

The performance of the biogas production process can be factored by a certain number of environmental conditions such as pH, temperature, redox potential, C:N ratio, volatile fatty acids (VFA); technical aspects - biogas potential of feedstock, agitation, pretreatment, retention time, nature of the substrate, loading rate etc (Merlin Christy et al., 2014). A change in conditions can affect the process stability, biogas yield and bacterial consortium. Therefore, for the effective fermentation process, numerous factors and technical aspects must be taken into consideration and be controlled.

1.4.1 The pH value and alkalinity

The pH value is an important variable that has essential influence on enzyme activity in microorganisms, since each enzyme is active only in a specific pH range and has maximum activity at the optimal pH value. The pH value in anaerobic digesters is mainly controlled by the bicarbonate buffer system and it depends on the partial pressure of CO_2, the concentration of alkaline and acid components in the liquid phase. Buffer capacity (the solution resistance to pH change) also plays an important role for the process stability. In a system with a low buffer capacity the organic acids have high influence on the pH level. High alkalinity level is necessary prerequisite to maintain a stable pH value. The composition of substrate also plays an important role, e.g. protein-rich feed due to the release of ammonia (Gerardi, 2003). The main buffer in anaerobic digesters presents in a form of bicarbonates which are in equilibrium with carbon dioxide (Equation 1.1).

$$CO_2 + H_2O \leftrightarrow H_2CO_3 \leftrightarrow H^+ + HCO_3^- \leftrightarrow 2H^+ + CO^{2-}{}_2 \quad (1.1)$$

Other compounds normally found in the digester also influence the pH balance if present at high concentration, for example, ammonia (NH_4^+/NH_3, pKa 9.3), hydrogen sulfide (H_2S /HS^- /S^{2-}, pKa 7.1 and 13.3) and hydrogen phosphate (H_3PO_4 /$H_2PO_4^-$/HPO_4^{2-} /PO_4^{3-}, pKa 2.1, 7.2 and 12.3) (Moosbrugger et al., 1993; Schön, 2009). In practice, when temperature and HRT have been defined, the pH value will be at a certain value which benefits the dominant microorganisms. For optimal performance of the microbes, the pH within the digester should be kept in the range of 6.8 - 7.2. If the pH value is below 6.5, the production of VFAs leads to a further decrease of the pH by the hydrolytic bacteria and a possible fermentation failure (Chawla, 1986).

1.4.2 Temperature

Temperature has a direct effect on physical-chemical properties of all components in the digester and also affects thermodynamics and kinetics. An increase in temperature normally leads to an increase of the metabolic activity. However, an increase in temperature has other effect as well. Increasing temperature decreases pKa of ammonia, therefore, increases the fraction of free NH_3 which inhibits microorganisms. Additionally, increasing temperature increases the pKa of VFAs, which increases its not dissociated

fraction (Marchaim, 1992). A rise in the temperature can cause the slowdown in the reaction rate, decrease or shift in yields or even increase in the death rate (Abbasi et al., 2012). There are various temperature ranges at which the anaerobic digestion (AD) runs: psychrophilic (< 30°C), mesophilic (30°C – 45°C), and thermophilic (45°C – 60°C) (Figure 1-3). Most of the methanogenic microorganisms belong to the mesophilic group. Methanogens are sensitive to rapid temperature changes. Thermophilic methanogens are more temperature sensitive than the mesophilic, and small temperature variations can result in a decrease in bacterial activity. Critical temperature for the mesophilic microorganisms is in the range of 40°C – 45° C when bacterial activity is irreversibly lost. Thus, temperature determines which kind of microorganism can survive in the reactor. Therefore, a constant temperature is very important for the microbial consortium because once it has adapted to a certain temperature value it can tolerate a small deviations in temperature (Deublein and Steinhauser, 2008).

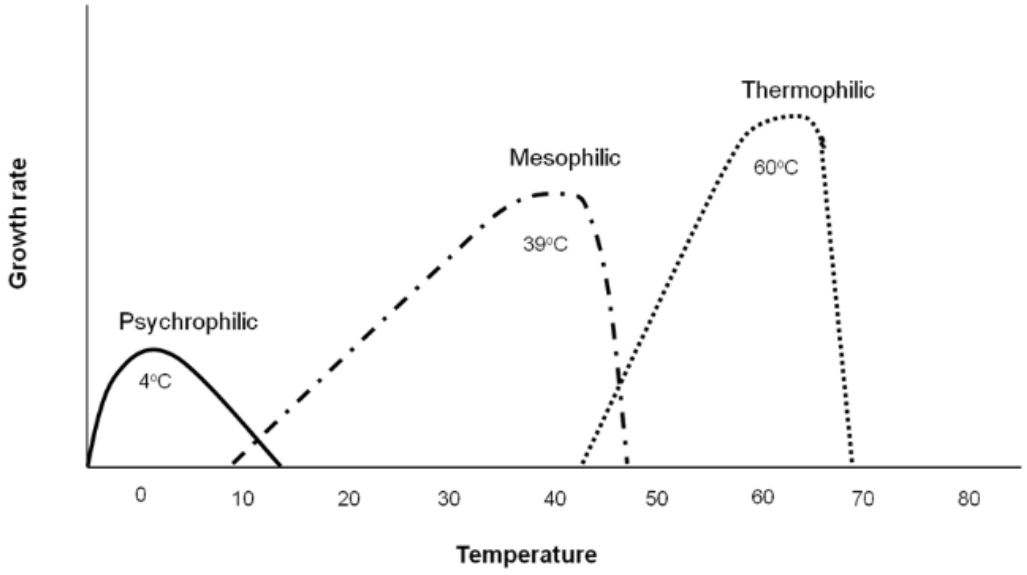

Figure 1-3: Growth of microorganisms at different temperatures (Schnürer and Jarvis, 2010)

1.4.3 Oxidation - reduction potential

The oxidation – reduction potential (ORP) is a measurement of the relative amount of oxidized oxygen (NO_2^-, NO_3^-, SO_4^{2-}, CHO) (Gerardi, 2003). Redox potential must be kept at low values. Methanogenic bacteria require a range between -300 and -330 mV. To

be able to maintain a low ORP value, oxidizing agents might be added such as sulfates, nitrates, absence of oxygen and nitrites. The optimum ORP range for hydrolysis/ acidogenesis phase is at - 400 and - 300 mV and for methane-forming bacteria it is at -300 mV (Deublein and Steinhauser, 2008).

1.4.4 Organic loading rate

The volumetric organic loading rate is related to the retention time through the active biomass concentration in the bioreactor and it is used to estimate the loading on anaerobic treatment systems. The OLR serves for the design and operation of anaerobic processes and gives information about the efficiency of the utilized reactor volume. The OLR is calculated using the following formula (Equation 1.2):

$$OLR = \frac{Q \cdot C}{V} = \frac{C}{HRT} \quad (1.2)$$

where OLR is the volumetric organic loading rate [kg VS m^{-3} d^{-1}], Q the influent flow rate [m^3 d^{-1}], C the concentration of volatile solids in the substrate [kg VS m^{-3}] and V the bioreactor volume [m^3] (Schön, 2009). In a mesophilic operation, values between 3.5 and 5 kg VS/$m^3 \cdot d^{-1}$ have been proved to be successful (Deublein and Steinhauser, 2008).

1.4.5 Hydraulic Retention Time

Hydraulic Retention Time (HRT) implies the average length of time the liquid influent (substrate) and it is calculated by dividing the daily amount of VS added by the total fermenter volume. For completely mixed anaerobic reactors operated without solids recycling the HRT and the (solid retention time) SRT are identical. Retention time and OLR are inversely proportional to each other and thus, have to be aligned when designing the reactor layout. The maximum possible OLR depends on both the process temperature and the retention time: the lower the temperature and the longer the retention time the higher the OLRs that can be processed. In tropical countries HRT varies from 30-50 days while in countries with colder climate it might reach 100 days (Lagrange, 1979). This maximum value depends also on the specific plant type. Feeding the system above its sustainable OLR, results in low biogas yield due to accumulation of inhibiting substances

such as fatty acids in the digester slurry. Typically, OLR ranges from 2 to 6 kg VS $m^{-3}d^{-1}$ (Deublein and Steinhauser, 2008).

1.4.6 Agitation/ Mixing

The close contact between microorganisms and the substrate material is very important for an efficient digestion process as well as to avoid the formation of scum and temperature gradients within the fermenter. This can be achieved due to daily feeding of the substrate instead of long interval gives and installation of certain mixing devices such as propeller, scraper, or stirrer in the plant (Yadvika et al., 2004).

1.5 Important characteristics of feedstock

The most important initial issue when considering the application of anaerobic digestion systems is the feedstock for the digestion. A broad variety of organic substrates can be anaerobically utilized (Chynoweth et al., 2001). Input materials vary in terms of gas yield and electricity production, and each feedstock has to be evaluated on its own merits and its influence on the overall feedstock mixture. Its nutrient load, composition, methane yield potential, and pretreatment cost play roles. For economic and technical reasons, some substrates are preferential than others. If the costs for biomass are high, then the economic benefits of its outputs (gas and slurry) will be low (Weiland, 2010). Carbon, oxygen, nitrogen, hydrogen and phosphorus are the main components in feedstock and microbial cell material is about 50, 20, 12, 8 and 2 % of those elements, respectively (Gerardi, 2003). Substrates for the methane production range from readily degradable wastewater to complex high solid material. According to a current survey from different operators based on the monitoring report on the Renewable Energy Sources Act – EEG there is the following distribution among the substrates digested at biogas plants nationwide: 54% renewable resources (maize, grain, grasses, sugar beet, cup plant such as *Silphium perfoliatum* and species of sorghum), 41% livestock excrements, 4% bio - waste, and 1% residual substances from industry and agriculture (Agency for Renewable Resources, 2013). The biomass classification which was suggested by Weiland (2010) is considered as a mixture of the following biomass input streams:

- agricultural (liquid manure from cows, pigs and other livestock waste; energy crops such as cereals, silage from maize, rye, sunflowers, sorghum, and grass clippings and agricultural byproducts, algal biomass and harvest remains);
- biodegradable industrial residues (residues from the food/beverage (Jayathilakan et al., 2012), cosmetic, pharmaceutical pulp and paper industry, residues from production processes, for instance, beer, sugar, wine, alcohol, meat products, milk, juice, vegetable processing, harvest surplus and fats);
- wastewater treatment (household sewage);
- waste disposal (solid and liquid wastes) (Weiland, 2010).

An example of the methane production from certain substrate types is shown on the Figure 1-4. The difference of the methane yield is due to the difference of the composition of the input substrates. Different combinations of waste such as manure and other biodegradable industrial residues may result in higher gas yield since industrial organics frequently have higher biogas potential. Besides, the proportion of proteins, carbohydrates and lipids in organic matter plays important role. Methane yields, the composition of various types of waste and their organic content are shown in the Table 1-3. Aside from the qualitative influence of the substrate one should consider the installation technology of the biogas plant and parameters of the fermentation process.

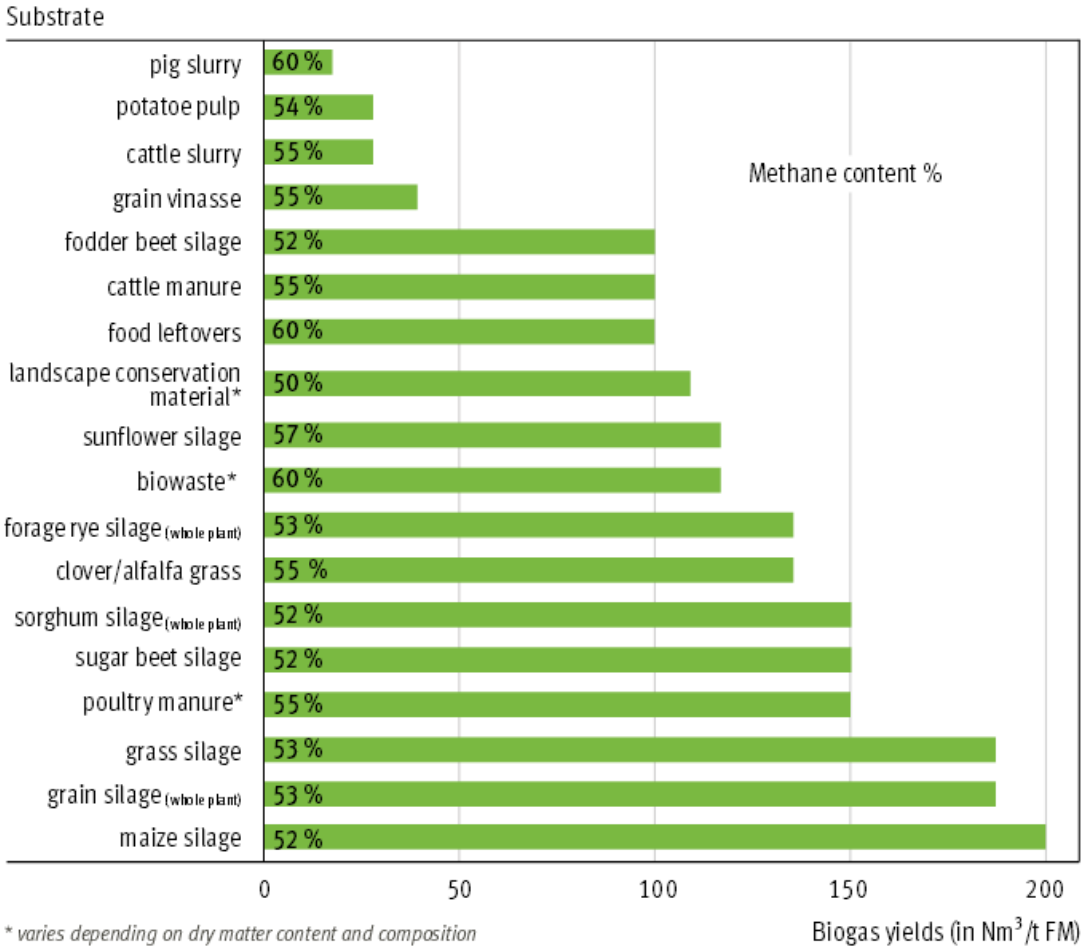

Figure 1-4: Generation of methane (%) from various feedstock (Agency for Renewable Resources, 2013)

Table 1-3: Dry matter, content of organics, biogas yield (Deublein and Steinhauser, 2008) and percent amount of proteins, carbohydrates and lipids in different types of waste (Angelidaki, 2008; Al Seadi, 2001), P-proteins, C- carbohydrates, L-lipids

Feedstock	DM [%]	oDM [%]	Biogas yield [m^3 kg^{-1} oTS]	Organic content	Resource for estimation of P,C and L relation in percent
Flotation sludge	5-24	90-98	0.7-1.2	P: 65-70%, L: 30-35%	Al Seadi T, 2001; Angelidaki, 2008
Greaves	2-70	75-98	1.2	P: 80-90%, L: 7-15%	Al Seadi T, 2001
Overstored food and leftovers	14-18	81-97	0.2-0.5	-	-
Fat residues	99.9	99.9	1.2	L: 85-95%	Al Seadi T, 2001
Mucilage	40-75	30-70	27	-	-
Whey	4-6	80-92	0.5-0.9	C: 75-80%, P: 20-25%	Al Seadi, 2001; Angelidaki, 2008
Blood	30-40	95-98	0.66-1.36	-	-
Stomach – intestine residues	12-15	80-84	0.3-0.4	P:33%,C:33%,L:33%	Al Seadi, 2001; Angelidaki, 2008
Glycerine	>98	90-93	1.0-1.1	-	-
Whey concentrate	95	76	0.7	P:20-25%, C:75-80%	Angelidaki, 2008
Manure (cattle)	7-17			P, C, L: 33.3%	assumed

1.5.1 Substrate composition

The process stability as well as velocity and decomposition rate is influenced by the chemical composition of the feedstock and the necessary supply of the microbial community with essential elements (Yen et al., 2007). Techniques are available to determine the compositional characteristics of the feedstock, whilst parameters such as solids, elemental and organic analyses are important for digester design and operation. Depending on the substrate composition, intermediate products produced in the acidogenic pathway can limit or inhibit further degradation and, consequently, biogas quantity and composition. For instance, the degradation of the substrate containing fats can lead to a rise of fatty acids, and following degradation restrictions. The decomposition of the substrates, which are rich in proteins, might cause a formation of ammonia and hydrogen sulfide and further inhibition the AD process. Anaerobes can breakdown material to varying degrees of success from readily in the case of short chain hydrocarbons such as sugars, to over longer periods of time in the case of cellulose and hemicellulose. Anaerobic microorganisms are unable to break down long chain woody molecules such as lignin (Gunaseelan, 1997). Such points ought to be taken into consideration during the biomass selection (Deublein and Steinhauser, 2008).

1.5.2 Carbon : Nitrogen (C:N) ratio

The relationship between the amount of carbon and nitrogen present in organic materials is also quite important in the AD process. The optimum C:N ratio for hydrolysis/ acidogenesis phase is at 10 - 45:1 and for methane-forming bacteria it is at 20 – 30:1. If the C:N ratio is very high, the nitrogen will be consumed rapidly by methanogenic bacteria to meet their protein requirements and will no longer react on the left over carbon content of the material, which can cause low gas production. On the other hand, if the C:N ratio is very low, nitrogen will be released and accumulated in the form of ammonia, which in turn can lead to an increase in the pH value. A pH value higher then 8.5, will have a negative effect on the methanogenic population. Therefore, biomass with a high C:N ratio should be mixed with that of a low C:N ratio to bring the average ratio of the composite input to a desirable level (Deublein and Steinhauser, 2008).

1.5.3 Volatile Fatty Acids

Volatile fatty acids (VFAs), which are produced by acidogenic and acetogenic bacteria, reflect a kinetic coupling between the acid producers and consumers (methanogenic bacteria). Accumulation of VFAs leads to decrease in the pH value. Normally the drop in pH is counterbalanced and buffered by formation of alkalinity through CO_2 production. VFAs concentration will change according to the changes in hydraulic loading, organic loading or temperature (Gonzales-Fernandez and Garcia-Encina, 2009). In anaerobic digesters with low buffering capacity, pH, and partial alkalinity VFAs are key indicators for process imbalance, however, in highly buffered systems, pH changes can be small, even when the process is extremely stressed, and only VFAs can be considered reliable for process monitoring and serve as an important parameter for process imbalance diagnosis (Franke-Whittle et al., 2014). For a stable process the concentration of VFA should be rather low (< 500 mg L^{-1}). The concentration can be higher if the digester is undersized for the organic load (Labatut and Gooch, 2012). VFAs comprise a group of six acids, and they are acetic acid (acetate), propionic acid (propionate), butyric acid (butyrate), valeric acid (valerate), caproic acid (caproate) and enanthic acid (enanthate), where acetic acid is predominant (Labatut and Gooch, 2012). Various VFAs have different effects on bacteria. Propionic acid is more toxic than acetic acid and accumulation of propionic acid often indicates the imbalance in any metabolic pathways in AD, e.g. Wang et al. (Wang et al., 2009) reported that 900 mg L^{-1} of the propionic acid had significant inhibition effect on bacterial activity, whereas 2400 mg L^{-1} of the acetate and 1800 mg L^{-1} of butyrate resulted in no inhibition of the activity of methanogens. Some authors suggested that the main indicators of the coming AD failure are i-butyric, i-valeric, propionic acid. However, different AD systems have own levels of VFAs meaning that certain level of VFAs which is inhibiting in one reactor can have an opposite effect in another reactor (Franke -Whittle et al., 2014).

1.5.4 Inhibitors

Inhibitory compounds are either present already in the substrate or generated during the degradation. The most common inhibitors are formed during degradation of the substrate, such as VFA (See 1.5.2), long-chain fatty acids (LCFA), ammonia and sulfide. LCFAs

are formed during the initial steps of treatment of the lipid-containing organic material and even the low concentration of LCFA can be responsible for inhibition of the gram-positive bacteria (Kabara et al., 1977). Due to adsorption onto the cell wall, LCFAs interfere with the transport and protective function of microorganism (Chen et al., 2008).

Treatment of protein-rich substrates can lead to accumulation of ammonia in the broth which occurs in the form of ammonium ion (NH_3^+) and in the form of free ammonia (NH_4). Ammonia concentration below 200 mg L^{-1} is beneficial for bacteria as a prestage of amino acid synthesis. It has been reported that TAN (total ammonia nitrogen) concentration in a range from 1.7 to 14 g L^{-1} results in the reduction of methane by 50% (Angelidaki and Ahring, 1994; Chen et al., 2008; Sung and Liu, 2003). The typical inhibition mechanisms of the digestion caused by ammonia are changes in the intracellular pH, increase of the maintenance energy equipment and inhibition of some enzymatic reactions. To remove ammonia from the substrate air stripping, chemical precipitation and increasing of biomass retention in the digester are applied (Chen et al, 2008).

Another reason of the inhibition can be H_2S which affects negatively the metabolic activity of methanogenic bacteria. In the case of the high accumulation of H_2S into the fermenter, the methanogens are inhibited what leads to the accumulation of acids, subsequent drop of pH and further increase of sulfide. To overcome the sulfide accumulation iron salts can be added into the fermenter or some oxygen (Gerardi, 2003).

Some inhibitors are present already in the substrate, such as some ions from mineral salts, heavy metals, detergents and antibiotics. A small quantity of ions (e.g. sodium, potassium, calcium, magnesium, ammonium and sulfide) also stimulates the growth of bacteria. The same is the case with heavy metals (copper, nickel, chromium, zinc, lead, etc.). In small quantities they are essential for the growth of bacteria but in higher concentrations they have toxic effects (Chen et al., 2008). Detergents such as soap and organic solvents inhibit the activities of methane producing bacteria and the addition of these substances in the digester should be avoided (Deublein and Steinhauser, 2008). Inhibitory effects of these compounds are not inherent but solely depend on concentration

and emerge when a certain threshold is exceeded (Deublein and Steinhauser, 2008). The main indicators of inhibition are drop in alkalinity and pH, increase in VFAs or disappearance of H_2 and CH_4 (Gerardi, 2003). This can be a reversible effect and activity will recover when concentrations fall below thresholds (Deublein and Steinhauser, 2008, Chen et al., 2008).

1.5.5 Nutrients

Macronutrients are the elements that are the nutrients of the anaerobic microorganisms. They include hydrogen, nitrogen, oxygen, carbon, sulfur, phosphorus, potassium, calcium, magnesium and iron. In addition to the micronutrients, a number of other elements, such as Ni, Fe, Zn and Co must be present in small amount (Kumar et al., 2013). For anaerobic treatment of mixed waste, such as sewage sludge, it is often assumed that the necessary nutrients are available and in non-limiting amounts. However, when the substrate is composed of single wastes or wastewater fraction, the degradation can be limited by the availability of certain nutrients (Deublein and Steinhauser, 2008).

1.5.6 Water content

Next consideration related to the moisture content of feedstock. The movement of bacteria and activity of extra cellular enzyme are highly determined by the water content in the digester. The wetter the material the more suitable it will be to handle with standard pumps instead of energy intensive concrete pumps and physical means of movement. The moisture content of the target feedstock will also affect what type of system is applied for its treatment. Optimum moisture content has to be maintained in the digester and the water content should be kept in the range of 60-95 % (Demetriades, 2008). However, the optimum water content is likely to differ with different input materials depending up on the substrates chemical characteristics and degradation rate.

1.5.7 Particle size

The production of biogas is also affected by particle size of the substrate. If the particle diameter is high, the microbial activity is reduced due to a reduced accessibility and it can also result in the clogging of the digester. Small particle size provides a large surface area

for substrate uptake and thus allows increased microbial activity followed by increase in gas production (Yadvika et al., 2004).

1.5.7 Microbial degradability of the biomass

The level of biodegradability is the key factor for successful application of any biodegradable material as substrate. The experience shows that fats require a long retention time due to their poor bioavailability, but provide a high biogas yield. Carbohydrates and proteins have much faster conversion rates but lower gas yield and proteins have faster conversion and a similar high biogas yield as compared to lipids (Deublein and Steinhauser, 2008).

1.6 Types of biogas digesters and modes of operation

Various AD configurations are applied for the installation of the biogas production (Table 1-4). Fermenters, in which the input material is composed of 25-40% DM, are defined as dry-matter anaerobic digesters, whereas those with less than 15% of DM are classified as wet-matter digesters (Nizami and Murphy, 2010). AD with 15-25% DM is considered to be a combination of dry - and wet - matter AD. Substances with more than 40% of DM must be diluted with water. In wet AD the feedstock is pumped and stirred and in dry AD it can be stacked. Mixing of dry systems is more difficult and there are three types of homogenization of the system: recirculation of the waste from the bottom to the top of a tank, recirculation in the horizontal tank equipped with rotating impellers and re-injection of biogas into the bottom of a tank (Erickson et al., 2004). Dry - matter AD tends to be cheaper to maintain as there is less water to heat and there is more gas production per unit feedstock. However, wet - matter AD has a lower set-up cost.

Depending on the type of feeding one can distinguish discontinuous or batch (e.g. percolation process), quasi- and continuous (e.g. plug-flow process). About 70% of biogas plants in Germany work according to the continuous feeding, where the feedstock is introduced either constantly or with some intervals (Agency for Renewable Resources, 2013).

Table 1-4: Different types of the biogas process production based on the certain criteria (Agency for Renewable Resources, 2013)

Criterion	Distinguishing features
Dry-matter content of the substrate	Wet digestion Dry digestion
Type of feeding	Discontinuous Quasi-continuous Continuous
Number of process phases	Single-phase Two-phase
Process temperature	Psychrophilic Mesophilic Thermophilic

When all four phases of AD take place in one digester, this is referred as single-phase process. Some systems have double digester to ensure each AD step is as efficient as possible, e.g. mesophilic operating conditions in one tank and thermophilic conditions in another one (Demirel and Yenigun, 2002). Thus, the AD process starts with acids formation phase and finishes with the biogas generation at the end. Optimized process conditions for hydrolysis and acidogenesis in the first digester and acetogenesis and methanogenesis in the second digester result in faster substrate degradation and consequent reduction of the HRT. However, an accumulation of ammonia and probably more hydrogen sulfide can take place during the acid phase (Erickson et al., 2004). Currently, about 90% off biogas plants in Europe operate on one stage process due to the lower cost (Bouallagui et al., 2005).

Some digesters operate at different temperature ranges. Thermophilic systems have a faster through put with faster biogas production per unit of substrate and a better hygienisation can be attained. At 35ºC the typical retention time ranges from 15 to 30 days, whereas at 55ºC it is only 12-14 days. However, the capital costs to maintain the thermophilic systems are much higher and they generally require a higher degree of operation and monitoring (Erickson et al., 2004).

In batch digesters, the reactor is loaded once with the inoculum and substrate and it is left until complete degradation occurred (Lissens et al., 2001). The HRT depends on the

temperature and other factors. The batch digester is the easiest and cheapest to build and also it is more robust against inhibitors. In continuous set-ups the substrate is constantly and regularly fed into the reactor vessel and an equal amount is pumped out from the system. In continuous systems the microorganisms can adopt to the inhibitor either with increasing of their concentration. As examples for continuous reactors are mentioned here continuously stirred tank reactor (CSTR), anaerobic filters, upflow anaerobic sludge blanket (UASB) and plug flow reactor (Nizami et al., 2010).

MODELING and SIMULATION of the BIOGAS PRODUCTION PROCESS

Even though that the anaerobic digestion is known for a long time, the steps of the processes behind are quite complex and need further investigation. Mathematical modeling of the AD processes was initiated by the need for the optimization and effective process operation since the late 1960's (Donoso-Bravo et al., 2011). Different models have been formulated in order to learn in depth the mechanisms influencing the biochemical and physical sides of the AD process. Numerical modeling is a tool for investigation of the static or dynamic processes without conducting or reducing the number of long-term running experiments. Ideally, biogas mathematical models are supposed to become a useful tool for qualitative and quantitative analysis of the microbial reactions including hydrodynamics and mass balance of all components in the AD system as well as bacterial dynamics in different plant configurations under different environmental and operational conditions (Yu et al., 2002). Such tools can be of great importance for development and testing of new optimization and control strategies (e.g. substrate exchange, identification the disturbances at the early stages of the fermentation). For this, models have to adequately capture the different fermentation phases and inhibition factors as well as the fermentation process dependencies on internal and external influences. Nevertheless, to obtain valid kinetic constants still remain a complicated task due to the fact that AD is a complex system implying the simultaneous performance of physical, chemical and biological reactions catalyzed by a consortium of various bacteria which composition may vary in an unknown way. Additionally, the mathematical prediction of the AD dynamics is further complicated by seasonal changes, retention time, temperature, reactor type and daily feeding. Moreover, the lack of knowledge regarding the specific bacteria involved, their particularities in metabolism as well as their physiological limitations also play a limiting role of predicting capability (Yu et al., 2013). Therefore, one should accept that it is still not possible to adopt a general mathematical model applicable under all circumstances and representing completely the overall process of biogas production with all reactions including all

process parameters of the process. Models represent a simplification of reality and the description the part of reality which is relevant to understand and to deal with. A model can be only successful when it fulfills the expectations (Henze et al., 2008). Thus, a typical feasible mathematical model is based on many assumptions resulting in neglecting of some real biological phenomena and should satisfy basic characteristics: cause-effect performance, relative simplicity, identifiability and predictive capability (Donoso-Bravo et al., 2011).

2.1 Classification of biogas models

Biogas models have allowed an understanding of important patterns of the AD process and have given rise to guidelines for the operation and optimization of anaerobic reactors. Dynamic modeling is a helpful tool during start-up phase, indication of the process failure due to inhibition and its possible recovery. Validated models also lead to a more in-depth knowledge of microbial biochemical kinetics, and stoichiometric relationships. Typically, the biogas fermenter is in a dynamical state which makes the modeling and simulation as valuable tool for the studies of the AD process.

Models can be classified according to a number of different criteria. Models are divided into structured and unstructured ones. The former subdivide biomass into compartments of different functionality, whereas the latter usually describe the biomass as one chemical compound (Bailey and Ollis, 1986; Birol et al., 2002; Fredrickson et al., 1970; Liu et al., 2004).

Considering time as variable, models can be either steady state or dynamic. Steady state models show the process performance under stable time invariant conditions. Such models are helpful for design of reactors, for the forecast of gas quality and effluent quality for stable reactor at given operating conditions (Budhijanto et al., 2012). Dynamic models can predict the AD process under time variant conditions and, therefore, they are quite useful when the biogas reactor is in transient phases depending on the mixed microbial populations. Dynamic models consist of ordinary differential equation (ODE), based on mass balance. For instance, the substrate balance of the AD process can be expressed by Equation 2.1:

$$\frac{dS}{dt} = (S_0 - S) \cdot D + (\frac{dS}{dt})_r \quad (2.1)$$

accumulation = input - output + reaction

where $\frac{dS}{dt}$ is the accumulation rate (change of the substrate concentration over change in time), D is the dilution rate (d^{-1}), S_0 is the initial substrate concentration, S is the substrate concentration and $(\frac{dS}{dt})_r$ is the reaction rate. In the equation one can define a technical part or mode of operation: $(S_0 - S) \cdot D$ and a chemical part - $(\frac{dS}{dt})_r$. The technical part is responsible for the transition phase and input and output flows while the chemical part describes the dynamical change of the compound or substrate. Besides ODE algebraic equations are necessary for calculation of flow of gaseous components or for other estimations.

There are theoretical (the first order) and experimental (empirical) models. A theoretical model is, as the name indicates, based on the theoretical knowledge of how the system works. It is expected to be able to predict the behavior of systems. An experimental model is developed by experimentally investigating the correlation between different parameters. An experimental model is therefore only valid for the particular system for which it was developed. Some of the models are more suitable for qualitative description while others provide with qualitative predictions. The first order models have high predictive power.

Taking into account that the difference between the first order models and empirical ones is not considerable, there are white-box, grey-box and black-box models. White-box models are deductive, and include necessary information to describe biochemical reactions in the AD process, contrasting with black-box models which inductively join the input with output excluding any prior knowledge about the process. In grey-box models some approximation and simplification of the AD process are needed where the parameters have a physical interpretation and are calculated by estimation procedure. The most dynamic models have a grey-box structure (Lauwers et al., 2013).

The mathematical formulation results in a mathematical model that can be used for quantitative analysis under certain conditions. There are some examples of non-dynamic white-box models based on stoichiometry and applied only for calculating biogas production (models of Amon et al., 2007a; Amon et al., 2007b; Boyle, 1976; Buswell and Müller, 1952). They are time independent models and based on data for basic elements or components of organic substrates. Such models are helpful for estimation of values CH_4 and CO_2 (Gerber, 2008). The examples of the stoichiometric models are shown in Table 2-1.

Table 2-1: Models for calculation of methane production

Structure	Application	Potentials	Limitations	Reference
$C_aH_bO_c + (a - -\frac{b}{4} - \frac{c}{2}) H_2O \rightarrow (\frac{a}{2} - \frac{b}{8} + \frac{c}{4}) CH_4 + (\frac{a}{2} - \frac{b}{8} - \frac{c}{4}) CO_2$	- Estimation of CH_4 and CO_2 yields	In the case of the absence of sufficient data from the laboratory AD experiments can provide valuable information during the feedstock change.	- The chemical composition has to be known - Synthesis of biomass and energy for growth is not included - Substrates are considered as a part of a complex mixture but only as an individual unit - Calculated CH_4 is always higher than what can be obtained in the AD process	Buswell and Müller, 1952
$C_aH_bO_cN_dS_e + (a - \frac{b}{4} - \frac{c}{2} + \frac{3 \cdot d}{4} + \frac{e}{2}) H_2O \rightarrow (\frac{a}{2} + \frac{b}{8} - \frac{c}{4} - \frac{3 \cdot d}{8} - \frac{e}{4}) CH_4 + (\frac{a}{2} - \frac{b}{8} + \frac{c}{4} + \frac{3 \cdot d}{8} + \frac{e}{4}) CO_2 + d\ NH_3 + e\ H_2S$	- Estimation of CH_4 and CO_2, ammonia and hydrogen sulfur fractions - Estimation of the theoretical maximum CH_4 production with an assumption of complete organic substrate ($C_cH_hO_oN_nS_s$) breakdown			Boyle, 1976
MEV [l_N CH_4 kg^{-1} VS] = x1 · XP [%DM] + x2 · XL [%DM] + x3 · XF [%DM] + x4 · XX [%DM]	- Estimation of the yield of methane from the nutrient composition of energy crops in mono fermentation - Estimation of the nutrient requirement of bacteria - Estimation of the produced power of agricultural biogas plants - Estimation of the CH_4 yield per hectare of energy crops	MEV considers the influence of nutrient composition on the production of CH_4	MEV model cannot predict the methane yield in an absolutely reliable way	Amon et al., 2007

MEV - methane energy value model
XP - crude protein
XL - crude fat
XF - crude fibre
XX - N-free extracts
a, b, c, d and e - the molar fraction of elements C, H, O, N and S in the organic fraction of substrate

2.2 Growth of biomass

The performance of the growth of microorganisms, degradation of substrate, and formation of products can be described by kinetic modeling. Biological kinetics for many models are based on the elementary microbial growth and rates of the substrate consumption which is strongly dependent on the specific growth rate, which is limited by availability of nutrients (substrate concentration S in g l^{-1}) and other ambient conditions such as inhibitors (inhibitor concentration I in g l^{-1}), the *pH* value or temperature T.

Microbial fermentation is conversion of the substrate to biogas by microbes with following generation of new cells. The kinetics can be divided into four phases: lag-phase, log-phase, steady-state phase and death phase (Figure 2-1).

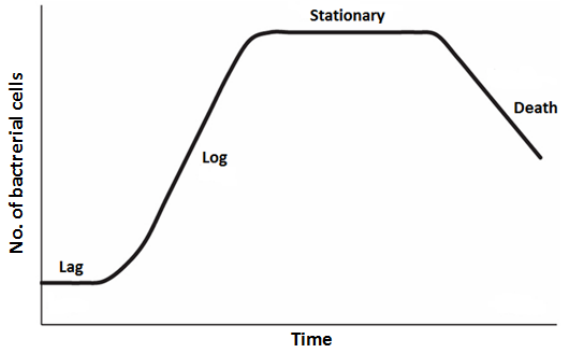

Figure 2-1: Microbial growth curve in a closed system

The lag - phase is an adaptation phase when bacteria become in contact to the organic matter and start to convert. It depends on the bacterial age and medium. When bacteria are already familiar with the substrate there is no need for the adaptation phase. During the exponential growth the bacteria reproduce themselves exponentially and this phase, basically, depends on the microbial population, substrate composition and process parameters. At some point the bacterial growth becomes limited because of the depletion of one or several substrates. As depletion continues growth may be equal to bacterial death which represents the stationary phase of the growth curve. Finally, the amount of dying cells exceeds that of the growth of the active population and additionally accumulation of inhibiting compounds, lack of food or cell lyses lead to the ending phase of the microbial growth.

2.3 Models for bacterial growth

In 1913 Michaelis and Menten published the model that describes the mechanism and kinetics of enzymatic catalysis. The mechanism begins with formation of an enzyme substrate complex ($E \cdot S$), proceeds with reaction of the complex to generate a product (P) and release the enzyme (E) (Equation 2.2):

$$E + S \underset{k_{-1}}{\overset{k_1}{\leftrightarrow}} E \cdot S \overset{k_2}{\rightarrow} E + P \tag{2.2}$$

Assuming that the concentration of the enzyme substrate complex C_{ES} is constant (Equation 2.3):

$$C_{ES} = \frac{k_1 \cdot C_{Et} \cdot C_s}{k_{-1} + k_2 + k_1 \cdot C_S} \tag{2.3}$$

where C_{Et} is the sum of free enzyme , C_{ES} is the substrate-enzyme complex, k_1, k_{-1}, k_2, and k_3 are the reaction constants for the corresponding reactions. The Michaelis –Menten constant is estimated as follows (Equation 2.4):

$$K_M = \frac{k_{-1}+k_2}{k_1} \tag{2.4}$$

The rate of the product generation equals to (Equation 2.5):

$$v = k_2 \cdot C_{ES} \tag{2.5}$$

Hence the velocity of the reaction is (Equation 2.6):

$$v = \frac{v_{max} \cdot S}{K_M + S} \tag{2.6}$$

The relationship demonstrates that the velocity of the reaction depends on the substrate concentration (Modhoo, 2012). Such relation can be applied for the bacterial growth as well (Chang, 2010). Based on the non-linear relation between specific growth rate and substrate concentration Monod formulated for microorganism growth (Monod, 1942) (Equation 2.7):

$$\frac{dX}{dt} = \mu = \mu_{max} \cdot \frac{S}{K_s + S} \cdot X \tag{2.7}$$

where X is concentration of bacteria degrading the substrate, μ is the specific growth rate, μ_{max} is the maximum specific growth rate, d^{-1}, K_s is the half-saturation constant equal to the concentration of substrate giving growth rate of μ_{max}, g L^{-1}, S is the concentration of growth-limiting substrate g L^{-1}. The specific growth rate increases strongly for low substrate concentration and slowly for high substrate concentration, until the saturation of growth rate is reached (Figure 2-2).

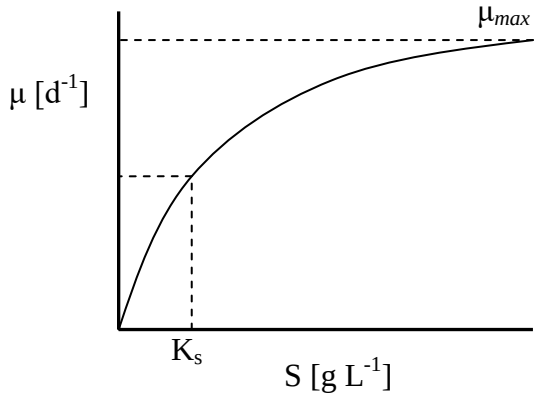

Figure 2-2: Specific growth rate depending on substrate concentration according to Monod kinetics

The substrate limits the specific growth rate due to its concentration. K_s (bacterial affinity to S) is always greater 0, therefore, $\frac{S}{S+K_S}$ is always less than 1 and the specific growth rate is less than μ_{max}. The accuracy of the Monod-model for homogenous cultures and simple substrates is very high, but not for heterogeneous cultures or complex substrates (Gerber, 2008). Similarly, the Monod kinetic cannot be used to describe the degradation of municipal wastes as complex substrates. That is because of the Monod-model has been developed as a model for bacterial growth. Additionally, the lag – phase is neglected. For this reasons the model needs to be modified depending on the requirements and specificity of the process. Other models for growth rate are known as Contois, Tessier and Moser (Dochain and Vanrolleghem, 2001; Najafpour, 2015). Table 2-2 categorized mentioned models for bacterial growth. Thus, for modeling AD process the kinetics of bacterial growth, substrate degradation and product formation should be included.

Table 2-2: Unstructured rate models with dependence on a substrate or biomass concentration (Dochain and Vanrolleghem, 2001; Edwards, 1970; Najafpour, 2015)

Model	Equation	Description	Reference
Monod	$\mu = \mu_{max} \cdot \frac{S}{K_s+S}$	A simple model is usually used as a basis model	Monod, 1942
Contois	$\mu = \mu_{max} \cdot \frac{S}{\beta X+S}$	Saturation term is a function of biomass concentration	Najafpour, 2015
Tessier	$\mu = \mu_{max}\left[\exp\left(\frac{-S}{K_s}\right) - \exp\left(\frac{-S}{K_s}\right)\right]$	The growth rate is sensitive to a low concentration of a substrate	Edwards, 1970; Najafpour, 2015; Tessier, 1942
Moser	$\mu = \mu_{max} \cdot \frac{S^{\lambda}}{K_s+S^{\lambda}}$	The model with the strong dependence on a substrate concentration	Layokun et al., 1987; Najafpour, 2015; Moser, 1958

2.4 The first-order kinetics of proteins, carbohydrates and lipids hydrolysis

As previously mentioned in Section 1.3, the AD process includes four main steps. Normally, one step is much slower than the others and can be referred to as a rate-limiting step. The rate-determining step depends on the waste composition and its properties, loading rate, temperature and reactor configurations. Many biogas models consider hydrolysis of complex waste as a rate-limiting unit. The most conventional describing hydrolysis is the first-order reaction in terms of the degradable organic waste concentration (Equation 2.8):

$$\frac{dS}{dt} = -k_{hyd}S \tag{2.8}$$

where S is concentration of waste in VS, k_{hyd} is the first-order rate coefficient. The rate coefficient for different substrates can be obtained from literature. Table 2-3 summarizes values for k_{hyd} for carbohydrates, lipids and proteins. The range in values can be explained by different experimental conditions and variation of feed to inoculum ratio.

First-order kinetics is not directly coupled to bacterial growth and can be applied only when the rate-limitation is due to the particulate substrate surface (Vavilin et al., 2008).

Table 2-3: Literature overview of hydrolysis constant (Vavilin et al., 2008)

Substrate	k_{hyd} [s^{-1}]	Reference
Carbohydrates	$5.78 \cdot 10^{-6}$ - $2.31 \cdot 10^{-5}$ (at 35ºC)	Garcia-Heras, 2003
	$4.74 \cdot 10^{-7}$ - $1.5 \cdot 10^{-6}$	Gujer and Zehnder,1983
	$2.89 \cdot 10^{-6}$ vary within (100%)	Batstone et al.,2002
Lipids	$1.16 \cdot 10^{-6}$ – $8.1 \cdot 10^{-6}$ (at 35ºC)	Garcia-Heras, 2003
	$9.25 \cdot 10^{-7}$ - $4.63 \cdot 10^{-6}$	Gujer and Zehnder, 1983
	$1.16 \cdot 10^{-6}$ vary within (300%)	Batstone et al.,2002
	$5.78 \cdot 10^{-8}$ – $1.157 \cdot 10^{-7}$ (at 55 ºC)	Christ et al., 2000
	$8.8 \cdot 10^{-6}$	Shimizu et al., 1993
	$7.3 \cdot 10^{-6}$ (at 25 ºC)	Masse et al., 2002
Proteins	$2.9 \cdot 10^{-6}$ - $9.3 \cdot 10^{-6}$ (at 35ºC)	Garcia-Heras, 2003
	$2.31 \cdot 10^{-7}$ - $3.47 \cdot 10^{-7}$	Gujer and Zehnder, 1983
	$2.31 \cdot 10^{-6}$ vary within (100%)	Batstone et al., 2002
	$1.7 \cdot 10^{-7}$ – $8.7 \cdot 10^{-7}$ (at 55 ºC)	Christ et al., 2000
Gelatine	$3.12 \cdot 10^{-6}$ ± 0.13	Raposo et al., 2011
	$7.5 \cdot 10^{-6}$	Flotats et al., 2006

2.5 Effect of inhibition on bacterial growth

Microbial growth can be inhibited either by substrate or product. The substrate may inhibit its own digestion when it has a high concentration. The model of Haldane is frequently used to represent the substrate digestion including the effect of substrate inhibition. Hypothetically, the substrate (S) combines with the enzyme-substrate ($E \cdot S$) complex for the formation a more complicated complex which inhibits the substrate degradation itself. The elementary enzymatic reactions are declared as follows (Equations 2-9 - 2.11):

$$E + S \underset{k_{-1}}{\overset{k_1}{\leftrightarrow}} E \cdot S \tag{2.9}$$

$$E \cdot S + S \underset{k_{-2}}{\overset{k_2}{\leftrightarrow}} S \cdot E \cdot S \tag{2.10}$$

$$E + S \overset{k_3}{\rightarrow} S + E \tag{2.11}$$

where k_1, k_{-1}, k_2, k_{-2} and k_3 are the reaction constants for the corresponding elementary reactions. The Haldane kinetic formula was developed based on the elementary reactions of enzymes and expressed as follows (Equation 2.12):

$$\mu = \mu_{max} \cdot \frac{S}{(K_s+S)\cdot(1+\frac{S}{K_i})} = \mu_{max} \cdot \frac{S}{K_s+S} \cdot \frac{K_i}{K_i+S} \tag{2.12}$$

where μ is the specific growth rate, μ_{max} is the maximum specific growth rate, d^{-1}, K_s is the half-saturation constant equal to the concentration of substrate giving growth rate of μ_{max}, g L^{-1}, S is the concentration of growth-limiting substrate g L^{-1} and K_i is substrate inhibition coefficient g L^{-1} (Cheng, 2010).

2.6 Literature overview on biogas models

The number of biogas models is large and they possess essential differences in the number of parameters, input variables and overall complexity of their structure. The first attempts for modeling anaerobic digestion regarded to models describing the limiting step. The first dynamic mathematical model emerged in 1960's as an attempt to explain the complex behavior of anaerobic digesters (Graef and Andrews, 1974). In this model, degradation of acetate was assumed to be a rate-limiting step, and only the acetoclastic methanogens took a part into the anaerobic degradation. Volatile fatty acids are expressed as acetic acid. The methanogenic bacteria are assumed to be $C_5H_7NO_2$. The overall reaction is modeled as follows:

$$CH_3COOH + 0.032\ NH_3 \longrightarrow 0.032\ C_5H_7NO_2 + 0.92\ CO_2 + 0.92\ CH_4 + 0.096\ H_2O$$

This model was used for the investigation of the response of a reactor to hydraulic and organic overloading and the addition of an inhibitor. According to this model, a digester is expected to crash when fatty acids increase. Such an increase leads to a pH drop and the rise of the acetic acid concentration which in turn causes a drop in the methanogens growth rate and the washing out of methanogens. The model demonstrates that simple

inhibition patterns could create a complex behavior during digestion although the specific types of inhibition have not been fully clarified. There is no experimental verification of this model (Graef and Andrews, 1974, Lyberatos et al., 1999).

In the sequel we will focus on basic models for the substrate conversion. Such simple models that assume substrate inhibited Monod kinetics of the methanogens are listed in Table 2-4. Hill´s and Barth´s model (1977) considers the hydrolysis, acidogenesis and ammonia inhibition (Figure 2-3). Kleinstreuer´s and Powegha‘s model (1982) involves hydrolysis of biodegradable solids, acetogenesis and methanogenesis, and has a dependence on pH and temperature (Figure 2-4). Moletta’s model (1986) involves an acidogenesis step that forms acetate from glucose, and is inhibited by not dissociated acetic acid (Figure 2-5). Smith’s model (1988) in which slow and fast hydrolysis is assumed, and acidogenesis of the soluble intermediates and methanogenesis are also taken into account (Lyberatos et al., 1999) (Figure 2-6).

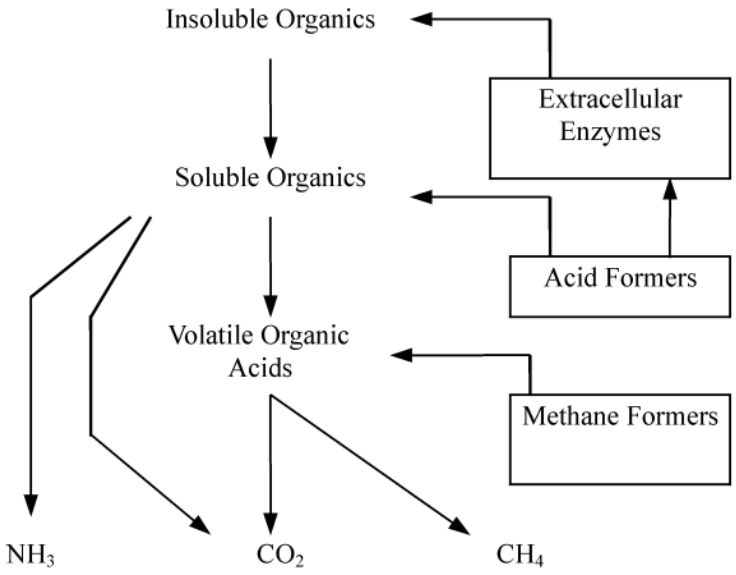

Figure 2-3: Schematic representation of the conversion of insoluble organics described by Hill´s and Barth´s model (Lyberatos et al., 1999)

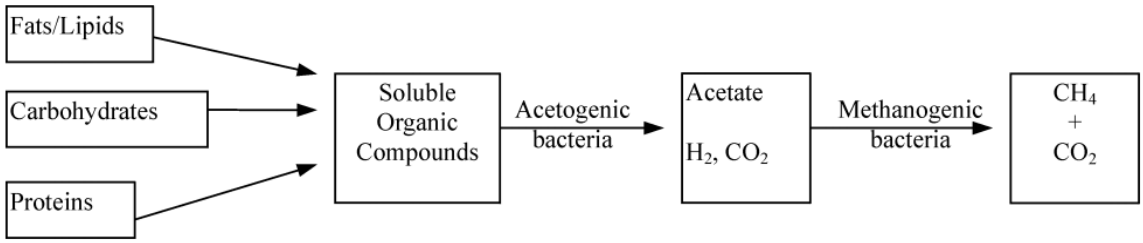

Figure 2-4: Scheme of the conversion of three types of substrates described by Kleinstreuer´s and Powegha‘s model (Lyberatos et al., 1999)

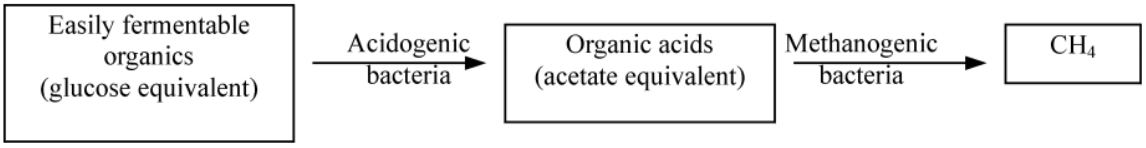

Figure 2-5: Scheme of the conversion of easily fermentable organics described by Moletta’s model (Lyberatos et al., 1999)

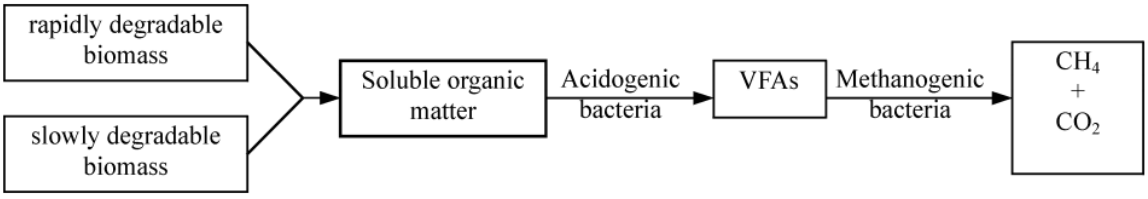

Figure 2-6: Scheme of the conversion of rapidly and slowly degradable organics described by Smith’s model (Lyberatos et al., 1999)

Other models are based on the mass and energy consumption, different growth and product formation or degradation kinetics (Bala et al, 1991; Vavilin et al., 2000; Zaher et al., 2003). Some other models are based on other mathematical methods and control theories, such as the fuzzy dynamic model, neural networks, and generic algorithms (Patzwahl et al., 2001; Ploit et al., 2002; Qdais et. al., 2010; Strik et al.; 2005; Wolf et al., 2009).

Table 2-4: Comparative characteristics of models that describe the organics conversion and assume substrate inhibited Monod kinetics (Lyberatos et al., 1999)

Model Name	Suitable for the following substrates	Inhibition	Output	Process type	Model application and potentials	Limitations
Graef and Andrews, 1974	particulate organics	VFA, external inhibitor	$C_5H_7NO_2$ (biomass), H_2O, CH_4, CO_2	steady-state, dynamic	- simulation of digester start-up phase - digester response to organic and hydraulic overloading - entry of an external inhibitor	- no experimental verification - one type of bacteria (methanogens)
Hill´s and Barth´s model, 1977	poultry waste	VFA, NH_3	biomass, CH_4, CO_2	dynamic	- prediction of digester failure by heavy organic loading and VFA accumulation	-
Kleinstreuer´s and Powegha‘s model, 1982	various substrates	Acetate, toxic substances	biomass, CH_4, CO_2	dynamic		-
Moletta’s model, 1986	easily fermentable substrates (glucose)	acetate	biomass, CH_4	batch	- prediction of digester failure by undissociated acetic acid	- limited substrate application - no hydrolysis phase
Smith’s model, 1988	biodegradable organic mater	VFA	biomass, CH_4, CO_2	dynamic	- prediction of digester failure by VFA accumulation - model assumes a fast and slow hydrolysis	-

The variety of the existing biogas models and their historical evolution shows that a high number of different models exist. Other detailed reviews can be recommended to find more information on this topic (Batstone, 2006; Gavala et al., 2003; Husain, 1998; Kythreotou et al., 2014; Lyberatos and Skiadas, 1999; Thorin et al., 2015; Tomei et al., 2009; Yu et al., 2013). Because of the fact that basics of the formulated biogas model in this study came from biogas models of Bernard (Bernard et al., 2001) and Blesgen (Blesgen and Hass, 2010), this literature review is aimed to focus on the most important features of these models and includes also ADM1 (Batstone et al., 2002) as the most used among AD models. Comparative information of three AD models is summed up in the Table 2-5.

2.7 Acidogenesis/Methanogenesis (AM2) model

In 2001 a dynamic two-step (acidogenesis-methanogenesis) mass-balance model, "Acidogenesis/Methanogenesis Model" (AM2) was developed jointly by researches of the INRA of Narbonne and the INRA of Sophia-Antipolis (Bernard et al., 2001). The AM2 model was inspired from the model of Graef and Andrews (1974), but after modification the model structure became simpler and a second bacterial population, acidogenic bacteria, was introduced. The AM2 model is based on the experimental material obtained on the fixed bed reactor of the INRA of Narbonne. It was assumed that lipids, carbohydrates, and proteins have similar hydrolysis and consumption rates, which can be considered as a realistic assumption as long as sufficient nutrients and other substrates are present. Hydrolysis and subsequent uptake of substrates are proposed as single steps that can be acceptable as long as the kinetic constants are adjusted to account for both processes. The acidogenesis of the influent substrate is modeled using Monod kinetics. In the first step the acidogenic bacteria (X_1) consume the organic substrate (S_1) and produce CO_2 and VFA (Bernard et al., 2001).

Acidogenesis (with reaction rate $r_1 = \mu_1 \cdot X_1$):

$$S_1 \rightarrow X_1 + S_2 + CO_2$$

The AM2 model describes inhibitory effects of accumulated VFAs which result in a drop of the pH value. The methanogenesis of VFAs is modeled using Haldane kinetics (see Table 2-1). During methanogenesis bacteria (X_2) consume the VFA (S_2) as substrate for the growth and produce CO_2 and CH_4.

Table 2-5: Comparative overview for the AM2 model (Bernard et al., 2001), the ADSIM model (Blesgen and Hass, 2010) and ADM1 (Batstone et al., 2002)

Characteristics/ Reference	AM2	ADSIM	ADM1
Model type	dynamic	dynamic	dynamic, steady state
Structure	single model	four sub-model structure	single model
Adapted substrate	microalgae	gelatine, sucrose, rapeseed oil	various substrates
Growth kinetics	Monod, Haldane	Monod	Modified Monod
Process reactions	2	2	19
Parameters:			
- stoichiometric	6	12	17
- kinetic	7	8	38
- physico-chemical	6	15	≥ 8
State variables	6, COD based	10, COD based	24, COD based
Bacterial groups	2	2	6
Hydrolysis kinetics	none	none	First order
Inhibition functions	none	3	4
Type of inhibition	NH_3, VFAs	pH, temperature, VFAs	H_2, pH, NH_3, butyric acid
Products	CH_4, CO_2, biomass	CH_4, CO_2, biomass, heat	CH_4, CO_2

Methanogenesis (with reaction rate $r_2 = \mu_2 \cdot X_2$):

$$S_2 \rightarrow X_2 + CO_2 + CH_4$$

The biogas production rate is proportional to the growth rate of methanogens. In addition, the AM2 model represents the gas release mechanism by acid base equilibrium as well as gas solubility in a pH dependent speciation. Based on the model an adaptive controller and a fuzzy controller were implemented to maintain the alkalinity, maintain stable process conditions and avoid VFAs accumulation in the case of organic load overcharge (Bernard et al., 2001). Besides, the AM2 model was used for design and simulation. In 2005 Méndez-Acosta et al. have designed a model-based controller for maintaining the COD of the reactor effluent at its set point, using the AM2 model (Méndez-Acosta et al., 2005). In 2015 Vargas and Moreno have developed a simple feedback controller that maximizes the biogas production rate using the AM2 model (Vargas and Moreno, 2015).

2.8 Anaerobic digestion simulator (ADSIM) model

In 2009, the biogas model of Bernard was chosen and adjusted to the requirements of a real-time interactive training simulator which can be used for design and testing of the process control strategies, industrial and academic education (Blesgen, 2009). The model was named as the anaerobic digestion simulator model. The AD process was modeled with regard to biological, biochemical, physicochemical, and reactor sub-models. The biological sub-model is based on the AM2 model and the basic structure is shown in Figure 2-7 (Blesgen and Hass, 2010).

Complex organic matter which consists of carbohydrates, proteins, and lipids is degraded by acidogens (X_{aci}) to produce VFAs. Byproducts of this first reaction are carbon dioxide (CO_2 and total inorganic carbon: TIC) and new biomass. The VFAs are further degraded by methanogens (X_{meth}) into methane, carbon dioxide, and new biomass. Both reactions consume water and produce some heat of reaction (Blesgen and Hass, 2010). The model code includes 13 single differential equations for calculating biomass, substrate and final product concentration. The acidogenesis of the influent substrate and the methanogenesis of VFAs are modeled using Monod kinetics. In addition, the model describes inhibition of the biological process by temperature, pH and VFAs concentration.

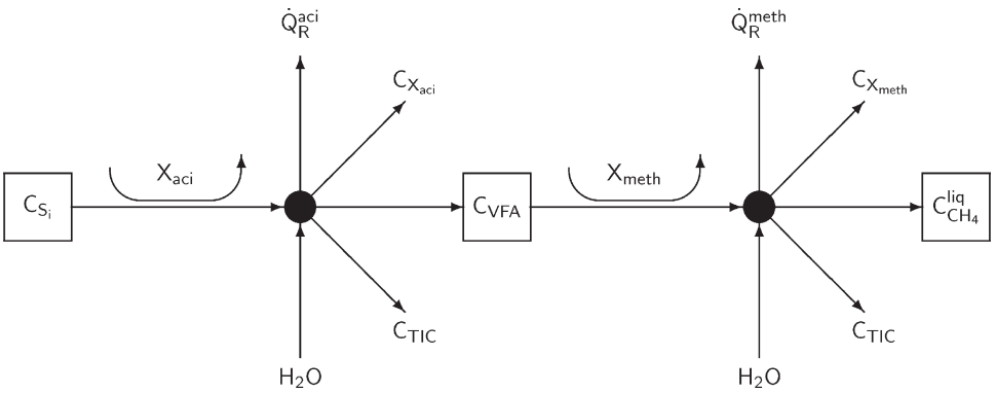

Figure 2-7: Structure of the biological sub-model: CSi, concentrations of substrates; CXaci, concentration of acidogenic bacteria; CXmeth, concentration of methanogenic bacteria; CVFA, concentration of volatile fatty acids; $\dot{Q}_R^{aci}$ and $\dot{Q}_R^{meth}$, heat of reaction produced by acidogenic and methanogenic bacteria, respectively; CTIC, concentration of inorganic carbon (CO2(aq) + HCO3- + CO32-); CCH4liq, concentration of methane in the liquid phase (Blesgen and Hass, 2010)

The pH value is influenced by substrates contents (e.g. proteins), VFAs and influent acid and alkali flows. The fractionation of total inorganic carbon is also included and presented by HCO_3^-, CO_3^{2-} and CO_2. Partial pressures of CO_2 and CH_4 in the liquid phase and transfer of the gases from the liquid phase into the headspace are included as well (Blesgen and Hass, 2010).

2.9 Anaerobic Digestion Model No.1 (ADM1)

Another widely used and complex kinetic model is the Anaerobic Digestion Model No.1 (ADM1) which is a result of international collaboration among experts from multiple disciplines (Figure 2-8). Conventional process variables like organic acids and NH_4 concentrations, the pH value, and gas flow rates were also used as model outputs. The ADM1 model offers the description of the AD process through different fermentation. These phases include disintegration, hydrolysis, acidogenesis, acetogenesis and methanogenesis. The physicochemical part is presented by liquid-gas transfer and liquid-liquid process (ion association and dissociation). The ADM1 model simulates degradation of complex solids into proteins, fats, carbohydrates, and inert compounds. These degradation products are then hydrolyzed to amino acids (AA), long-chain fatty acids (LCFA), and sugars (MS), respectively.

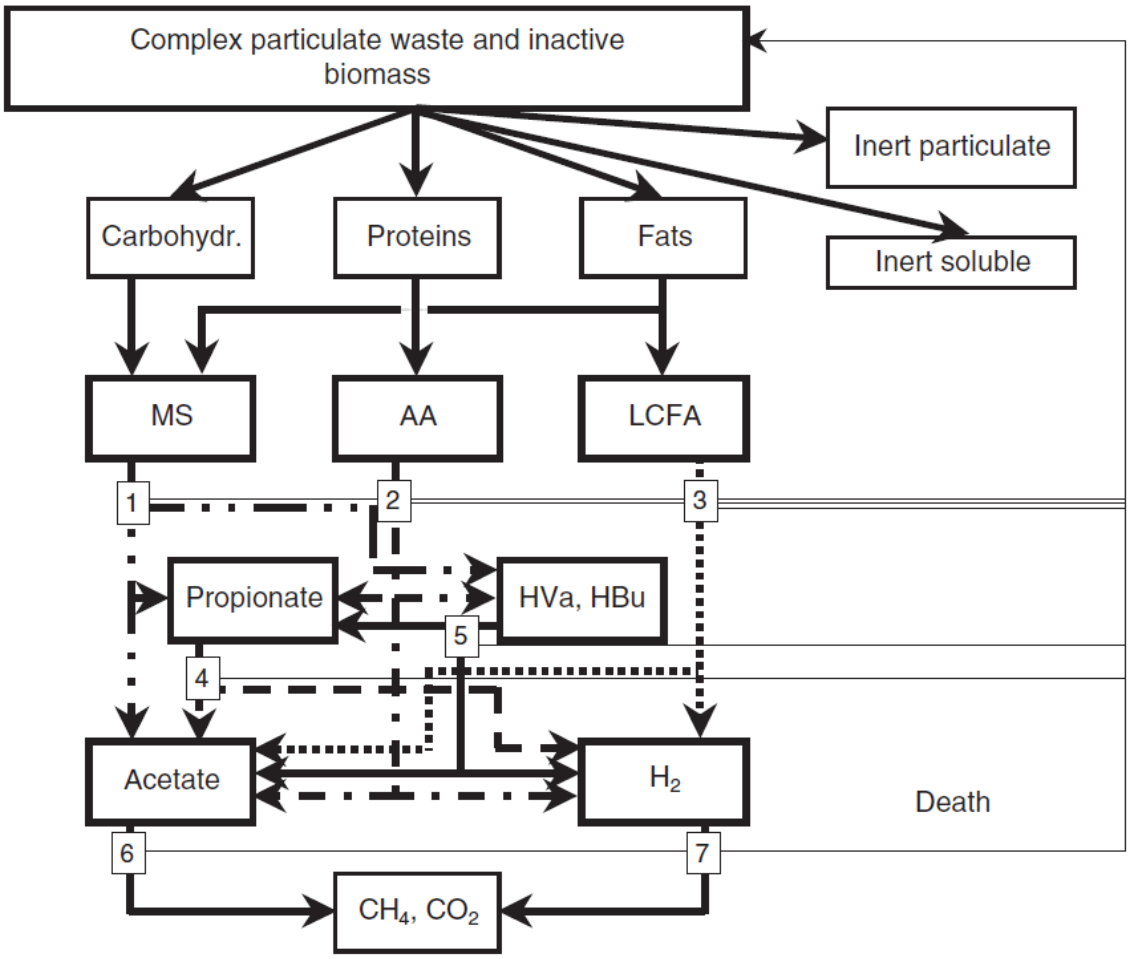

Figure 2-8: The main pathways for ADM1 model: (1) acidogenesis from sugars, (2) acidogenesis from amino acids, (3) acetogenesis from LCFA, (4) acetogenesis from propionate, (5) acetogenesis from butyrate and valerate, (6) aceticlastic methanogenesis, and (7) hydrogenotrophic methanogenesis; MS - monosaccharides, AA -amino acids, LCFA -long-chain fatty acids (Batstone et al., 2002)

Volatile fatty acids (acetate, propionate, valerate and butyrate) and H_2 can then be generated via the acidogenic fermentation of proteins and carbohydrates. Methane is produced by both aceticlastic methanogenic cleavage of acetate and hydrogenotrophic methanogenic reduction of CO_2 by H_2. Extra-cellular biochemical reactions are based on the first - order rate law kinetics, and intra-cellular biochemical reactions are described by Monod-type kinetics. Substrate uptake reaction rates are proportional to the biomass growth rate and biomass concentration (Batstone et al., 2002). One of two empirical functions expresses inhibition by pH for all types of bacteria. Non- competitive functions calculate H_2 and free NH_4 inhibition for acetogenic and aceticlastic methanogenic

microorganisms, respectively. Physicochemical reactions are independent of bacteria. Gas-liquid transfer and ion association/dissociation are fast comparing to biochemical process. Therefore, they can be assumed to be in equilibrium and expressed by algebraic equations instead of ODE.

Since development of the ADM1 model in 2002 and up to now it has been widely tested and applied. For example, it was used in theoretical analysis of new implemented parameters, extensions and modifications (Batstone and Keller, 2003; Nopems et al., 2009; Wolfsberger and Holubar, 2006) and for monitoring and simulation of the AD process of various organic wastes: sludge from waste water treatment plants (Kerroum et al., 2010), olive pulp (Kahlfas et al., 2006), grass silage (Koch et al., 2010), sewage sludge (Shang et al., 2005; Mendes et al., 2015).

The ADM1 is well studied for its limitations as well. In the ADM1 model, 32 dynamic concentration variables are used, which increase the effort of parameter identification and manipulation and validation. The numerical solution of the numerous differential equations is a sophisticated and time-consuming process. Moreover, the model assumes a constant-volume, completely-mixed system which is difficult to achieve in any digester. Another weakness lies in inaccuracies in the stoichiometry (Kleerebezem and van Loosdrecht, 2006).

MOTIVATION and SCOPE

3.1 Problem Statement

Due to the rapidly growing interest in anaerobic digestion processes, the development and improvement of anaerobic digestion process and optimization techniques are intensively examined. From literature overview it is known that anaerobic digestion has to deal with a huge variety of organic waste (see Section 1.5). In operating plants the process stability and velocity are influenced by the chemical composition of the organic waste and the full supply of the microbial community with essential elements (see Sections 1.5.1 and 1.5.5). Process disturbances can be caused by ranging the feedstock quantity and quality on daily basis due to addition of different substrate types in different amounts which depends on the feedstock supplier. Obviously, it affects bacterial growth, and therefore, the biogas composition and methane yield. As it was described in Sections 1.3, 1.5.3 and 1.5.7, the hydrolysis and final content of CH_4 in biogas is depended on the type of the substrate, accumulation of intermediate products and presence or generation of inhibitors. Literature sources (Figure 1.4) and online calculators can provide biogas plant owners with biogas rate, methane yields and electricity production, but not with the information how new substrates influence the adaptation of the AD process in long-term and which combination of available substrates results in stable AD and efficient performance. Therefore, there is a need in a simple approach to map huge variety of organic waste and foresee the effect of the newly introduced organics on the AD process and final methane yield.

Currently, there are two common approaches for the biogas production process study and optimization. The first one is to use lab-scale digesters equipped with extensive laboratory and online- measurements for testing new optimization strategies, for example, optimizing various operation parameters: temperature, retention time, pH, satisfying the nutritional requirements of microbes, and manipulating the feed proportions of substrates. However, not every biogas plant can be provided with advanced equipment for process monitoring or laboratory facilities. Dynamic simulation models can be considered as a

promising alternative to waste timing and financially unprofitable techniques (Wolf et al., 2009). As it was shown in earlier studies (see Section 2.3), models with focus on the substrate conversion were successfully used for studies of anaerobic digestion for various types of organics. In principle, their structures have a lot in common but with varying level of complexity and amount of unknowns (AM2, ADSIM and ADM1) (see Sections 2.7 – 2.9). Some of them were tested only for certain types of organics, e. g. the AM2 model was validated by experimental data of the AD of microalgae, the ADSIM model – by experimental data of the AD of gelatine, sucrose, rapeseed oil and ADM1 was validated by experimental data of the AD with various types of waste. In this study we decided to combine features of already existing models to prove the proposed hypothesis of the substrate linearity.

3.2 The substrate linearity hypothesis

Accordingly to this hypothesis, proteins (gelatine), carbohydrates (sucrose) and lipids (rapeseed oil) as basic master biomass can be used to mimic the properties of any organic substrate as a linear combination of different biomass (e.g. domestic and industrial wastes, silage, leftovers, manure, agricultural residues and food industry waste).

3.3 Goal of the study

The present study was aimed to formulate a relatively simple dynamic model on the basis of the AM2 and the ADSIM models (see Section 2.3). The biogas model allows the description of anaerobic fermentation in a quantitative and qualitative way for the digestion of three main components: proteins, carbohydrates and lipids.

3.4 Objectives of the study

This study has four objectives:

1. *Development and verification of the model*

The model consists of three steps of anaerobic digestion: hydrolysis, acidogenesis, and methanogenesis. A complex substrate is converted to methane and carbon dioxide as final products of the AD process. VFAs and LCFA have an inhibition effect on acidogenic and methanogenic bacteria. The growth of bacteria, substrate digestion and the product

generation depend on the concentration and chemical composition of the digested substrate and VFAs. The fundamental characteristics of the proposed model are accuracy of the prediction, simplicity in parameterization and explanation of the discovered phenomenon. The model has to be able to simulate the AD process of different organic waste in batch and continuous mode. The developed model is calibrated using the experimental data obtained in batch experiments for each substrate: gelatine, sucrose and rapeseed oil.

2. *Validation of the model*

For the validation of the calibrated model the data set of the batch experiment with a mixture of three easy degradable substrates is used: gelatine, sucrose and rapeseed oil. The model has to predict the volume of biogas and methane, the volumetric concentration of CH_4 and CO_2, the biogas flow rate and COD_{Tot}.

3. *Cross-validation of the model*

For the independent validation of the calibrated model the data set of continuous experiments with potato waste water and starch is used. The model is supposed to foresee the dynamics of the volumetric concentration of CH_4 and CO_2. The model has to predict the changes of the methane concentration according to the changes of the waste input.

4. *Simulations of the substrates dynamics for a big-scale biogas plant with a tanks cascade system*

The model structure has to be adapted to the tanks cascade system, scaled-up and simulate the dynamics of the waste composition and, consequently, changes in the volumetric concentration of CH_4 in continuous mode.

3.5 Expectation of scientific outcome of the study

1. Proof of the substrate linearity hypothesis by applying the parameterized model for the forecasting of the AD for different types of organic wastes.

2. Application of the parameterized model for batch and continuous biogas process as well as for laboratory-scale reactors and industrial scale biogas fermenter.

3. Study of the influence of the proportion of master substrates in organic waste and their quantity on the final product and stability of the AD in long-term dynamics.

MATERIALS and METHODS

4.1 Batch setup

4.1.1 Inoculum and substrates characteristics for batch experiments

The inoculum was a seeding sludge blend originating from a wastewater treatment plant (Farge, Bremen, Germany), a pig and cattle manure digestion plant (Ritterhude, Lower Saxony, Germany) and sludge from corn and silage digesting plant (Osterholz-Scharmbeck, Lower Saxony, Germany). In order to reduce the endogenous methane production by inoculum, the sludge was pre-incubated at 38±0.2°C during one week prior to feeding. HRT for each batch trial was equaled 28 days (German Engineers Association, 2006).

Three different substrates, sucrose (Nordzucker AG), gelatine (Backfee) and rapeseed oil (EUCO GmbH), were digested in batch mono-digestions and finally in a random mixture of three. The input concentration of substrates was defined according VDI 4630 (German Engineers Association, 2006), with exception of the ratio oTS substrate/oTS sludge which was doubled and equaled to 1. The final $VS_{Inoculum}$ had to be in a range between 1.5 and 2 % (by weight) and the ratio of oTS to TS has to be more than 50% (German Engineers Association, 2006). The used concentration of substrates were: sucrose - 16.0 g L^{-1}, gelatine -15.8 g L^{-1}, rapeseed oil – 8.2 ml L^{-1}, and for the mixture the sucrose - 5 g L^{-1}, gelatine - 6 g L^{-1}, rapeseed oil -3 g L^{-1}, in total -14g L^{-1}. Table 4-1 summarizes the characteristics of the used substrates and inoculum.

4.1.2 Equipment for running batch anaerobic digestion

The batch tests were conducted in glass flasks at mesophilic conditions maintained at 38±0.2°C controlled by thermostat (Haake DC 30/K10). The tests were conducted in triplicates. The scheme of the batch setups are presented in Figure 4-1 and Figure 4-2. The digesters were manually mixed several times per day. Every digestion included the negative control - inoculum only. After filling with the substrate and inoculum in total of

Table 4-1: Characterization of Inoculum and substrates used

Inoculum/ Substrate/ Unit	COD_{Tot} [g L^{-1}]	Mass [g L^{-1}]	Mixture Mass [g L^{-1}]	TS to FM [%]	oTS to FM [%]	oTS/ TS [%]
Inoculum $_{Gelatine}$	25.600					
Inoculum $_{Rapeseed\ oil}$	25.586					
Inoculum $_{Sucrose}$	25.400					
Inoculum $_{Mixture}$	23.690					
Gelatine	11.440	15.8	6.0	2.44	1.61	66.73
Sucrose	15.316	16.0	5.0	2.73	1.65	61.69
Rapeseed oil	15.420	8.2	3.0	2.21	1.34	60.66
Mixture	14.466		14.0	2.44	1.64	60.31

1,0 L, the air was flushed out with 100% N_2 gas for 2 min at 2 bars. The discharge of biogas occurred through a port in the fermenter cap. The outlet tube was connected to a CO_2 capture unit (3M NaOH) when bio-methane recordings were needed. In the case of the biogas production recording, the sodium hydroxide unit was omitted. Generated methane and biogas passed through a condensate trap for vapor removal and was recorded in a gas volume sensor (gasUino). The gasUino device (Falk, 2011) is a gas volume counter based on the low-cost gas sensor developed by Liu et al. (Liu et al., 2003) where the recordings are adapted to standard conditions. A 75% NaCl solution (pH2) served as a sealing liquid for decreasing the gas solubility (Walker et al., 2009). Finally, the biogas is collected in a biogas bag.

The total methane and biogas volumes were deduced by subtracting the average blank sample respectively. The data acquisition (date, time, temperature, pressure and amount of clicks made by gas counter) was developed in Processing (Processing. org) and stored in a comma separated text file. LabVIEW VI automatically corrects the biogas and CH_4 volumes to standard conditions, reproduce it on the screen and saves the data in a MySQL database (Falk, 2011).

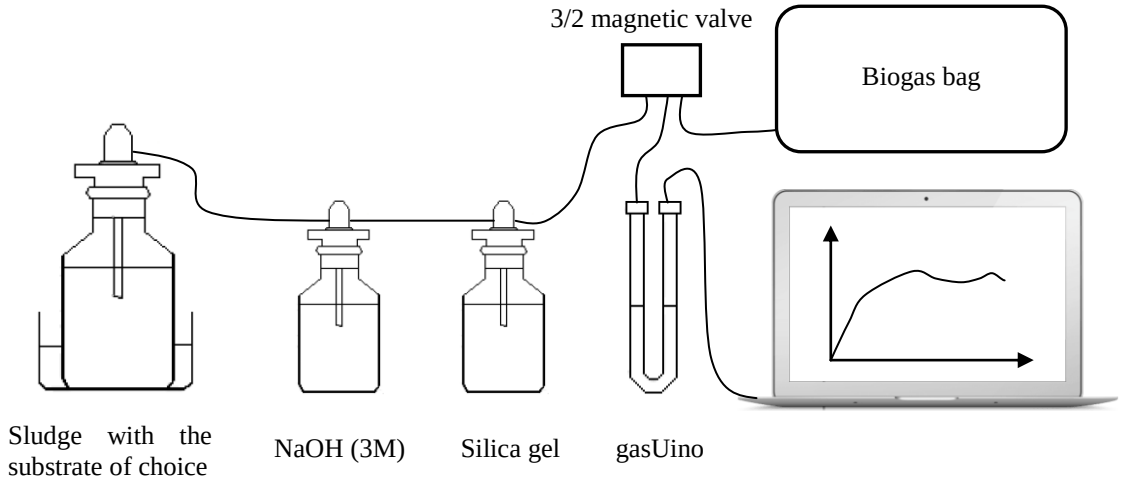

Figure 4-1: The sketch of the batch setup unit for the CH_4 volume production is shown. For the biogas production estimation one should neglect the NaOH solution. Blanks without substrate were maintained as control to measure biogas and methane production from the sludge

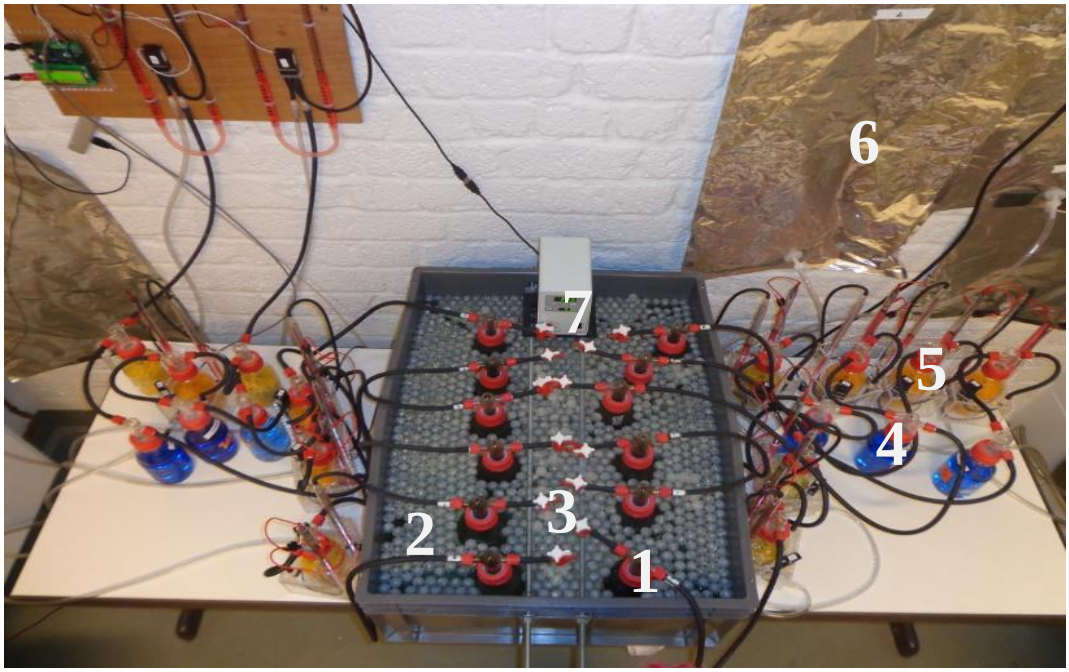

Figure 4-2: Picture of the batch setup including 12 units. There are digesters (1) immersed into the water bath (2), the valve for the sample (3), bottles with NaOH (4), condensate trap and gas counter - gasUino (5), biogas collecting bag (6), and thermostat (7)

4.1.3 Analytical methods

The following measurements were performed: Total solids (TS) and volatile solids (VS or oTS) were measured by drying and calcinating samples at 105°C and 550°C, respectively, for 24 h (P300, Nabertherm), and total COD (Hach-Lange, Germany) was determined of samples taken on daily basis. The pH was measured at beginning and end of the experiments.

4.2 Continuous setup

4.2.1 Inoculum and Substrates characteristics for continuous experiments

Two substrates were used in the research, starch (Roth, Germany) (COD = 12.6 g L^{-1}) and potato waste water (PWW) (COD = 24.7 g L^{-1}), as an example of an industrial waste substrate, and was provided by Emsland Group, Emlichheim, Germany (http://www.emsland-group.de/en/home). The used PWW was obtained during the very first stages (potato washing, grinding and pressing stages) of the starch production process. The chemical content of potato juice is shown in Table 4-2. Inoculum was taken from the operating biogas plant in Raiffeisen Agil, Oehmer Feld Leese, Germany. COD of inoculum equaled 60.2 gCOD L^{-1}.

Table 4-2: Biochemical content of potato waste water (Trojanowski et al., 2006)

Component	Amount
Total Carbon (%)	36.5
Total N (%)	6.01
Starch (%)	0.0
Protein (%)	37.3
Free amino acids (μM/g)	949.3
Ca (mg/g)	4.3
Mg (mg/g)	65.8
Fe (mg/g)	1.7
Cu (μg/g)	0.2
Mn (μg/g)	23.7
Zn (μg/g)	90.1

4.2.2 Equipment for running continuous anaerobic digestion

Here, the most important details of laboratory experiments in CSTR are described. More information on equipment description can be found from previous studies (Blesgen, 2009; Korjik, 2010). Experiments were carried out in 10 L laboratory - scale fermenter. The temperatures in the reactor and in the heating bath were controlled by temperature sensors and maintained at 38±0.2°C. The reactor content was mixed with a speed 70 rpm. Two pumps were adjusted for the effluent and influent flows. Both were controlled manually or automatically by the stirrer. The discharge of biogas occurred through a port in the reactor lid. A tube was connected with a condensate trap. Further, the biogas passed through a concentration measurement device, where the methane and carbon dioxide concentrations were measured by the Monogas Analyzer (Pronova, Berlin, Germany). Further the biogas flowed through the MilliGascounter (Dr. Ing. Ritter Apparatebau GmbH, Bochum, Germany), and finally, biogas was collected in a gas bag. The reactor lid had several ports for the pH electrode Ega 140/143 with an integrated temperature sensor (Sensor Technology Meinsberg, Germany), the redox potential electrode33 Emc. (Sensor Meinsberg, Germany), the openings for influent and effluent flows, the biogas outlet and a conductivity sensor LTC 1 / 24 (Sensor Meinsberg, Germany) which detects a possible foam formation and overflow of the reactor. The online signals were measured and recorded every 10^{th} sec by the process control system WinErs (Figure 5-7): pH (0..14), temperature within the reactor (0...100ºC),temperature within the heating bath (0...100ºC), redox potential (-1,000...+1,000mV), conductivity (overflow in the reactor or foam formation, 10 µS cm^{-1} – 20 µS cm^{-1}), CH_4 concentration (0...100 Vol.-%), CO_2 concentration (0...100 Vol.-%), volumetric gas flow (1...1,200 ml h^{-1}), speed 4...2,000 min^{-1}, level in the heating bath and substrate level. The piping and instrumentation diagram of the CSTR set-up, the screen shot of the virtual biogas reactor and the picture of the complete laboratory equipment are shown in the Figures 4-3 – 4-5.

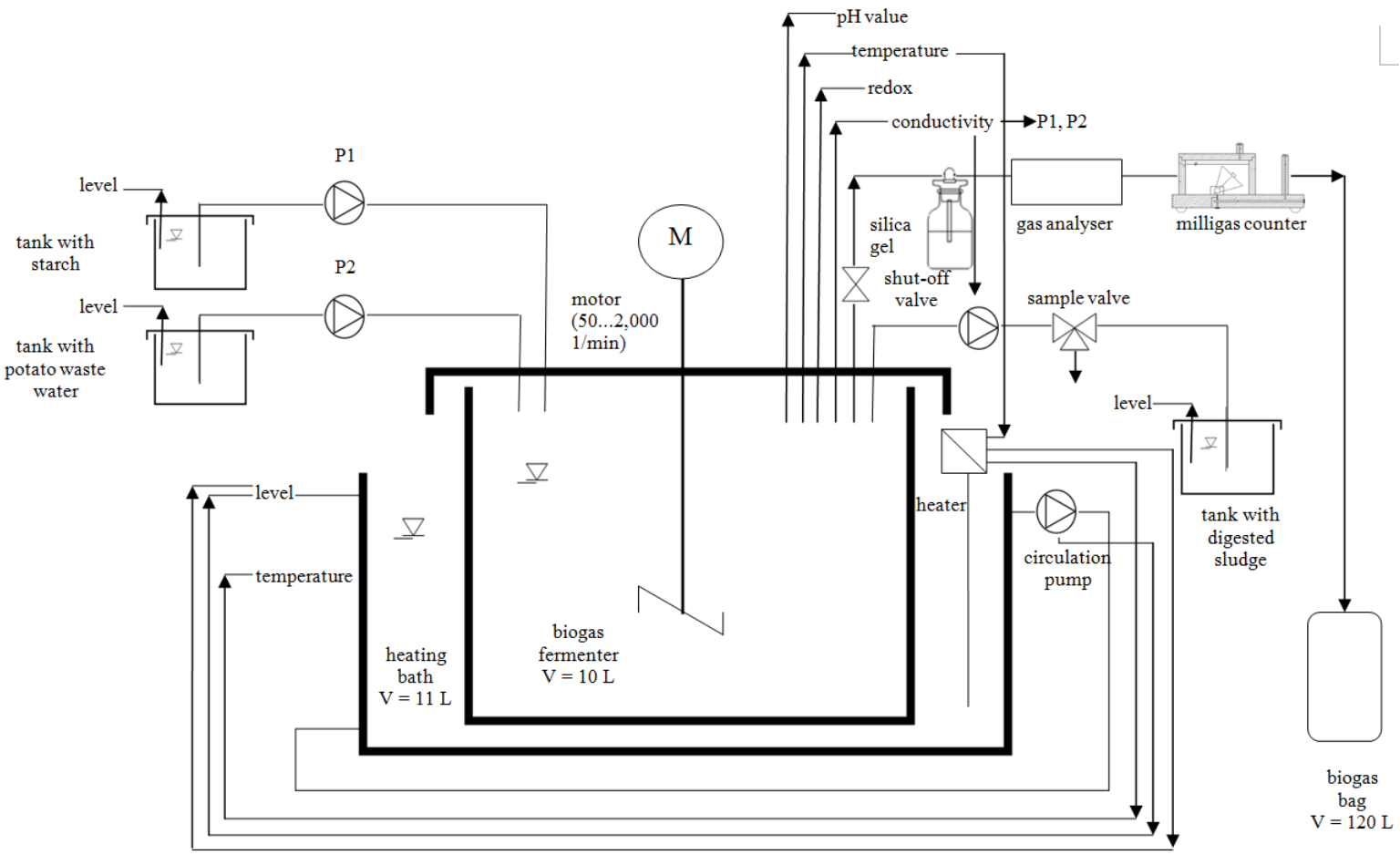

Figure 4-3: Piping and instrumentation diagram of the biogas generation from starch and PWW using CSTR set-up. P1 and P2 are inflow pumps. In the case of overloading, the sensor detects it and shuts down the pumping in, as well as it controls the effluent pump. The temperature sensor regulates the heater in the heating bath by turning it off or on depending on the temperature inside the reactor

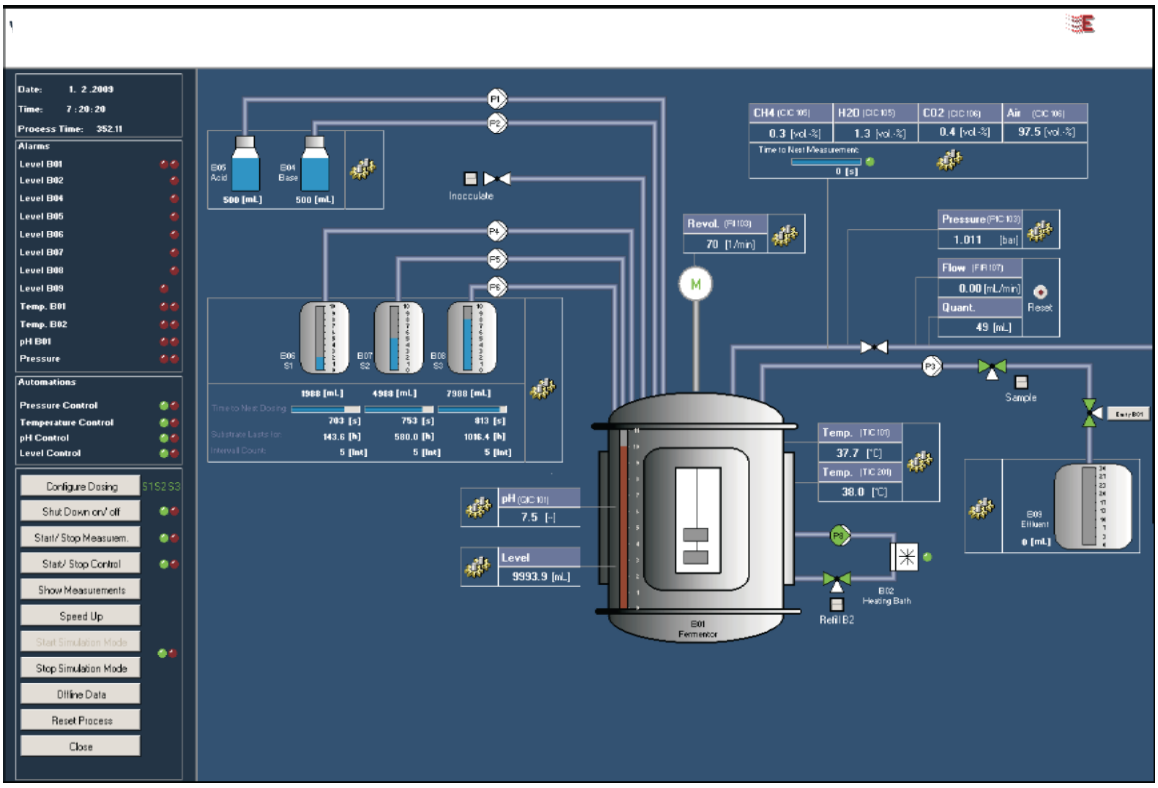

Figure 4-4: The screen shot of the virtual biogas reactor (Blesgen, 2009). The present scheme includes additional units which were neglected in the experiments like: the acid and base bottles and third bottle with the substrate. The simulator was served for the monitoring and data collection as well as for the performance of the biogas process production. By activating a certain buttons one could start inflow and effluent flows, adjust the interval dosing and a certain COD feeding per day, as well as temperature value inside the reactor and in the heating bath and the stirrer speed their maintenance can be kept in automatic mode. The decrease of the pH value, a drop of the water level in the heating bath, or organic substrate in the storage bottles, overfeeding in the reactor are immediately detected by the system by a special signal or blinking red buttons

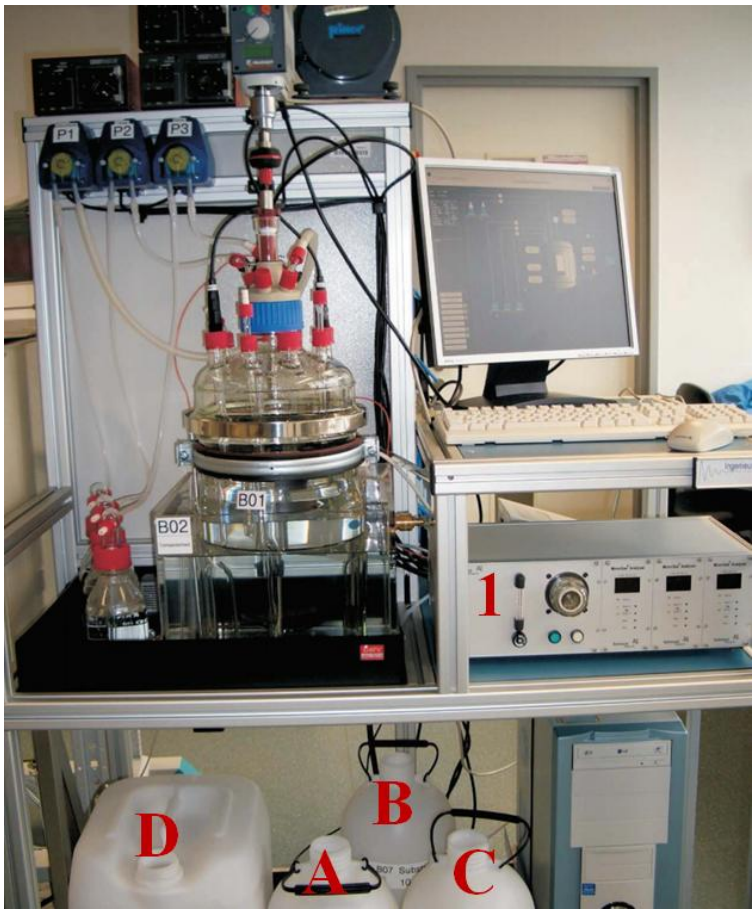

Figure 4-5: Picture of 10 L laboratory- scale fermenter. BO1- biogas fermenter, BO2 – the heating bath, P1-P3- pumps, biogas analyzer – 1, influent tanks A, B, C and effluent tank - D (Blesgen, 2009)

BIOGAS PROCESS MODEL

5.1 Procedure of biogas model development

The procedure of the model development usually includes several steps. General modeling procedure is shown on the Figure 5-1. In the very beginning the problem has to be specified, where the aim of the model should be defined, the future usage of the model (research, operation/control or for design), and the required degree of accuracy and complexity because there is no need for the complete match with reality. Mathematical and practical demands require simplicity and easy overview. In principle the level of complexity of a model can be increased by introducing additional details (Henze et al., 2008). The level of complexity must be balanced against the purpose and use of a model. With high complexity models offer high adaptation and allows for explanation of many details. On the other hand the calibration process becomes more difficult with increasing complexity due to longer runtimes and parameter interference. The next step in a model development is the derivation of the governing equations that should represent the process. The third step is preliminary verification, in which a first analysis of the model ability to be identified is tested, and the parameters ranges (in which interval does the model behave as predicted) are defined. The forth step is design of experiments and the estimation of parameters against the set of experimental data. The key of calibration implies the change of input parameters in an attempt to match field conditions in reality. After, it allows describing and understanding the system under study and simulating different scenarios with reasonable predictions. Additionally, the calibration procedure can be a very useful exercise to understand the sensitivity of the model to various influences. Finally, the calibrated model has to be validated by comparison with independent sets of experimental data in order to determine whether the model accurately predicts the behavior of the real process.

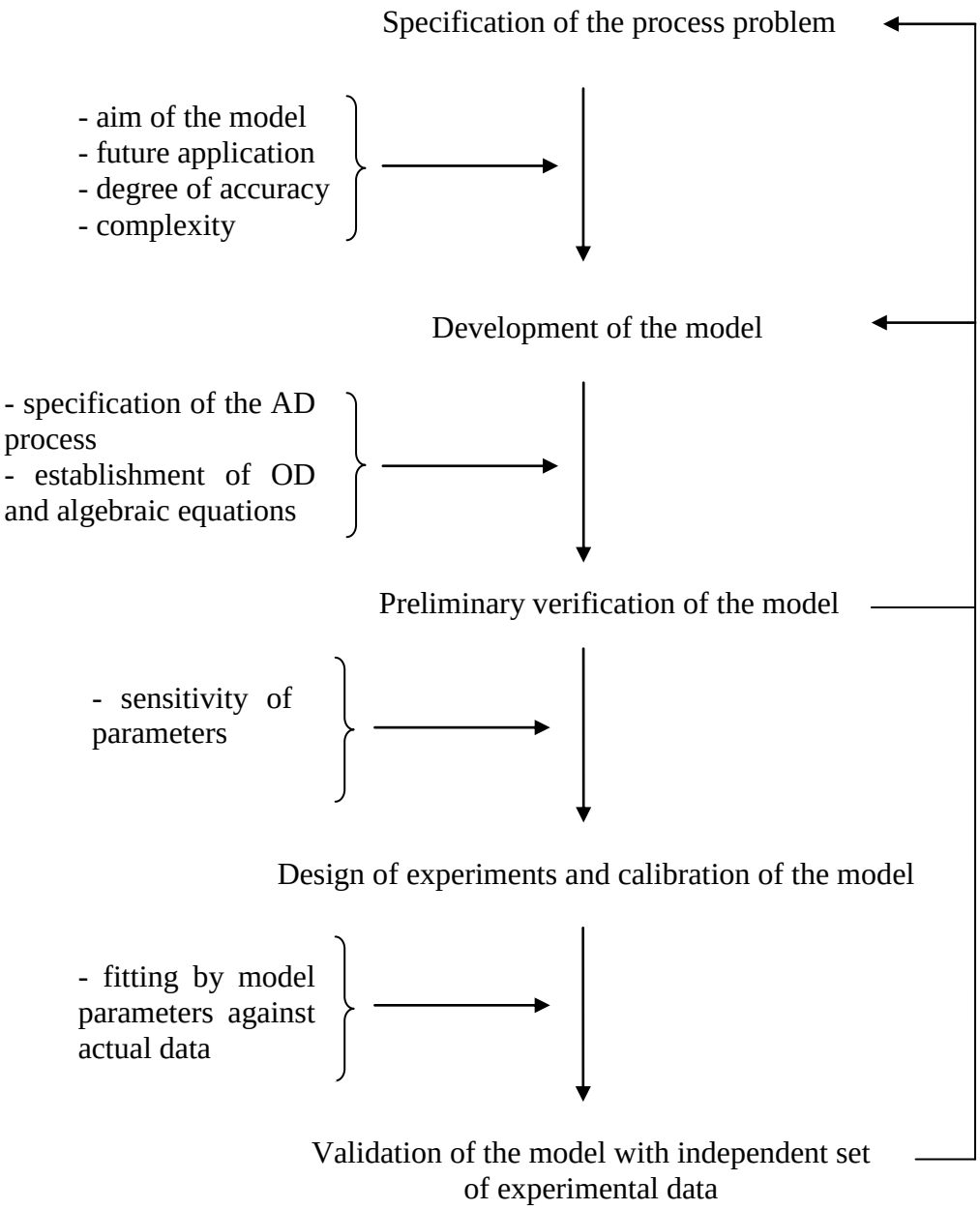

Figure 5-1: General scheme of the modeling procedure for anaerobic digestion (Sanders, 2001)

5.2 Structure of the biogas model

The AM2 model (Bernard et al., 2001) and the ADSIM model (Blesgen, 2009; Blesgen and Hass, 2010) were reformulated and simplified in order to reduce the amount of unknowns and assumptions. The developed process model for the AD process is based on closed mass balance, realized as differential equations, and specific reaction rates for each of the components, described by Monod kinetics. The system is assumed to be ideally mixed, meaning the absence of concentration gradients and it has a constant volume. The input variables are the influent feed rates ($\dot{q}_C^0, \dot{q}_P^0$ and $\dot{q}_L^0$), the initial concentrations of the components (C_p^0 , P_p^0 and L_p^0), the initial bacterial concentrations (X_{Aci}^0 and X_{Meth}^0) (Appendix 1). For the calculation of the concentrations change in the biogas fermenter, for each component the mass balance is estimated. The solution is manifold and depends on chosen initial values and the model parameterization. Microsoft Visual Studio 8.0 64-bits is used in this study as the tool to calculate numeric model solution. The code of the model is written in C++ (see Appendix 2). Model parameters, initial values, time variable and state variables are made available to the model as text files. The results of the calculation by solution of the set of differential equations are provided in text files as well. The dynamic state variables and model parameters are listed in Appendix 1. The simplified scheme of the biogas digester showing plant, state variables and control quantities is given by on Figure 5-2.

The programmed model is compiled to an executable (*.exe) with help of a Visual C+ + compiler. During execution the initial values of the differential equations, the user default of chosen solution algorithms and model parameter are imported and depending of the chosen solving algorithm (called adaptation of DASSL (Petzold, 1982)) the model is solved with static or dynamic step size. The executable program can be used for testing and verification of the described model. For the graphical representation of data Gnuplot was used which allows generating images of graphs from data files in a scripted environment.

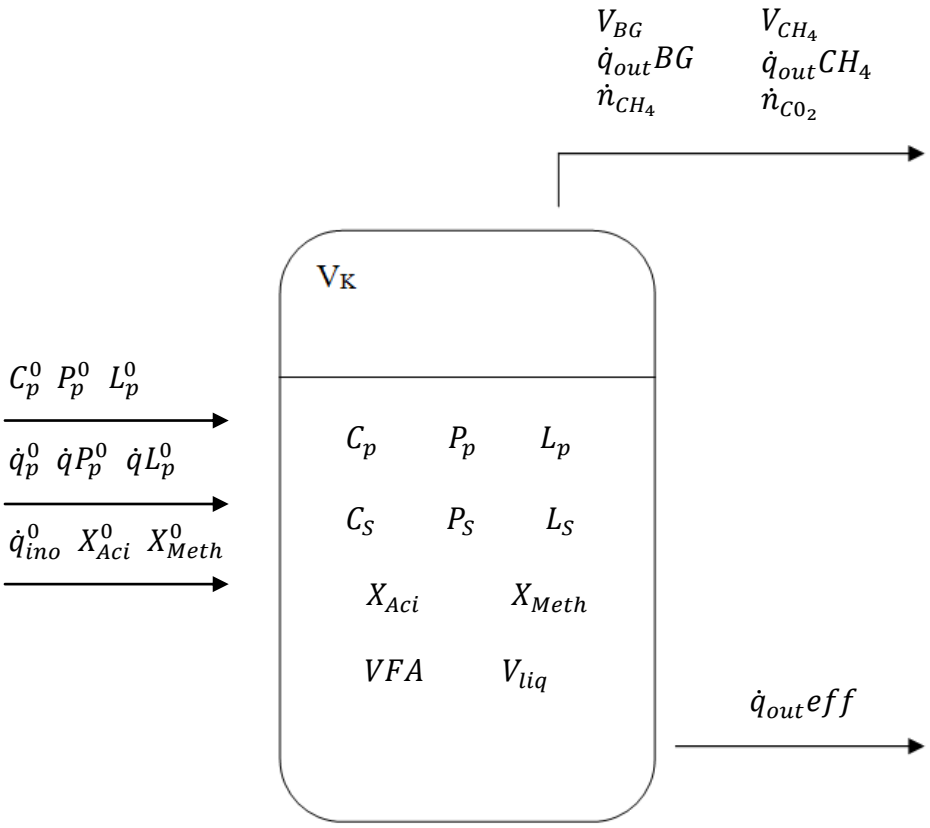

Figure 5-2: Schematic structure of biogas fermenter with the substrate components C_p^0 , P_p^0 and L_p^0 – initial concentrations of proteins, carbohydrates, lipids, respectively; C_p, P_p and L_p - concentrations of *primary* proteins, carbohydrates and lipids, respectively; C_S, P_S and L_S - simple accessible mono-/oligomers carbohydrates, proteins and lipids, respectively; $\dot{q}_C^0$, $\dot{q}_P^0$ and $\dot{q}_L^0$ – inflow rate of proteins, carbohydrates and lipids, respectively; $\dot{q}_{ino}^0$- inflow of inoculum into the digester; X_{Aci}^0 and X_{Meth}^0 – inflow of acidogenic and methanogenic bacteria; X_{aci} - acid forming bacteria and X_{meth}- methanogenic bacteria; *VFA*- volatile fatty acids; V_{liq} – volume in a digester; V_K – volume in the head space; V_{BG} – volume of biogas; V_{CH_4}- volume of methane; $\dot{q}_{out}BG$ and $\dot{q}_{out}CH_4$ - biogas and methane flow rates, respectively; $\dot{n}_{CH_4}$ and $\dot{n}_{CO_2}$ - molar flow rates of methane and carbon dioxide; $\dot{q}_{out}eff$ - effluent flow rate

5.3 Biogas process via mathematical overview

Hydrolysis is declared as one of the limiting step of anaerobic digestion. It is described by the 1st order reaction kinetics. The model describes the AD by three steps. After hydrolysis of particulate substrates (*Cp*, *Pp*, and *Lp*: *primary* carbohydrates, proteins and lipids, respectively) into accessible soluble substrates (C_S, P_S and L_S: carbohydrates, proteins and lipids, respectively), acidogenic bacteria (*Xaci*) cause the decay into CO_2 (total inorganic carbon: *TIC*) and volatile fatty acids (*VFA*). Finally, methanogenic bacteria (*Xmeth*) convert VFA (*VFA*) into methane (CH_4) and carbon dioxide (CO_2). The scheme of transformation of particulate substrates into CH_4 and CO_2 is shown in Figure 5-3.

5.4 Calculations

Bacterial growth rates

The biochemical reactions are associated to two bacterial populations (acidogenic and methanogenic bacteria). Bacterial growth rate is considered as proportional to substrate uptake. The growth rates [s^{-1}] for acidogenic bacteria (Equations 5.1 - 5.3) and methanogenic bacteria (Equation 5.4) are calculated using Monod-type kinetics. Inhibition by long chain fatty acids is described by Haldane kinetics (Equations 5.3 - 5.4).

$$r_{XP} = r_P^{max} \cdot X_{aci} \cdot \frac{P_S}{P_S + K_{P_S}} \tag{5.1}$$

$$r_{XC} = r_C^{max} \cdot X_{aci} \cdot \frac{C_S}{C_S + K_{C_S}} \tag{5.2}$$

$$r_{XL} = r_L^{max} \cdot X_{aci} \cdot \frac{Ip_{L_S}}{Ip_{L_S} + L_S} \cdot \frac{L_S}{L_S + K_{L_S}} \tag{5.3}$$

$$r_{VFA} = r_{VFA}^{max} \cdot X_{meth} \cdot \frac{Ip_{L_S}}{Ip_{L_S} + L_S} \cdot \frac{VFA}{VFA + K_{VFA}} \tag{5.4}$$

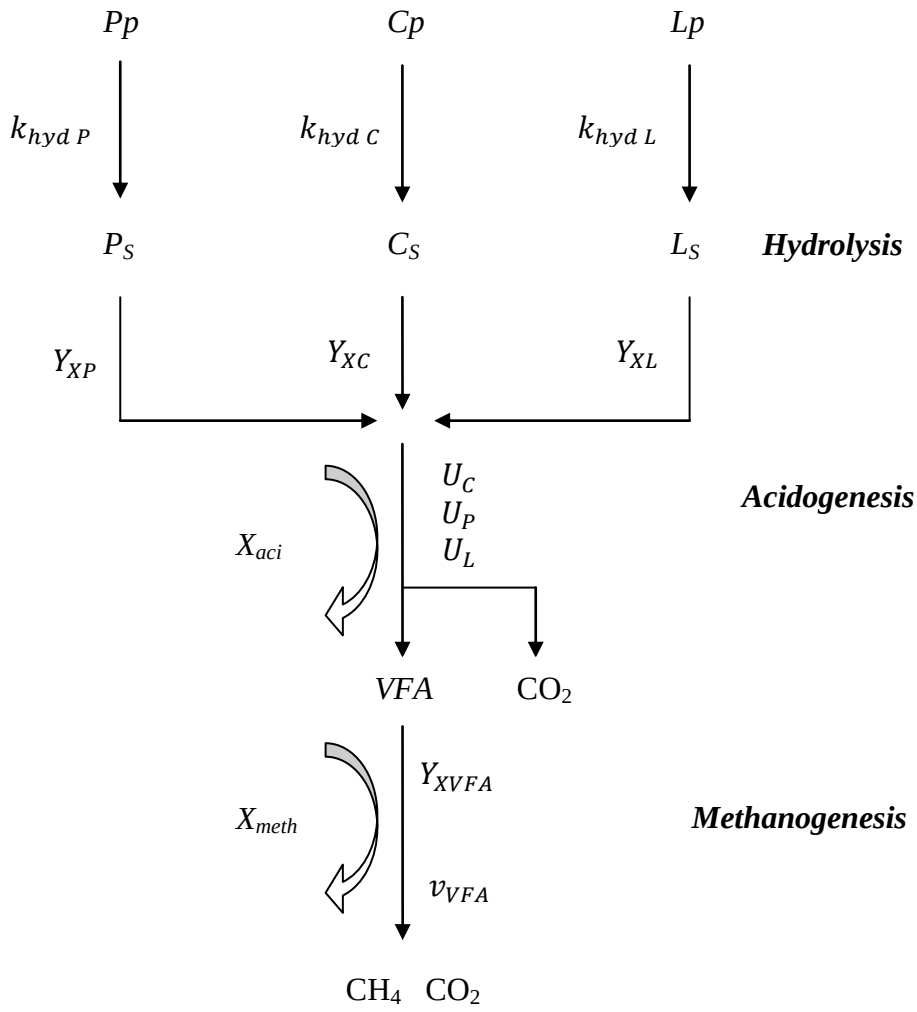

Figure 5-3: Schematic presentation of the biogas generation described by the model including parameters: (*Cp*, *Pp*, and *Lp*: *primary* carbohydrates, proteins and lipids, respectively; $k_{hyd\ C}$,$k_{hyd\ P}$ and $k_{hyd\ L}$ - hydrolysis constant for carbohydrates, proteins, lipids, respectively*;* C_S, P_S and L_S - simple accessible mono-/oligomers carbohydrates, proteins and lipids, respectively; Y_{XC} , Y_{XP} and Y_{XL} - yield factor for primary carbohydrates, proteins, lipids degradation, respectively; X_{aci} - acid forming bacteria; U_C, $U_P$and U_L - yield factor for VFAs production from carbohydrates, proteins, lipids, respectively; *VFA*- volatile fatty acids; Y_{XVFA} - yield factor VFA degradation; v_{VFA} – yield factor for CH_4 production from VFA; X_{meth}- methanogenic bacteria; CH_4 - methane and CO_2 - carbon dioxide (*TIC*)

where $r_P^{max}, r_C^{max}, r_L^{max}$ and r_{VFA}^{max} are the maximum bacterial growth rates on proteins (P_S) carbohydrates (C_S), lipids (L_S) and volatile fatty acids (VFA), K_P, K_C, K_L and K_{VFA} are the half-saturation constants associated with the substrate, IpL_S is the inhibition coefficient.

Volume of reactor and total influent rate

Dynamical change of the volume of biogas production is integrated from the biogas flow rate (Equation 5.5) [$m^3 \cdot s^{-1}$]:

$$\frac{dV_{BG}}{dt} = \dot{q}_{out} Ga \tag{5.5}$$

The total influent rate $\dot{q}_{tot}^0$ [$kg \cdot m^{-3} \cdot s^{-1}$] is calculated by sum of influent rates of three compounds and inflow of inoculum (Equation 5.6):

$$\dot{q}_{tot}^0 = \dot{q}_C^0 + \dot{q}_P^0 + \dot{q}_L^0 + \dot{q}_{ino}^0 \tag{5.6}$$

Concentration of bacteria

Dynamical change of acidogenic (Equation 5.7) and methanogenic (Equation 5.8) bacteria [$kg \cdot s^{-1}$] is calculated:

$$\frac{dX_{aci}}{dt} = \frac{\dot{q}_{ino}^0 \cdot X_{Aci}^0 - \dot{q}_{tot}^0 \cdot X_{Aci}}{V_{liq}} + Y_{XC} \cdot r_{XC} + Y_{XP} \cdot r_{XP} + Y_{XL} \cdot r_{XL} \tag{5.7}$$

$$\frac{dX_{meth}}{dt} = \frac{\dot{q}_{ino}^0 \cdot X_{Meth}^0 - \dot{q}_{tot}^0 \cdot X_{Meth}}{V_{liq}} + Y_{XVFA} \cdot r_{VFA} \tag{5.8}$$

Hydrolysis

Hydrolysis rates for carbohydrates, proteins and lipids are determined by using the first order kinetic model (Equation 5.9 - 5.11):

$$r_{hyd\,C} = k_{hyd\,C} \cdot C_p \tag{5.9}$$

$$r_{hyd\,P} = k_{hyd\,P} \cdot P_P \tag{5.10}$$

$$r_{hyd\,L} = k_{hyd\,L} \cdot L_p \tag{5.11}$$

Concentration of primary carbohydrates, proteins and lipids

Disintegration of *primary* carbohydrates (C_p) (Equation 5.12), *primary* proteins (P_p) (Equation 5.13) and *primary* lipids (L_p) (Equation 5.14) [kg·s^{-1}] is calculated:

$$\frac{dCp}{dt} = \frac{\dot{q}_C^0 \cdot C_p^0 - \dot{q}_{tot}^0 \cdot C_p}{V_{liq}} - r_{hyd\,C} \tag{5.12}$$

$$\frac{dPp}{dt} = \frac{\dot{q}_P^0 \cdot P_p^0 - \dot{q}_{tot}^0 \cdot P_p}{V_{liq}} - r_{hyd\,P} \tag{5.13}$$

$$\frac{dLp}{dt} = \frac{\dot{q}_L^0 \cdot L_p^0 - \dot{q}_{tot}^0 \cdot L_p}{V_{liq}} - r_{hyd\,L} \tag{5.14}$$

Concentration of simple carbohydrates, proteins and lipids

Hydrolysis of simple accessible mono-/oligomers: carbohydrates (C_S) (Equation 5.15), proteins (P_S) (Equation 5.16) and lipids (L_S) (Equation 5.17) [kg·s^{-1}] is calculated:

$$\frac{dC_S}{dt} = \frac{-\dot{q}_{tot}^0 \cdot C_S}{V_{liq}} + r_{hyd\,C} \cdot r_{XC} \tag{5.15}$$

$$\frac{dP_S}{dt} = \frac{-\dot{q}_{tot}^0 \cdot P_S}{V_{liq}} + r_{hyd\,P} \cdot r_{XP} \tag{5.16}$$

$$\frac{dL_S}{dt} = \frac{-\dot{q}_{tot}^0 \cdot L_S}{V_{liq}} + r_{hyd\,L} \cdot r_{XL} \tag{5.17}$$

Concentration of volatile fatty acids

Dynamical change of an intermediate product - volatile fatty acids (Equation 5.18) [mol·s^{-1}] is calculated:

$$\frac{d_{VFA}}{dt} = \frac{-\dot{q}_{tot}^0 \cdot VFA}{V_{liq}} + (1 - Y_{XC}) \cdot U_C \cdot r_{XC} + (1 - Y_{XP}) \cdot U_P \cdot r_{XP} + (1 - Y_{XL}) \cdot U_L \cdot r_{XL} - r_{VFA} \tag{5.18}$$

Inorganic carbon rate

In Equation 5.19 ***the inorganic carbon release*** (TIC) rate is estimated [mol·s^{-1}]:

$$rTIC = (1 - Y_{XC}) \cdot (1 - U_C) \cdot r_{XC} + (1 - Y_{XP}) \cdot (1 - U_P) \cdot r_{XP} + (1 - Y_{XL}) \cdot (1 - U_L) \cdot r_{XL} + (1 - Y_{XVFA}) \cdot (1 - v_{VFA}) \cdot r_{VFA} \quad (5.19)$$

Molar release of CO_2 and CH_4 [mol·s^{-1}] is in Equation 5.20 and in Equation 5.21, respectively:

$$\dot{n}_{CO2} = \frac{rTIC}{MWCO2} \cdot V_{liq} \quad (5.20)$$

$$\dot{n}_{CH4} = \frac{(1-Y_{XVFA}) \cdot v_{VFA} \cdot r_{VFA}}{MWCO2} \cdot V_{liq} \quad (5.21)$$

Molar fractions of CO_2 and CH_4 [Vol.-%] are given in Equations 5.22- 5.23:

$$y_{CO2} = \frac{\dot{n}_{CO2}}{\dot{n}_{CO2} + \dot{n}_{CH4}} \cdot 100\% \quad (5.22)$$

$$y_{CH4} = 1.0 - y_{CO2} \quad (5.23)$$

Biogas flow rate [m^3·s^{-1}] is estimated from molar release of CO_2 and CH_4 and the ideal gas law (Equation 5.24) [m^3·s^{-1}]:

$$\dot{q}_{out} Ga = (\dot{n}_{CO2} + \dot{n}_{CH4}) \cdot R \cdot TGas/P \quad (5.24)$$

The volume of biogas production is integrated from the biogas flow rate (Equation 5.25) [m^3·s^{-1}]:

$$\frac{dV_{BG}}{dt} = \dot{q}_{out} Ga \quad (5.25)$$

Kinetic coefficients, calculations of hydrolysis rates and rates of bacterial growth, and state variables are summarized in Table 5-1.

Table 5-1: Biochemical rate coefficients and kinetic rate equations for carbohydrates, proteins and lipids including inhibition coefficient determined by Haldane-kinetics (see Section 2.4)

Rate	X_{aci}	X_{meth}	C_p	P_p	L_p	C_s	P_s	L_s	*VFA*	*TIC*	CH_4
r_{hydC}[a] = $k_{hyd\,C} \cdot C_p$			-1								
r_{hydP}[b] = $k_{hyd\,P} \cdot P_P$				-1							
r_{hydL}[c] = $k_{hyd\,L} \cdot L_p$					-1						
r_{XC}[d] = $r_C^{max} \cdot CX_{aci} \cdot \frac{C_S}{C_S+K_C}$	Y_{XC}					-1			(1-Y_{XC}) $\cdot U_C$	(1-Y_{XC}) $\cdot (1-U_C)$	
r_{XP}[e] = $r_P^{max} \cdot CX_{aci} \cdot \frac{P_S}{P_S+K_P}$	Y_{XP}						-1		(1-Y_{XP}) $\cdot U_P$	(1-Y_{XP}) $\cdot (1-U_P)$	
r_{XL}[f] = $r_L^{max} \cdot CX_{aci} \cdot \frac{Ip_{L_S}}{Ip_{L_S}+L_S} \cdot \frac{L_S}{L_S+K_L}$	Y_{XL}							-1	(1-Y_{XL}) $\cdot U_L$	(1-Y_{XL}) $\cdot (1-U_L)$	
r_{VFA}[g] = $r_{VFA}^{max} \cdot CX_{meth} \cdot \frac{Ip_{L_S}}{Ip_{L_S}+L_S} \cdot \frac{VFA}{VFA+K_{VFA}}$		Y_{XVFA}							-1	(1-Y_{XVFA}) $\cdot (1-v_{VFA})$	$(1-Y_{XVFA}) \cdot v_{VFA}$

Acidogenic bacteria [kg·m^{-3}]
Methanogenic bacteria [kg·m^{-3}]
primary carbohydrates [kg·m^{-3}]
primary proteins [kg·m^{-3}]
primary lipids [kg·m^{-3}]
accessible carbohydrates [kg·m^{-3}]
accessible proteins [kg·m^{-3}]
accessible lipids [kg·m^{-3}]
Volatile fatty acids [mol·s^{-1}]
Total Inorganic carbon [mol·s^{-1}]
Methane gas [kg·m^{-3}]

r_{hydC}[a] - rate describing the hydrolysis of carbohydrates
r_{hydP}[b] - rate describing the hydrolysis of proteins
r_{hydL}[c] - rate describing the hydrolysis of lipids

r_{XC}[d] - rate describing the acidogenesis carbohydrates
r_{XP}[e] - rate describing the acidogenesis proteins
r_{XL}[f] - rate describing the acidogenesis lipids

r_{VFA}[g] - rate describing methanogenesis

5.4 Estimation of parameter

The parameters estimation and the model calibration were performed on the basis of least squares procedure by measuring the deviation between the model and real system outputs.

$$\Psi(\theta) = \sum_{i=1}^{N}\left(\frac{y_{exp}\,(\theta) - y_{sim(\theta)}}{\sigma_t}\right)^2 \quad (5.26)$$

where Ψ(θ) is the objective function, y_{exp} are the collected measurements, y_{sim} are the model-predicted outputs, θ represents the parameters to be determined and N is the number of measurements. When the errors of the measurements do not have a constant standard deviation, then it is generally required to introduce weighting factors (σ_t), leading to a weighted least-square criterion (Donoso-Bravo et al., 2011). The calculation of the most probable parameter (James, 2004) was achieved by the Numerics library Minuit. The software allows sharing of any subset of the model parameters to minimize the sum of squares (Equation 5.26). In addition, the identification space of the model parameters can be limited individually for each parameter. The robustness of the parameter estimation results from the possibility to restrict the identification space, thus, it excludes critical parameter values that cause numerical instability.

5.5 Calculation of theoretical methane and biogas yield

The theoretical methane and biogas yield were calculated based on the observation of the mono-substrate digestion. Equations 5.27 - 5.28 represent the mathematical way to calculate theoretical volume of biogas and methane which were produced after the AD of substrates mixture.

$$V_{BG\,Tot,mix} = \frac{V_{BG\,Tot,\ S}}{m_S} \cdot m_{S,mix} + \frac{V_{BG\,Tot,G}}{m_G} \cdot m_{G,mix} + \frac{V_{BG\,Tot,R}}{m_R} \cdot m_{R,mix} \quad (5.27)$$

$$V_{CH4\,Tot,mix} = \frac{V_{CH4\,Tot,\ S}}{m_S} \cdot m_{S,mix} + \frac{V_{CH4\,Tot,G}}{m_G} \cdot m_{G,mix} + \frac{V_{CH4\,Tot,R}}{m_R} \cdot m_{R,mix} \quad (5.28)$$

RESULTS

6.1 Batch experiments with sucrose, gelatine and rapeseed oil

6.1.1 Batch experiments with sucrose

Experimental results of the AD with table sugar are shown on Figure 6-1, A. Initially, 16 g of sucrose were added to the inoculum sludge. The biogas process production stopped after 16th day. In total, during 28 days of experiment 9.2L of biogas and 4.96 L of methane were produced. The volumetric concentrations of methane and carbon dioxide were calculated from the measured corresponding volumes as well as the biogas flow rate. The minimum methane concentration was reached at day 9 and showed 50.18%. Subsequently, it increased and reached 53.62%. The biogas flow rate was quite high at the first day and reached 0.145 L h^{-1}. Starting from the second day till the fifth it increased from 0.01 L h^{-1} to 0.071 L $h^{-1.}$ Subsequently, it was dropping and at day 10 it showed 0.002 L $h^{-1.}$ Afterwards, the flow rate was increasing slightly till 0.007 Lh^{-1} and then was stopped at day 16. COD_{Tot} was depleting from 15.31 to 0.04 g COD L^{-1} during 16 days.

6.1.2 Batch experiments with gelatine

For the AD of gelatine 15.8 g L^{-1} was added into the sludge. The experimental results are shown on the Figure 6-1, B. The end of the biogas generation was at the day 20 and, 7.19 L of biogas and 3.93 L methane were produced during 28 days. The volumetric methane concentration was fluctuating between 53.1 to 54.5 %. The biogas flow rate was increasing in the 6 days and reached its maximum - 0.035 L h^{-1}. After the flow was dropping until it stopped after the day 21. COD_{Tot} was depleting from 15.96 to 0.97 gCOD L^{-1} during 16 days.

6.1.3 Batch experiments with rapeseed oil

The experimental results from the AD of 8 ml L^{-1} rapeseed oil are presented on the Figure 6-1, C. After the day 25 the biogas production was stopped. The total amount of produced

biogas and methane was 6.9 L and 5.22 L, respectively. From the data it can be observed that the hydrolytic step took nearly 5 days. The volumetric methane concentration was increasing till the day 10 and was subsequently maintained at 75.4%. The first 15 days the biogas flow rate maintained between 0.006 - 0.002 L h^{-1}. After five days, the flow strongly increased and reached its maximum at 0.045 L h^{-1} and later was dropping. Within the first five days COD_{Tot} was increasing from 10.63 to 20.43 gCOD L^{-1}. Further it was dropping till the day 26 of the experiment.

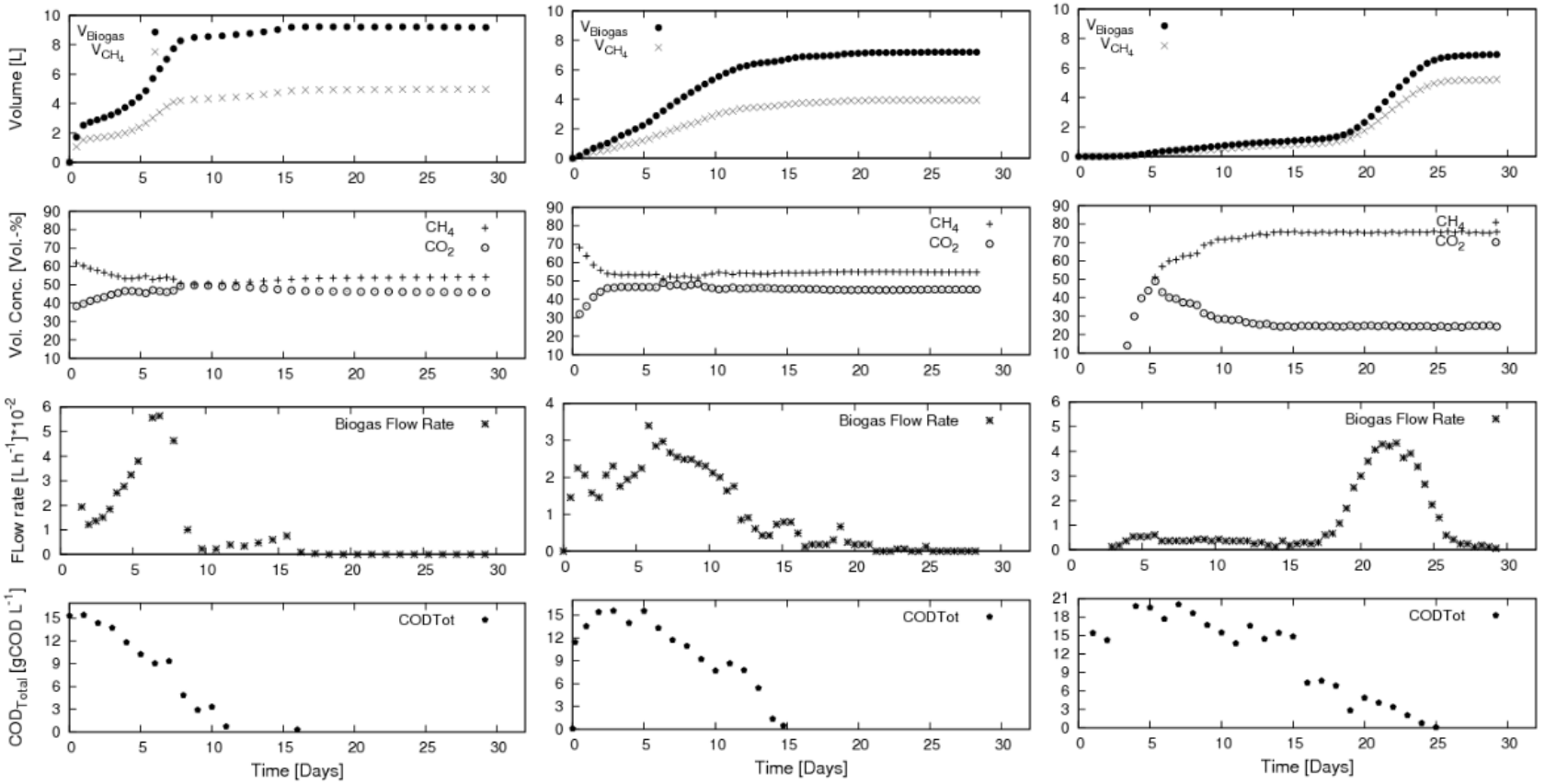

Figure 6-1: Experimental data of anaerobic mono-digestion in batch of 16 g L^{-1} sucrose (A), 15.8 g L^{-1} gelatine (B) and 8 ml L^{-1} rapeseed oil (C). Biogas and methane volume production, volumetric concentration of CH_4 and CO_2, biogas flow rate and COD_{Tot} are displayed during 30 days. Blank biogas and methane formation were subtracted

6.1.4 The anaerobic digestion with a mixture of sucrose, gelatine and rapeseed oil

For the final experiment it was decided to take the arbitrary substrate mixture with sucrose -5 g L^{-1}; gelatine – 6 g L^{-1}; rapeseed oil - 3 ml L^{-1}, in total 14 - g L^{-1} (Figure 6-2). The maximum biogas production was achieved after 25 days. Within 28 days of the AD, 8.14 L of biogas and 4.62 L of methane were produced. The hydrolysis took nearly 6 days. The mean volumetric methane concentration was steady at 58.8%. Starting from the day 6, the biogas flow rate was smoothly increasing and reached its maximum at 0.025 L h^{-1} on the day 17, after which it decreased and completely stopped the production at the day 26.

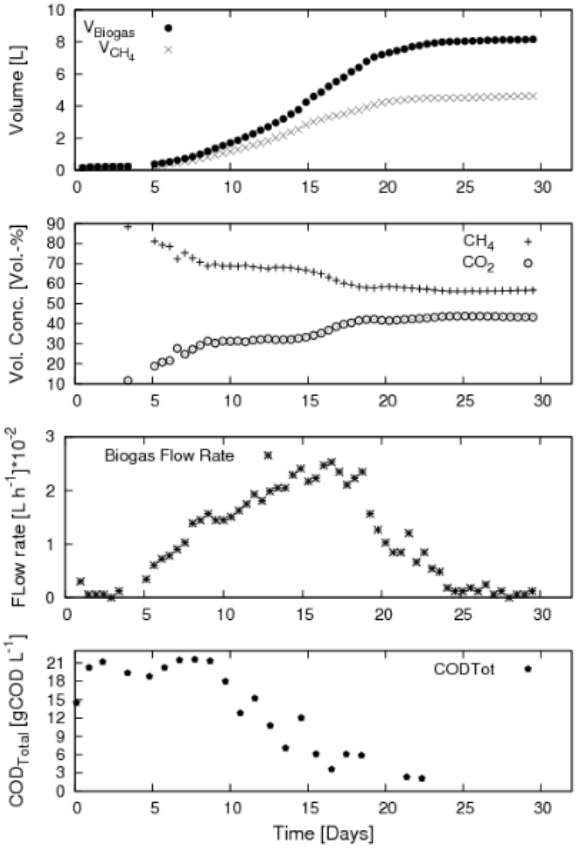

Figure 6-2: Experimental results of AD in batch of sucrose -5 g L^{-1}, gelatine – 6 g L^{-1}, rapeseed oil - 3 ml L^{-1}, in total -14 g L^{-1}. Biogas and methane volumes, volumetric concentration of CH_4 and CO_2, biogas flow rate are shown. Blank biogas and methane formation were subtracted

6.1.5 Estimation the theoretical methane and biogas yield for the AD of the mixture

In order to estimate the reproducibility of the experiments, the theoretical methane and biogas yield which can be obtained from the mixture of digested substrates was calculated. The estimation was based on the experimental observation of the mono-substrate digestion (see Section 6.1.1). Equations 5.27-5.28 (see Section 5.5) and the experimental values were used for the calculations (Table 6-1). The total theoretical V_{Biogas} production is equaled to 8.22 L while V_{CH4} was 4.75 L. Comparing the experimental yields there is a difference of 135 ml in outcome from theoretical CH_4 and 80 ml in biogas yield. The graphical summary of the total methane and biogas volume is shown in Figure 6-3.

Table 6-1: Summary of the generated volume of biogas and methane and used substrates concentrations for mono-digestions and their mixture

Symbol	Value	Unit
$V_{BG\,Tot,\ S}$	9.2	L
$V_{BG\,Tot,\ G}$	7.19	L
$V_{BG\,Tot,\ R}$	6.95	L
$V_{CH4\,Tot,\ S}$	4.96	L
$V_{CH4\,Tot,\ G}$	3.93	L
$V_{CH4\,Tot,\ R}$	5.22	L
$V_{BG\,Tot,mix}$	8.14	L
$V_{CH4\,Tot,mix}$	4.62	L
m_S	16.5	gVS L^{-1}
m_G	16.1	gVS L^{-1}
m_R	13.4	gVS L^{-1}
$m_{S,mix}$	5.94*	gVS L^{-1}
$m_{G,mix}$	6.97*	gVS L^{-1}
$m_{R,mix}$	3.48*	gVS L^{-1}

*the values represent a proportional relation of each master substrate in the mixture and m_{mix} is 16.4 [gVS L^{-1}]

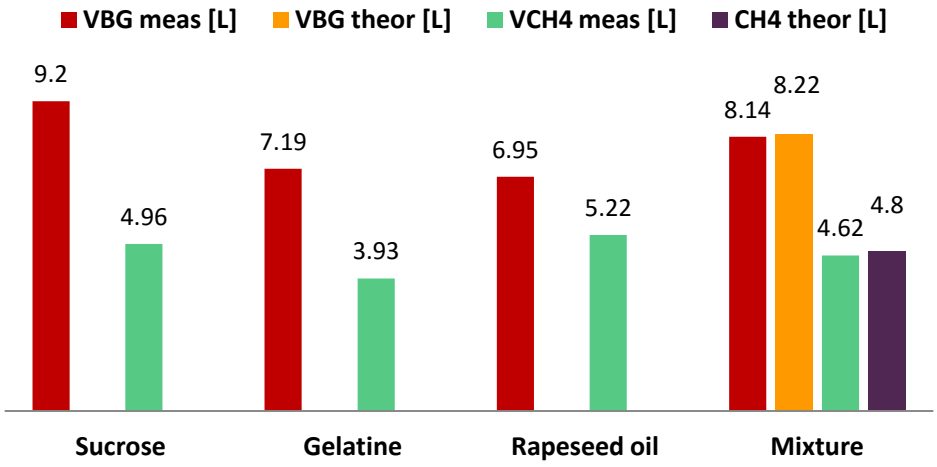

Figure 6-3: Summary of cumulative production of volume of biogas and methane in AD batch tests with 16.5 gVS L^{-1} sucrose, 16.1 gVS L^{-1} gelatine, 13.4 gVS L^{-1} rapeseed oil and 16.4 gVS L^{-1} substrates mixture. Theoretical biogas and CH_4 were calculated based on the product yields obtained during mono-fermentations. VBG is defined as volume of biogas, VCH_4 - volume of methane, meas - measured, theor - theoretical

6.2 Calibration of the model using the batch experiments with sucrose, gelatine and rapeseed oil and validation of the model using the experimental data set of their digested mixture

6.2.1 Estimation of parameters

In order to find the best agreement between simulated and experimental data, an appropriate criterion for the optimal solution of the model parameter identification must be selected. The values for the kinetic coefficients of the first-order rate of hydrolysis were based on the previous studies (see Section 2.4, Table 2-3). For the rest parameters estimation and final model calibration least squares procedure was performed (see Section 4.3). The summary of the estimated parameters is presented in Table 6-2.

Table 6-2: Kinetic parameters used in the model for AD of mixture: gelatine, sucrose, rapeseed oil

Parameter	Definition	Value	Unit
$k_{hyd\,C}$	Hydrolysis constant for carbohydrates	$7.9 \cdot 10^{-6}$	s^{-1}
μ_C^{max}	Maximum uptake rate for carbohydrates	$4.2 \cdot 10^{-6}$	s^{-1}
K_{C_s}	Half-saturation constant carbohydrates	6.5	$kg \cdot m^{-3}$
Y_{XC}	Yield factor for primary carbohydrates degradation	0.22	$kg \cdot kg^{-1}$
U_C	Yield factor for VFA production from carbohydrates	0.65	$kg \cdot kg^{-1}$
$k_{hyd\,P}$	Hydrolysis constant for proteins	$5.1 \cdot 10^{-6}$	s^{-1}
μ_P^{max}	Maximum uptake rate for proteins	$3.3 \cdot 10^{-6}$	s^{-1}
K_{P_s}	Half-saturation constant proteins	5.0	$kg \cdot m^{-3}$
Y_{XP}	Yield factor for primary proteins degradation	0.50	$kg \cdot kg^{-1}$
U_P	Yield factor for VFA production from protein	0.68	$kg \cdot kg^{-1}$
$k_{hyd\,L}$	Hydrolysis constant for lipids	$4.56 \cdot 10^{-6}$	s^{-1}
μ_L^{max}	Maximum uptake e rate for lipids	$5.6 \cdot 10^{-6}$	s^{-1}
K_{L_s}	Half-saturation constant lipids	3.2	$kg \cdot m^{-3}$
Y_{XL}	Yield factor primary lipids degradation	0.55	$kg \cdot kg^{-1}$
U_L	Yield factor VFA production from lipids	0.96	$kg \cdot kg^{-1}$
μ_{VFA}^{max}	Maximum uptake rate for VFA	$8.20 \cdot 10^{-6}$	s^{-1}
K_{VFA}	Half-saturation constant VFA	0.01	$kg \cdot m^{-3}$
Y_{XVFA}	Yield factor VFA degradation	0.35	$kg \cdot kg^{-1}$
v_{VFA}	Yield factor for CH_4 production from VFA	0.552	$mol \cdot kg^{-1}$
IpL_S	Inhibition coefficient	0.045	$kg \cdot m^{-3}$
VR	Volume of the reactor	1.1^{-2}	m^3
TR	Temperature in the reactor	311.0	K

The estimated set of parameters was found during the calibration of the model with each substrate (sucrose, gelatine, and rapeseed oil) and after summarizing the proposed set of parameters was applied for prediction of the AD of the mixture of these master substrates. The initial concentrations of acidogenic and methanogenic bacteria and VFA were different for each digestion as it is shown in the Table 6-3. The values were adjusted by using the least square method and then by a manual approach.

Table 6-3: The summary of applied state variables for simulation of the AD of sucrose, gelatine and rapeseed oil and prediction of the AD of mixture

State variable	Sucrose	Gelatine	Rapeseed oil	Mixture	Units
X_{aci}	8.97	6.54	2.95	0.6073	[kg·m^{-3}]
X_{meth}	5.981	4.85	3.0	3.588	[kg·m^{-3}]
C_P	16.0	-	-	5.0	[kg·m^{-3}]
P_P	-	15.8	-	6.0	[kg·m^{-3}]
L_P	-	-	8.0	3.0	[kg·m^{-3}]
VFA	0.08	$6.6 \cdot 10^{-8}$	$2.9 \cdot 10^{-4}$	0.03	[mol·m^{-3}]

6.2.2 Calibration of the model using the batch experiments with sucrose

The agreement between the experimental and simulated data during the AD of 16 g L $^{-1}$ sucrose is shown on Figure 6-4. The simulations showed initially a discrepancy with the experimentally measured volume of biogas and methane. The simulated biogas (9.59 L) and methane volume (5.273 L) was 397 ml and 313 ml less, respectively, as compared to the experimental volume of biogas which was 9.2 L and CH_4 - 4.96 L. The first five days the simulated methane volumetric concentration had a discrepancy in dynamics. After the day 5 concentration was maintained at 52.67% for CH_4 which coincided with the experimental values. The model predicted the biogas flow rate with a shift to the left in the very beginning of the batch experiment.

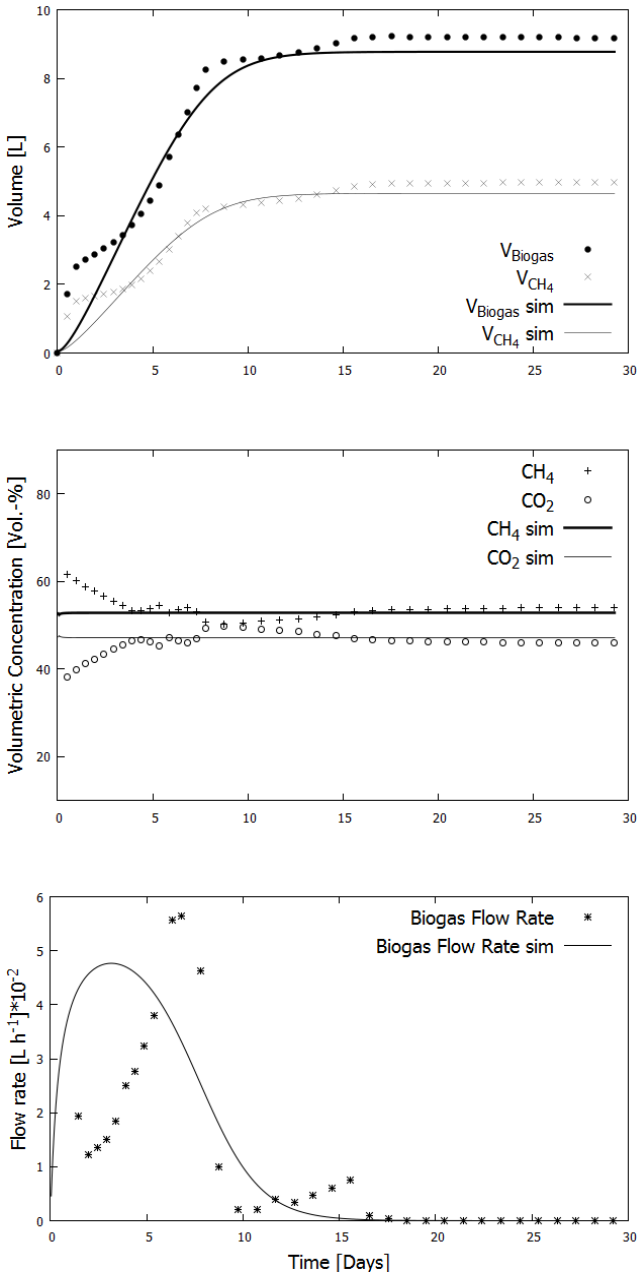

Figure 6-4: Experimental and simulation data of anaerobic mono-digestion in batch of 16 g L $^{-1}$ sucrose. Biogas and methane volume production, volumetric concentration of CH_4 and CO_2 and biogas flow rate are displayed

On the Figure 6-5 the simulated COD_{Tot} and concentration of VFA are shown. The simulated COD_{Tot} had a slightly faster degradation as compared to the experimental measurements. The model simulated degradation of 15.3 gCOD L^{-1} organics which was fermented within next sixteen days. The change of the C_{VFA} is presented only by theoretical data. Accordingly to the model the maximum of VFA was reached at the day 3 and reached its maximum at $2.3 \cdot 10^{-3}$ mol m^{-3}. After that the concentration of VFA was dropping till the day 16.

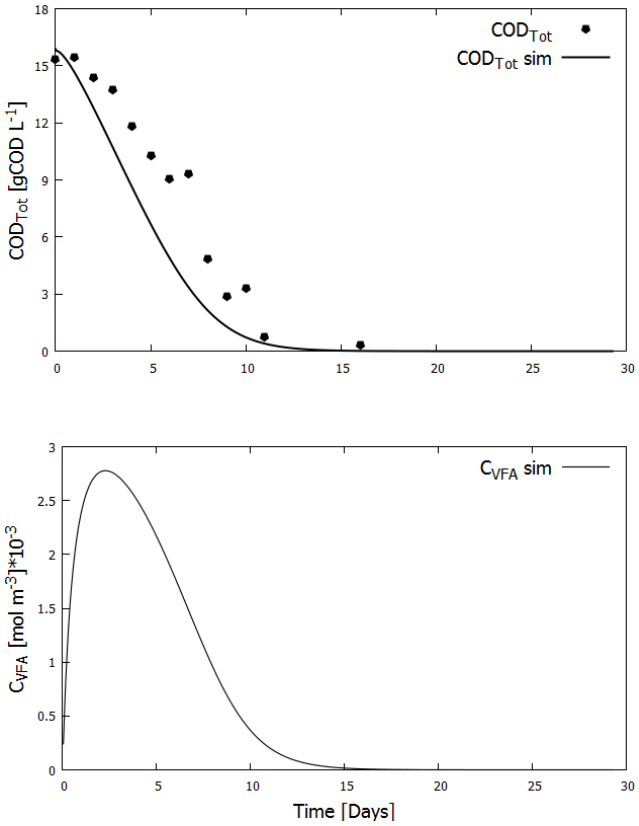

Figure 6-5: Experimental and simulation data of anaerobic mono-digestion in batch of 16 g L^{-1} sucrose. COD_{Tot} and concentration of VFA are displayed over 30 days. Blank biogas and methane formation were subtracted

6.2.3 Calibration of the model using the batch experiments with gelatine

The simulation of the AD of 15.8 g L^{-1} gelatine showed a good agreement with the corresponding experimental measurements: in particular for the biogas and methane volume production and biogas flow rate (Figure 6-6). The simulations predicted less production for biogas - 6.83 L and for methane 3.705 L as compared to the measured biogas and methane - 7.19 L and 3.93 L, respectively. The simulated volumetric concentration of CH_4 was maintained at 54.5 % from the day 2 which found an agreement with experimentally measured CH_4. On figure 6-7 the simulated biogas flow rate, COD_{Tot} and concentration of VFA are shown. Simulated biogas flow was increasing till the 6 days and after reaching its maximum - 0.035 L h^{-1} . The flow rate started to dropped until it stopped after the day 21.

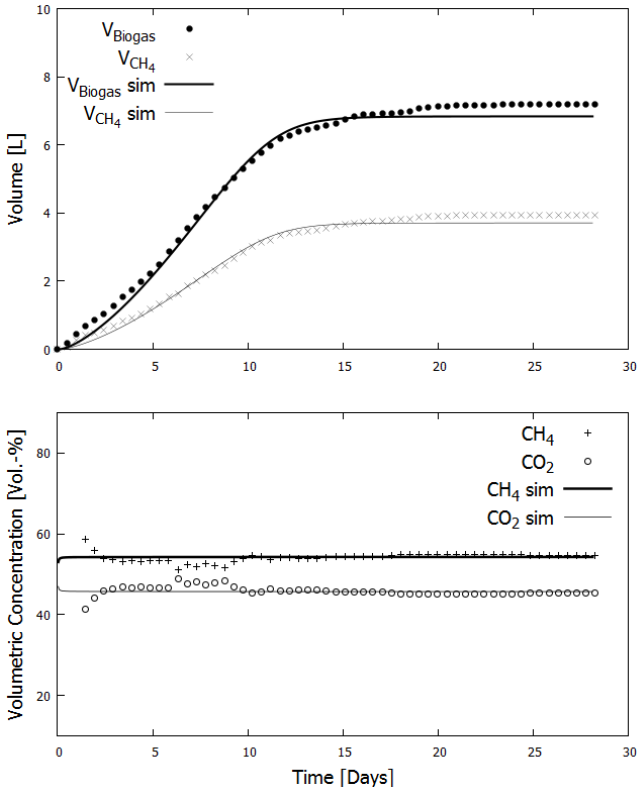

Figure 6-6: Experimental and simulation data of anaerobic mono-digestion in batch of 15.8 g L^{-1} gelatine. Biogas and methane volume production and volumetric concentration of CH_4 and CO_2 are displayed over 30 days

After day 6 the simulated COD_{Tot} degradation was slightly faster than experimental results. At day 6 the theoretical C_{VFA} reached 1.85 $\cdot 10^{-3}$ mol m^{-3} and after that the concentration of VFA was completely consumed at day 18.

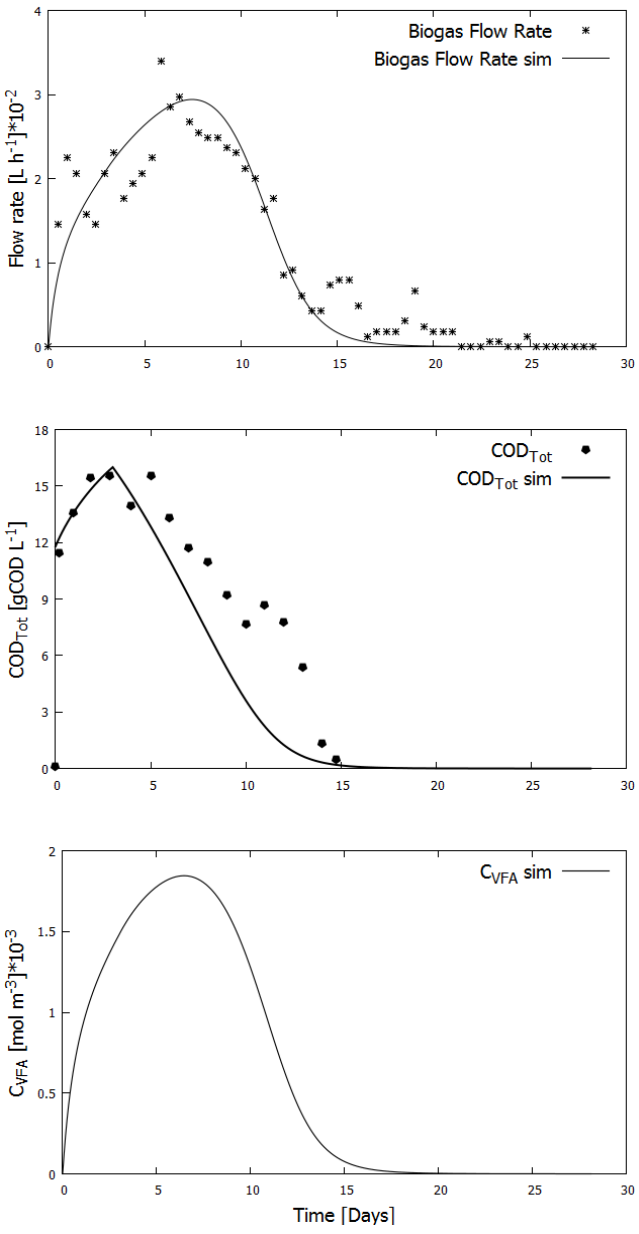

Figure 6-7: Experimental and simulation data of anaerobic mono-digestion in batch of 15.8 g L^{-1} gelatine. Biogas flow rate, COD_{Tot} and concentration of VFA are displayed over 30 days. Blank biogas and methane formation were subtracted

6.2.4 Calibration of the model using the batch experiments with rapeseed oil

The simulated results from the AD of 8 ml L^{-1} rapeseed oil are presented on the Figure 6-8. The model simulated the production of volume of biogas and methane which had a longer hydrolytic phase by 2 days as compared to experimental data. At day 6 the volume of biogas and methane started to grow and reached 6.9 L and 5.2 L after day 25, respectively. The simulated volumetric concentration of CH_4 and CO_2 could find a match with measured data after the day 12 and CH_4 concentration was kept 75.4%. On figure 6-9 the simulated biogas flow rate, COD_{Tot} and concentration of VFA are shown. Simulated biogas flow was generated after the day 6 which was 2 days later as compared to experimental flow. Starting from day 15 the flow rate rose sharply and with the slight shift to the right reached 0.045 L h^{-1} as compared to measured biogas flow.

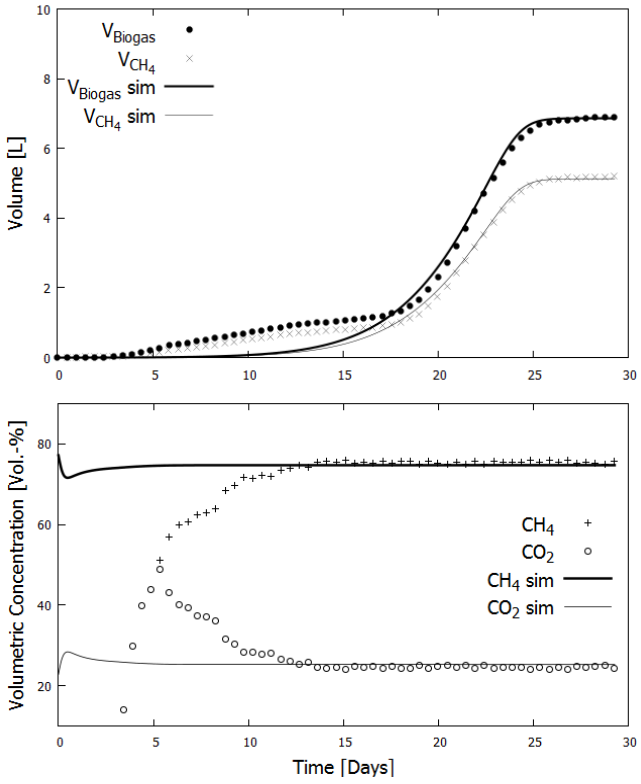

Figure 6-8: Experimental and simulation data of anaerobic mono-digestion in batch of 8 ml L^{-1} rapeseed. Biogas and methane volume production and volumetric concentration of CH_4 and CO_2 are displayed over 30 days

Simulated COD_{Tot} was increasing from 10.63 to 20.43 gCOD L^{-1} and thereafter dropped slower as compared to the measured values. The simulated concentration of VFA was increasing from $2.9 \cdot 10^{-4}$ to $3.2 \cdot 10^{-3}$ mol m^{-3} at day 6. After that the amount of VFA rose considerably and reached the maximum value - $7.2 \cdot 10^{-3}$ mol m^{-3} at day 21 After that the concentration of VFA was dropping till day 26.

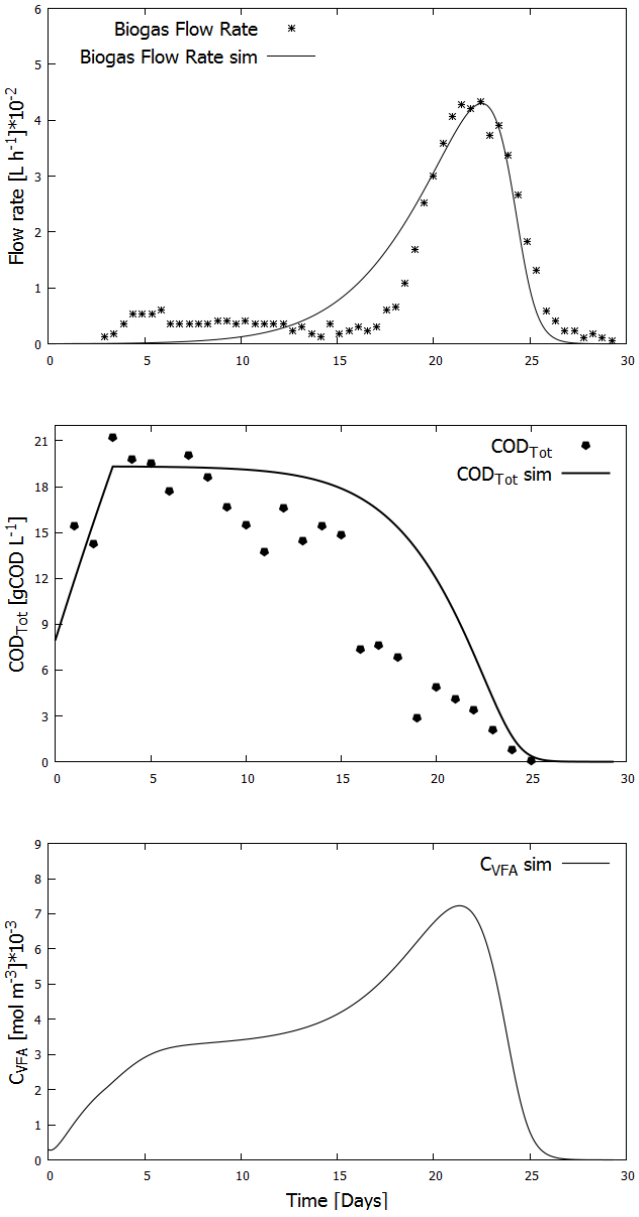

Figure 6-9: Experimental and simulation data of anaerobic mono-digestion in batch of 8 ml L^{-1} rapeseed. Biogas flow rate, COD_{Tot} and concentration of VFA are displayed over 30 days. Blank biogas and methane formation were subtracted

6.2.5 Validation of the parameterized model using experimental data of the synchronous anaerobic digestion with sucrose, gelatine and rapeseed oil

The calibrated model was applied for the prediction of the AD dynamics of the chosen substrates mixture: sucrose -5 g L^{-1}, gelatine – 6 g L^{-1}, rapeseed oil - 3 ml L^{-1}, in total -14 g $L^{-}1$. Figure 6-10 shows the dynamics of the volume of biogas and CH_4 production. The final theoretical volume of biogas and methane was higher as compared to the measured data and equaled to 8.64 L and 4.97 L, respectively. The simulated concentration of CH_4 reached the best agreement with the experimental concentration of CH_4 at day 22. On the Figure 6-11 the biogas flow rate, COD_{Tot} and concentration of VFA are presented. The biogas flow rate was growing and reached $2.7 \cdot 10^{-2}$ L h^{-1} at day 14 which was a bit higher as compared to the experimental measurements. Simulated COD_{Tot} was rising from 14.36 to 20.7 gCOD L^{-1}. The degradation of COD_{Tot} was completed at day 27.

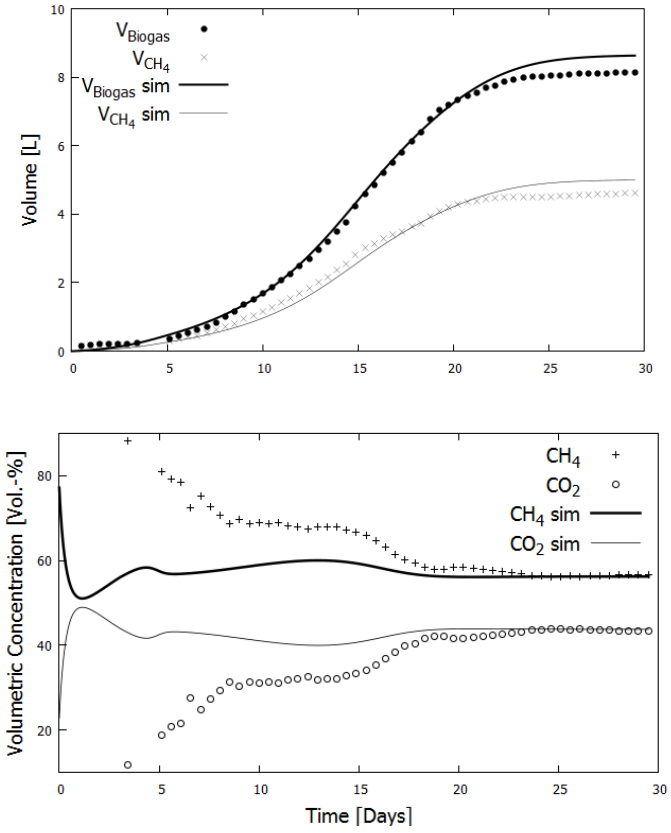

Figure 6-10: Simulation and experimental results of AD in batch of substrates mixture. Biogas and methane volumes, volumetric concentration of CH_4 and CO_2 are shown

The simulated concentration of VFA was increasing from $2.9 \cdot 10^{-2}$ to $4.5 \cdot 10^{-2}$ mol m^{-3} at day 3. After that the concentration of VFA was dropping sharply till day 7. The model simulated the complete degradation of VFA at day 27.

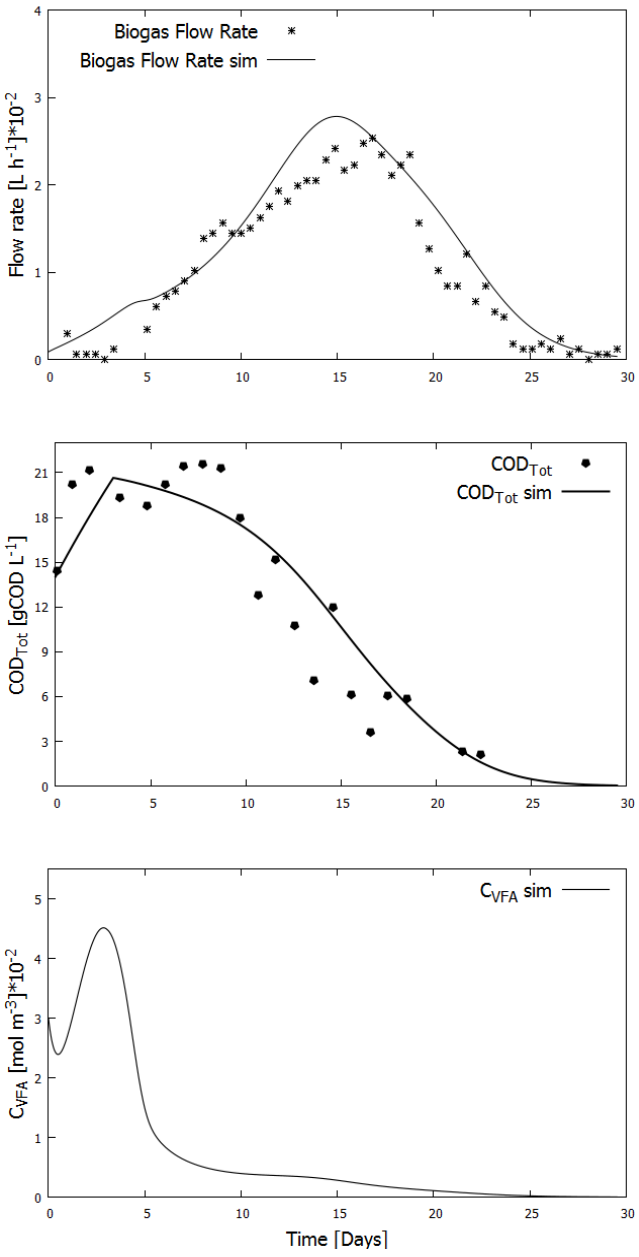

Figure 6-11: Comparison of simulation and experimental results of AD in batch of sucrose -5 g L^{-1}, gelatine – 6 g L^{-1}, rapeseed oil - 3 ml L^{-1}, in total -14 g L^{-1}. Biogas flow rate , COD_{Tot} and concentration of VFA are shown. Blank biogas and methane formation were subtracted

6.2.6 Simulated and experimental biogas and methane yields

The simulated and experimental volumes of biogas and CH_4 generated from the AD with each substrate and their mixture are displayed as a column chart including the error bars on the Figure 6-12. The quality of prediction of the biogas and methane volume are estimated for each digestions shown in Figure 6-13. The difference between simulated and measured volume varied between 0.7 and 7%.

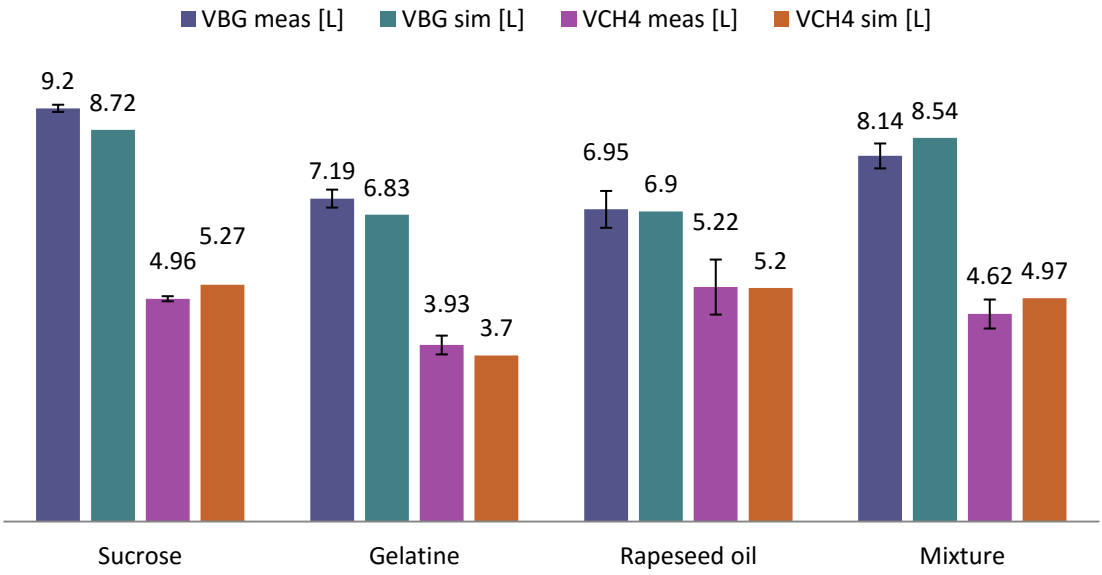

Figure 6-12: Summary of cumulative production of volume of biogas and methane in AD batch tests with 16 g L^{-1} sucrose, 15.8 g L^{-1} gelatine, 8 ml L^{-1} rapeseed oil and substrates mixture: of sucrose -5 g L^{-1}, gelatine – 6 g L^{-1}, rapeseed oil - 3 ml L^{-1}, in total -14 g L^{-1}.VBG is defined as volume of biogas, VCH_4 - volume of methane, sim is simulated and meas - measured

The amount of CH_4 per g of VS added was calculated and shown in Figure 6-14. The amount of VS added in the reactor is listed in Table 4-1. For the calculation of CH_4 per g of VS added, the total volume of CH4 was divided by VS added. The highest amount of methane was produced during rapeseed oil digestion while the lowest was attained in a batch test with gelatine. The amount of biogas produced per g of substrate added and per g of COD added is demonstrated in Figure 6-15 an 6-16. For calculation biogas per g of added substrate and per g of COD added, the total volume of biogas was divided by mass of the substrate in g and g COD, respectively.

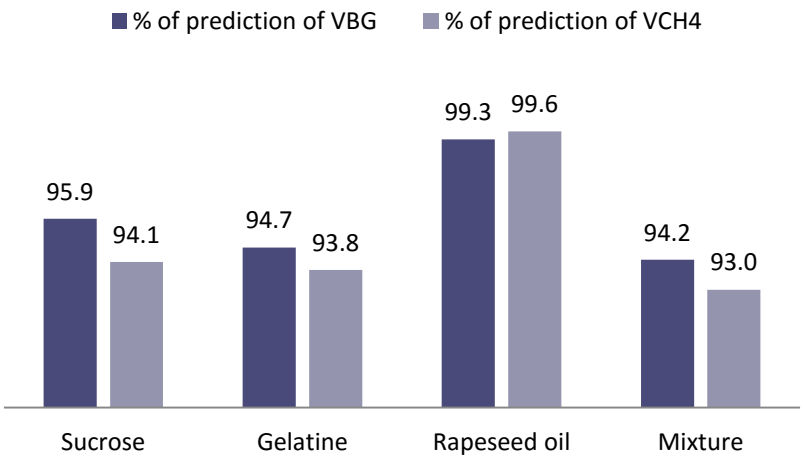

Figure 6-13: Estimation of the prediction performance in %. VBG is defined as volume of biogas, VCH_4 - volume of methane

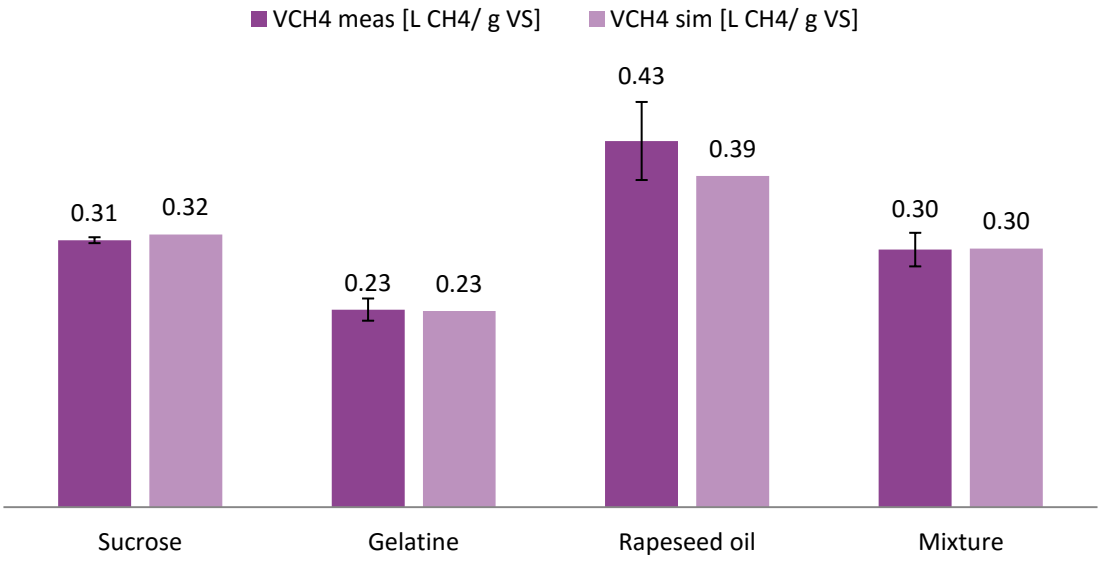

Figure 6-14: Comparative generation of the volume of methane experimentally and predicted by the model for each substrate and their mixture per g VS added. V CH_4 is defined as volume of methane, meas - measured, sim – simulated

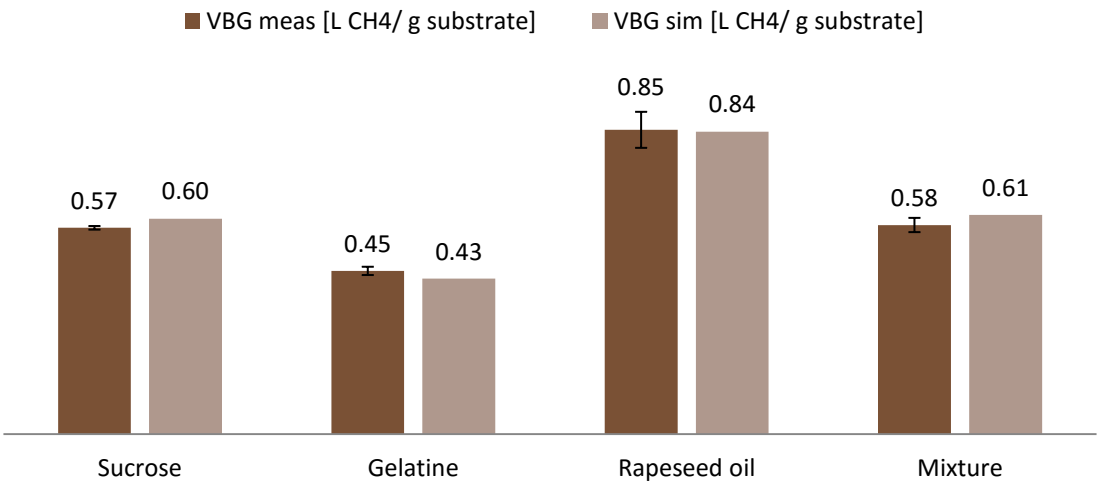

Figure 6-15: Comparative generation of the volume of biogas experimentally and simulated by the model for each substrate and their mixture per g of substrate added. VBG is defined as volume of biogas, meas - measured, sim – simulated

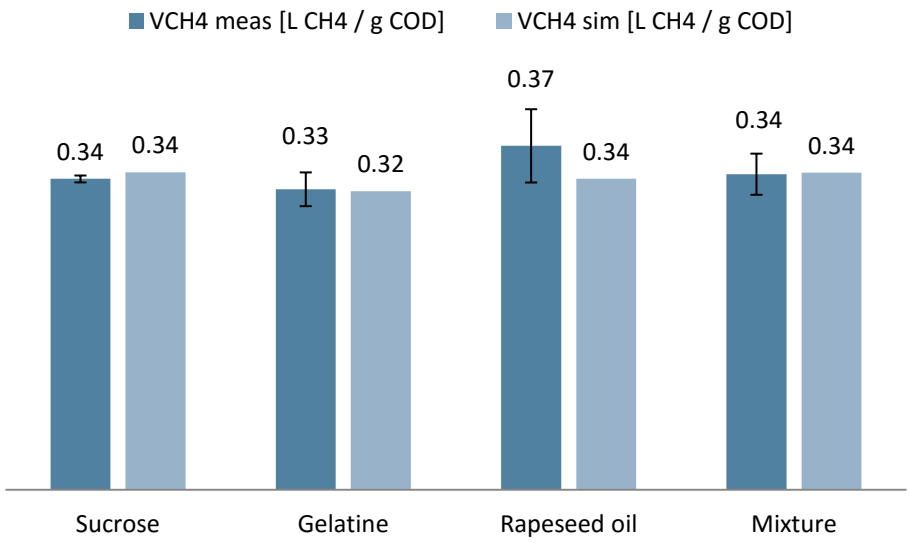

Figure 6-16: Comparative generation of the volume of biogas experimentally and simulated by the model for each substrate and their mixture per g of COD added. VBG is defined as volume of biogas, meas - measured, sim – simulated

6.3 Comparative characteristics of ADM1, ADSIM and biogas model

In order to mark the distinctive features of the developed biogas model, we compared it with the most widely applicable biogas model - ADM1 - and with the ADSIM model. The comparative characteristics are shown in Table 6-4a and 6-4b.

Table 6-4a: Comparative characteristics of ADM1, ADSIM and proposed biogas model

Characteristics	ADM1	ADSIM	Biogas model
Structure	single model	four sub-model structure	single model
Data set for validation	various types of substrates are used for calibration and validation	gelatine, sucrose, rapeseed oil	gelatine, sucrose, rapeseed oil
Purpose	development of a generic model as common platform for dynamic simulations of a variety of anaerobic processes	adjustment of a model for training simulator	development of a biogas model for representation of variety of organic waste based on three master substrates
Model application	- a unified basis for anaerobic digestion modeling - promotion of application of modeling and simulation as a tool for research, design, operation and optimization of anaerobic processes worldwide	- design and testing process control strategies - industrial and academic education	- prediction of anaerobic fermentation with dynamical change of waste in amount and composition - anaerobic digestion modeling for batch and continuous fermentations, scaling up from laboratory to industrial plant
Growth kinetics	modified Monod	Monod	Monod

Table 6-4b: Comparative characteristics of ADM1, ADSIM and the proposed biogas model

Characteristics	ADM1	ADSIM	Biogas model
Parameters:			
- stoichiometric	17	12	8
- kinetic	38	20	20
- physico-chemical	≥ 8	3	-
Process reactions	19	2	3
State variables	24	10	18
Bacterial groups	6	2	2
Hydrolysis kinetics	the 1st order	none	the 1st order
Inhibition functions	4	3	2
Type of inhibition	H_2, pH, NH_3, butyric acid	pH, temperature, VFAs	LCFA,VFA
Products	CH_4, CO_2	CH_4, CO_2, biomass, heat	CH_4, CO_2, biomass
Potentials	- since ADM1 is the most applicable among other models, it had been modified and improved for a certain AD conditions	- basis for development of a biogas simulator - foresees the dynamics of CH_4 and CO_2, biogas flow rate, biogas volume	- despite the much simpler structure, the model has a good potential to predict the AD dynamics - closed material balance
Limitations	- requires a detailed substrate definition - cannot reproduce intimate variations of the different parameters because of some default parameters taken from literature -missing rate limitations for TIC	- not closed material balance - no hydrolysis step - no decay constant - imbalanced gas release	- decay constant is missing - it doesn't consider the inhibition by free ammonia on X_{Meth}
Reference	Batstone et al., 2002	Blesgen and Hass, 2010	Schneider et al., 2015

6.4 Cross-validation of the model using the data sets of continuous experiments with potato waste water and starch

6.4.1 Overview of the continuous experiments and discussion

The continuous experiments were subdivided into the following stages (Table 6-5). The aim was to study the substrate dynamics in a real time and influence of the substrates manipulations on the final product generation. Potato waste water and starch were used as substrates. Figures 6-17 and 6-18 show the experimental data and prediction of the model for volumetric concentrations of methane and carbon dioxide, biogas volume.

Table 6-5: The summary of the continuous experiments

Time [d]	Substrate Name	Substrate [g L^{-1}]	Experimental phases
1-10	Starch	12.6	Start - up phase
10-20	Starch/PWW	12.6/24.7	Step-wise substrate replacement
20- 61	PWW	24.7	Digestion of PWW
61-81	PWW/Starch	24.7/12.6	One-step replacement of PWW by starch
81-100	Starch/PWW	12.6/24.7	One-step replacement of starch by PWW

Start-up phase lasted about a month until a fermentation process was stabilized. During this phase starch (12.6 g COD L^{-1}) was feeding with the rate of 0.5 L day^{-1}, the HRT was 20 days. The average concentration of methane was about 51 %, whereas for carbon dioxide reached 39 %. On Figure 6-15 only last 10 days of start-up phase are shown. At the next step starch was replaced by PWW (24.7 g COD L^{-1}) by daily decrease of the starch amount in the influent bottle on 10 % and the amount of PWW was increased on 10%, respectively. During the substrate exchange the volumetric concentration of methane was growing from 52% to 72% within two weeks. Nearly 144 L of biogas were produced at this step. A part of data set from day 41 to day 57 was lost due to the technical reasons. Nevertheless, the CH_4 concentration reached 72 % before the data loss and had the same value after the problem was solved. On the day 61 PWW was exchanged by starch in one step and after 20 days of the HRT starch was replaced by PWW back in one step.

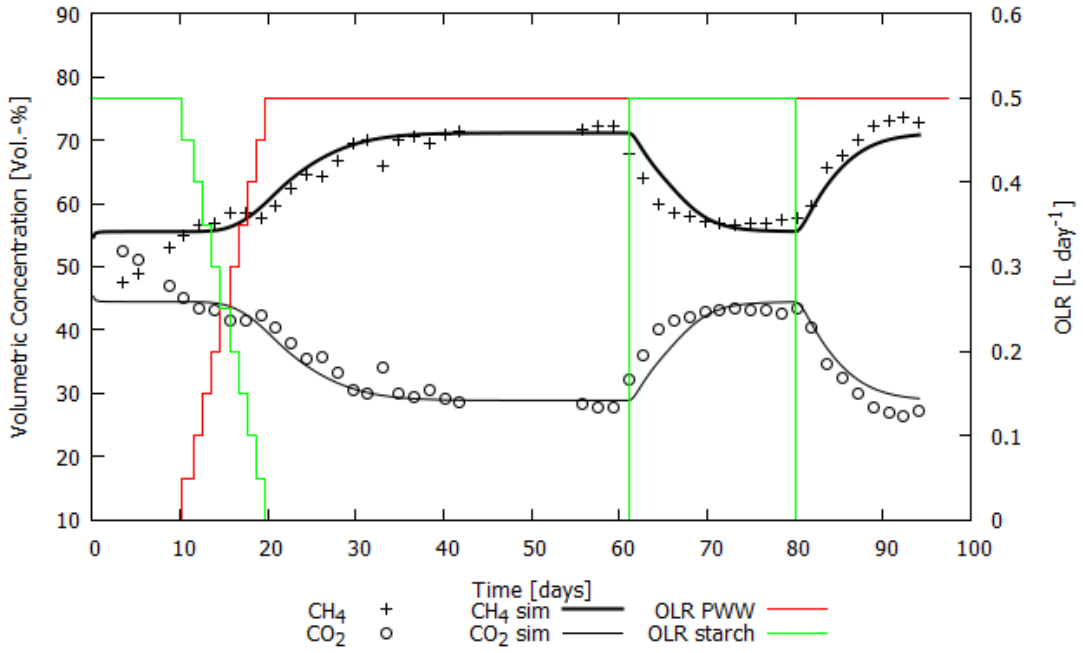

Figure 6-17: Comparison of simulation and experimental results of AD in CSTR of starch - 12.6 g L^{-1} and PWW – 24.7 g L^{-1}. The volumetric concentration of CH_4 and CO_2 and OLR of starch and PWW are shown here

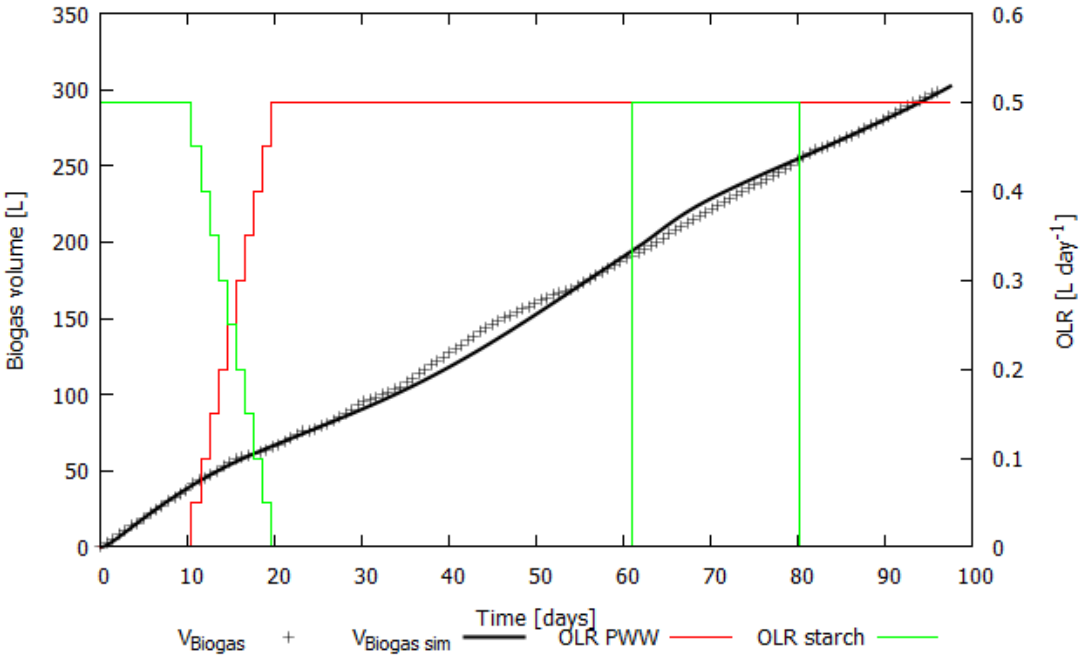

Figure 6-18: Biogas volume generated and predicted by the model over the continuous experiments with substrates replacement. The biogas volume and OLR of starch and PWW are shown here

After the substrates replacement the volumetric concentration of methane dropped sharply from 72% to 57% but it was resumed right after the return substrate replacement. In total, 299 L of biogas volume were generated over the study. Accordingly to the chemical content of the substrates we represented the PWW as a protein-substrate and starch as a carbohydrate-substrate for the substrates initial concentrations in the model.

6.4.2 Parameters for the prediction of the continuous experiments

For the simulations the same set of parameters was applied which was estimated after the parameterization using the batch experiments of gelatine, sucrose and rapeseed oil (Table 6-2). The initial concentrations of acidogenic and methanogenic bacteria and VFA were different as compared to the batch experiments as it is shown in the Table 6-6. The only one parameter has been changed - yield factor for VFA production from proteins, U_P , it was increased from 0.68 to 0.88 $kg \cdot kg^{-1}$. Obvious difference for simulation of the volumetric concentration when U_P equaled 0.68 $kg \cdot kg^{-1}$ is shown on Figure 6-17. After starch was replaced by PWW the volumetric concentration of CH_4 reached only 57 Vol.-% from 55 Vol.-% instead of 71 Vol.-%. Figure 6-18 demonstrates less production of simulated biogas volume on 6.5 L.

Table 6-6: The list of applied state variables for prediction of the continuous AD of PWW and starch

State variable	Value	Units
X_{aci}	4.0	$[kg \cdot m^{-3}]$
X_{meth}	2.0	$[kg \cdot m^{-3}]$
C_P	12.6	$[kg \cdot m^{-3}]$
P_P	24.7	$[kg \cdot m^{-3}]$
L_P	-	$[kg \cdot m^{-3}]$
VFA	$7.2 \cdot 10^{-4}$	$[mol \cdot m^{-3}]$
U_P	0.88	$[kg \cdot kg^{-1}]$

The difference in the simulation results when U_P had the initial value - 0.68 $kg \cdot kg^{-1}$ and after it was changed to 0.88 $kg \cdot kg^{-1}$ is shown on the Figures 6-19 and 6-20.

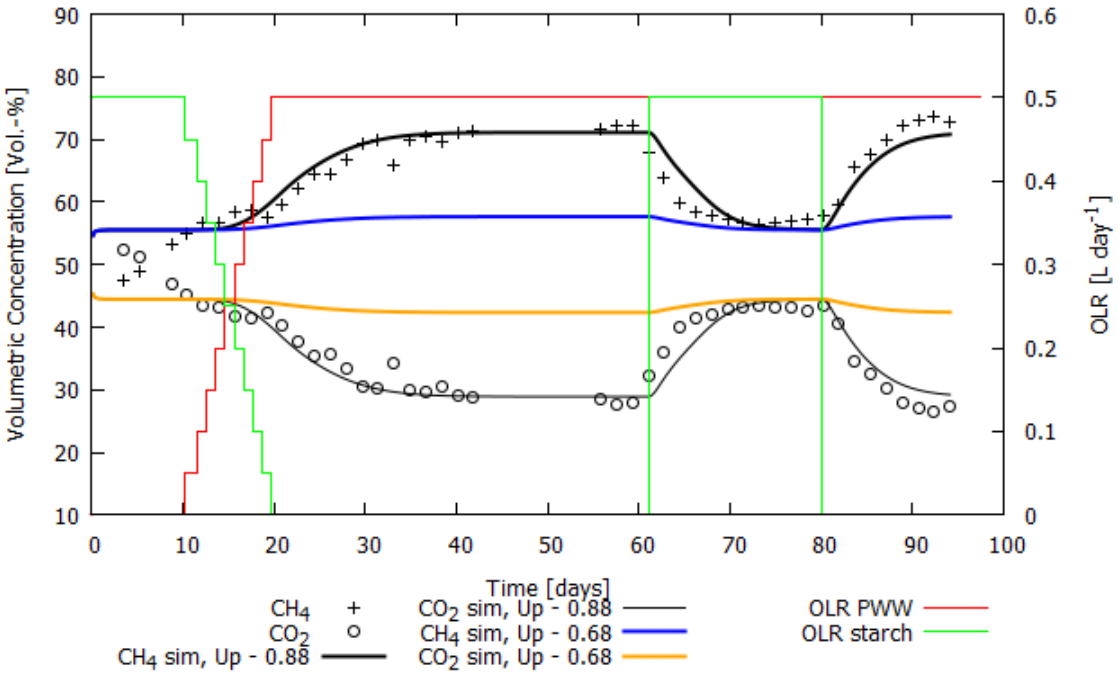

Figure 6-19: Comparison of the simulation results of the volumetric concentration of CH_4 and CO_2 when U_P is 0.68 and 0.88 kg·kg^{-1}

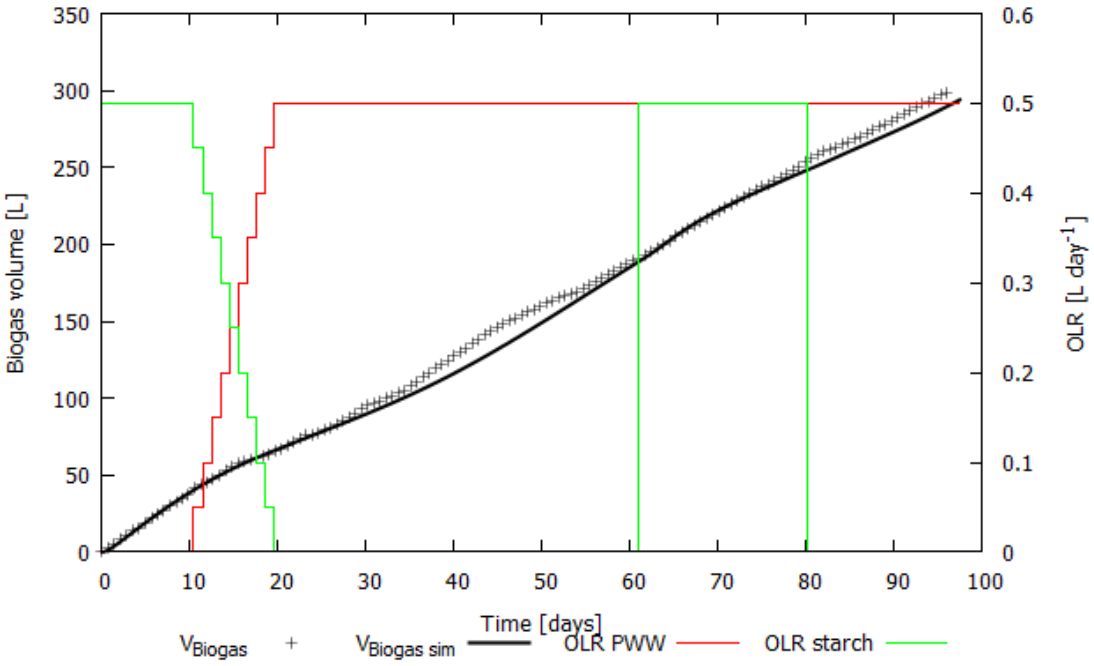

Figure 6-20: Prediction of the volume of biogas when U_P is 0.68 and 0.88 kg·kg^{-1}

6.5 Simulations of the substrates dynamics, methane and biogas volume based on the adjustment of the chemical composition of the feedstock for a big-scale biogas plant

6.5.1 Overview of the biogas process production in EWE Biogas GmbH, Surwold

For further study of the prediction capability of the proposed model, it was decided to simulate the AD process for a big-scale level. The employees of the biogas plant in EWE Biogas GmbH in Surwold, Germany kindly provided us with the process data of the operating plant where the input substrates (manure and waste) were delivered through the tank cascade (receiving, sanitation and buffer tanks) into the biogas fermenter (EWE Biogas GmbH in Surwold, Germany). The scheme of the process is shown on Figure 6-21. The aim of the simulation was to examine the dynamics of the organic input concentrations starting from the receiving tanks and ending with biogas fermenter and their effect on the volumetric concentration of CH_4.

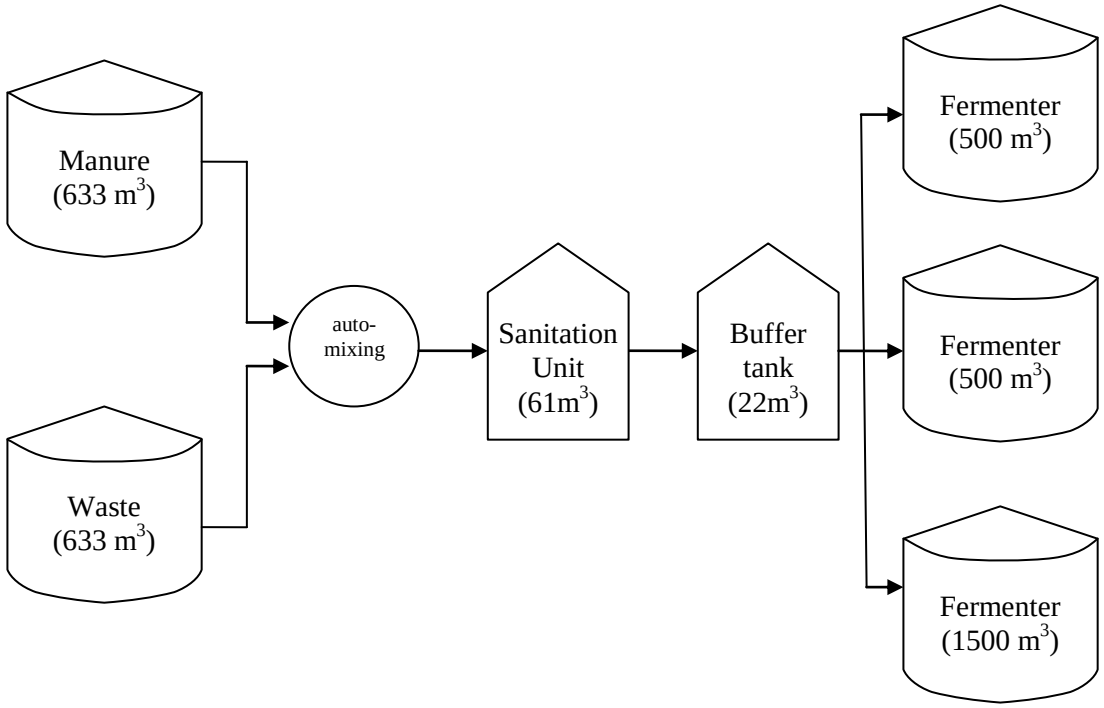

Figure 6-21: The incoming raw materials are received in the manure and the waste tanks, respectively. The raw materials are then thoroughly mixed before the hygienisation process. The substrate mixture then follows to the buffer tank. This allows for continuous material flow into the biogas digesters with total capacity of 2500m^3 (EWE Biogas GmbH in Surwold, Germany)

6.5.2 Simulation of the biogas process production in EWE Biogas GmbH, Surwold

The proposed model was modified to predict the EWE biogas plant by implementation of additional pre-steps before the biogas fermenter: manure and substrate receiving tanks, sanitation and buffer tank and adaptation to the continuous stirred tank reactor. The expanded model structure of the model is located in Appendix 3. For the prediction the set of parameters from the Table 6-2 was applied. The used state variables are listed in the Table 6-7. The maximum uptake rate for VFA was increased from $8.20 \cdot 10^{-6}$ to $2.52 \cdot 10^{-5}$ s^{-1}. The flow of waste and manure through the tanks cascade with the state variables in the biogas fermenter is shown on the Figure 6-22. The process scheme displays dynamics of the master substrates and corresponding inflow and outflow rates (F_{in} and F_{out}, F_{min} and F_{mout}, F_{sout}, F_{bout} and F_{fout}). The composition of waste was presented as a varying mixture of carbohydrates (C_{S10}), proteins (C_{S20}) and lipids (C_{S30}). Manure and waste were mixed together in a sanitation unit. The content of manure was assumed to be equal parts of the master substrates. From the sanitation tank master substrates: C_{S1s}, C_{S2s} and C_{S3s}, were mixed in a buffer tank. Finally, the master substrates from the buffer tank: C_{S1sb}, C_{S2sb} and C_{S3sb}, were anaerobically utilized in the biogas fermenter. The master substrates coming from the buffer tank were disintegrated with generation of particulate substrates (*Cp*, *Pp*, and *Lp)* which were hydrolyzed to produce accessible soluble substrates (C_S, P_S and L_S). Acidogenic bacteria (*Xaci*) consumed the simple organics and produced CO_2 and *VFA.* The intermediate product was converted by methanogenic bacteria (*Xmeth*) into methane (CH_4) and carbon dioxide (CO_2). More detailed description of the transformation of particulate substrates into biogas is depicted in Sections 5.2 - 5.4.

Table 6-7: The list of applied state variables for prediction of the substrates dynamics through the tanks cascade with the biogas fermenter at the final step

State variable	Value	Units
X_{aci}	9.8	$[kg \cdot m^{-3}]$
X_{meth}	8.3	$[kg \cdot m^{-3}]$
C_P	2.67	$[kg \cdot m^{-3}]$
P_P	5.33	$[kg \cdot m^{-3}]$
L_P	7.33	$[kg \cdot m^{-3}]$
VFA	$7.15 \cdot 10^{-5}$	$[mol \cdot m^{-3}]$
μ_{VFA}^{max}	$2.52 \cdot 10^{-5}$	$[s^{-1}]$

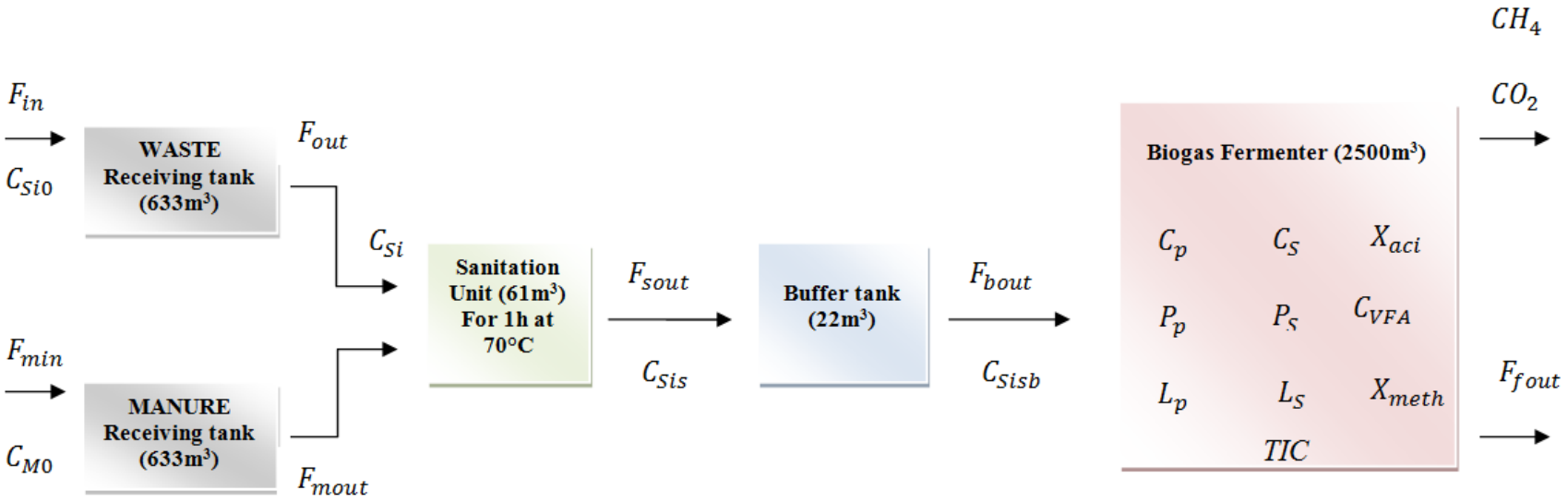

Figure 6-22: The Surwold process scheme of the substrates feed through the tanks cascade and final product generation. C_{Si0}, C_{M0} – initial concentrations of waste and manure, respectively, where *i* equals 1, 2, 3 and correspond to carbohydrates, proteins and lipids, respectively; C_{Si} - the waste concentration after receiving tank, C_{Sis} - the feedstock concentration after sanitation unit; C_{Sisb} - the feedstock concentration after the buffer tank; *CpP*, *CpC*, and *CpL*: *primary* carbohydrates, proteins and lipids, respectively are hydrolyzed into simple accessible mono-/oligomers: C_S, P_S and L_S: carbohydrates, proteins and lipids, respectively by the acidogenic bacterial group (X_{aci}) which produce CO_2 (total inorganic carbon: *TIC*) and volatile fatty acids (*VFA*). Finally, methanogenic bacteria (X_{meth}) convert VFA (*VFA*) into methane (CH_4) and carbon dioxide (*TIC*). F_{in} and F_{out}, F_{min} and F_{mout} - influent and effluent flows of waste and manure into and from the receiving tank. F_{sout}, F_{bout} and F_{fout} - effluent of mixture of substrates mixtures from sanitation unit, buffer tank and biogas fermenter, respectively

6.5.3 Characteristics of the used feedstock in EWE Biogas GmbH, Surwold

During one year (2010) various types of waste were utilized such as flotation sludge, fats and fat residues, blood, glycerol, mucilage, greaves, food residues, whey, grease, stomach- intestinal residues, food leftovers, and ice cream. The substrates quantity and quality were varied from day to day and its usage depended only on the feedstock supplier. EWE Biogas GmbH in Surwold, shared with us the following information:

- A daily input of substrates and manure (the name of the substrate, the amount per day). The list of the substrates digested and their mass is located in Appendix 3.
- Substrate feeding rate of waste and manure (mean value) which was calculated from the total organic material input per month over number of calendar days is shown on the Figure 6-23. The inflow rate of manure was varying between 47 - 68 $m^3 d^{-1}$ and inflow rate of organic waste was in a range of 80 - 111 $m^3 d^{-1}$.
- The generation of the volume of biogas is shown on the Figure 6-24. The total amount of gas yielded 2,026,640.63 m^3.
- The volumetric concentrations of methane and carbon dioxide which was measured 4-6 times per month are presented on the Figure 6-25. The average CH_4 concentration was 70.2 Vol.-% and for CO_2 – 28.8 Vol.-%.

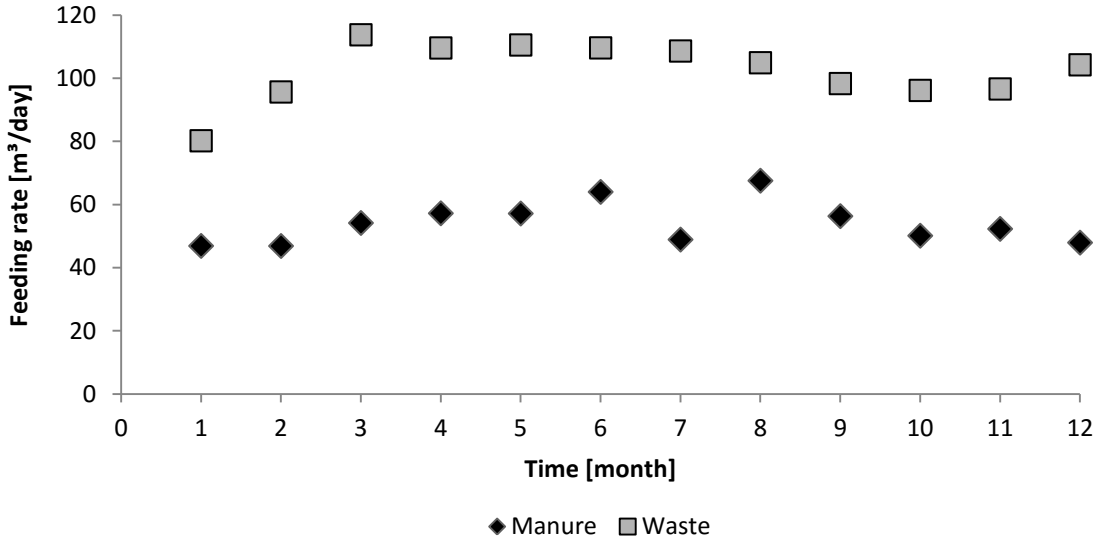

Figure 6-23: Feeding rate of manure and waste into the receiving tank which was defined from the total monthly feed over the calendar number of days (EWE Biogas GmbH in Surwold, Germany)

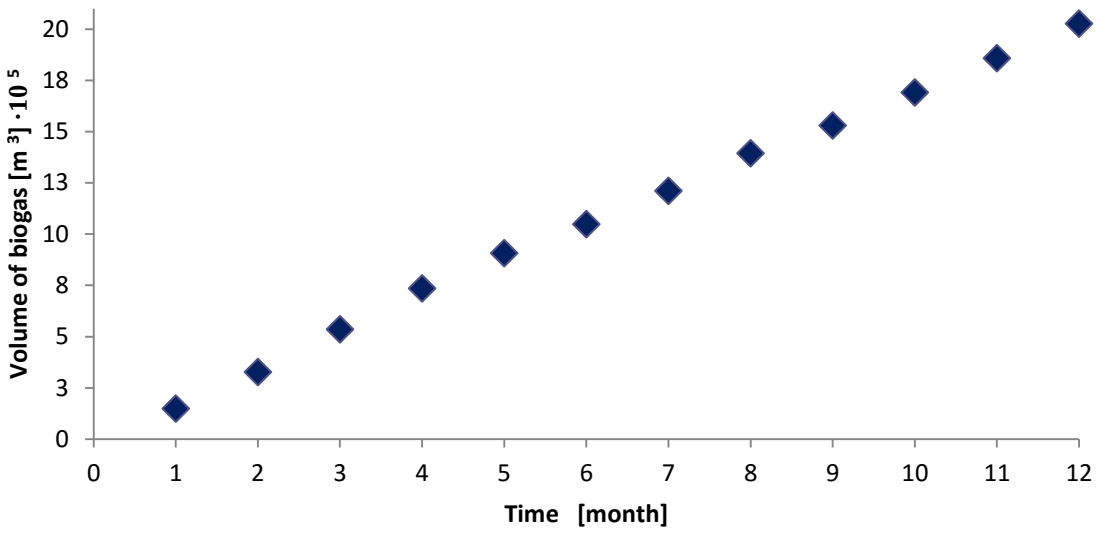

Figure 6-24: Biogas volume was measured monthly and summed up with a total amount of 2,026,640.63 m^3 (EWE Biogas GmbH in Surwold, Germany)

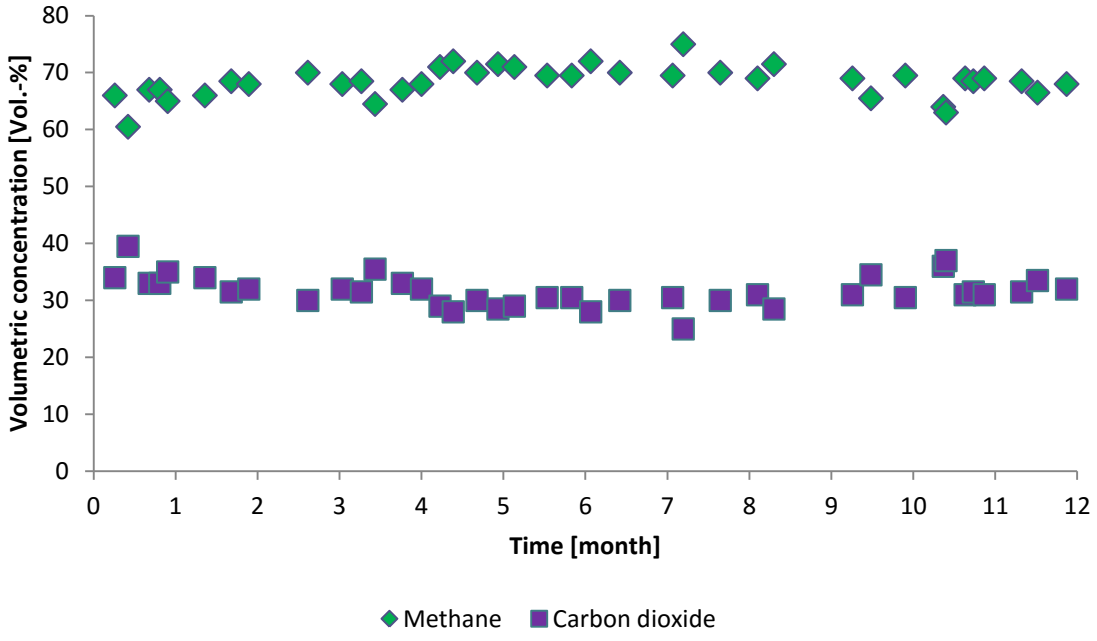

Figure 6-25: The volumetric composition of biogas from 04.01.2010 - 27.12.2010; the average CH_4 concentration was 70.2 Vol.-% and for CO_2 – 28.8 (Vol.-%) (EWE Biogas GmbH in Surwold, Germany)

6.5.4 Estimation of the substrates concentration

For the prediction of the AD process for the tanks cascade system it was decided to make some assumptions and the following calculations:

1. *Chemical composition of the substrate*

In order to fulfill the lack information about the chemical composition of the waste substrates and manure it was decided to rely on the literature data. In the case when the composition was unknown we assumed the equal content of proteins (P), carbohydrates (C) and lipids (L) for each substrate. The list of chemical composition of the utilized waste which was based on the literature data is shown in Table 1-3, Section 1.5. The assumed proportion of the used substrates is presented in Table 6-8. The following calculations of the substrate concentration accounted that the mass of the substrate varied each time, the different types of substrate were digested, the amount of substrates was varying daily meaning of digestion only one type of waste or four different per day.

Table 6-8: Assumed percent amount of proteins, carbohydrates and lipids in different types of waste, P-proteins, C- carbohydrates, L-Lipids

Feedstock	Organic content
Overstored food and leftovers	P, C, L: 33.3%
Mucilage	P: 20%, C:80%
Blood	P:10% , C, L
Glycerin	L:100%
Manure (cattle)	P, C, L: 33.3%

2. Calculation of the substrate concentration from the data

For estimation of the composition of the master substrates the following procedure was applied:

- calculation the amount of P, C and L for each added substrate by multiplication the daily input of organics on percent amount of P, C and L. The percent amount of the master substrates in waste is shown in Table 1-3, Section 1.5. The assumed proportion is shown in Table 6-8;

- calculate the amount of the master substrates digested per day by summarizing the P, C and L for each added substrate;

- from the obtained mass the water content and non-degradable parts were subtracted. The dry mass of the digested substrates is shown in Table 1.3 (Deublein and Steinhauser, 2008). The non-degradable part was assumed as 30% of DM (see Appendix 3).

3. Feeding rate of substrates and manure

The inflow and outflow rates F_{in} and F_{out}, F_{min} and F_{mout}, F_{sout}, F_{bout} and F_{fout} were converted from the measured data of t month^{-1} to kg s^{-1} (see Appendix 3)

6.5.5 Simulation results: studies of the dynamics of the organic matter concentrations through the tanks cascade and within the biogas fermenter

Having applied all mentioned calculations above, the biogas model generated the following results of simulations shown in the Figure 6-27. The graphs represent the substrate concentration dynamics through the tanks cascade for proteins, carbohydrates and lipids individually. During 12 month simulation the concentration of proteins was varying from 5 to 30 kg m $^{-3}$. The concentration of carbohydrates was ranging between 5-25 kg m $^{-3}$ while the concentration of lipids was changing between 2-20 kg m^{-3}. By comparing the dominance of the master substrates during the year the proteins among the others had relatively stable increase and decrease picture. The most amount of the simulated concentration of carbohydrates was digested during March, May and June, then from August till the middle of September. Figure 6-27 shows that the first four months the concentration of lipids was dropping and rising from 2-20 kg m $^{-3}$. Starting from April the concentration started to increase smoothly and by the December it reached 15 kg m $^{-3}$. After mixing waste and manure together in the sanitation unit, the components concentration decreased due to dilution by manure. Besides, there is a shift to the right side of the components concentrations accordingly to the tanks order in the row. The change of the manure concentration is not shown because we assumed that components proportion in the manure are constant and only the feeding rate of manure was deviating monthly. The feeding rate of manure is shown in Appendix 3.

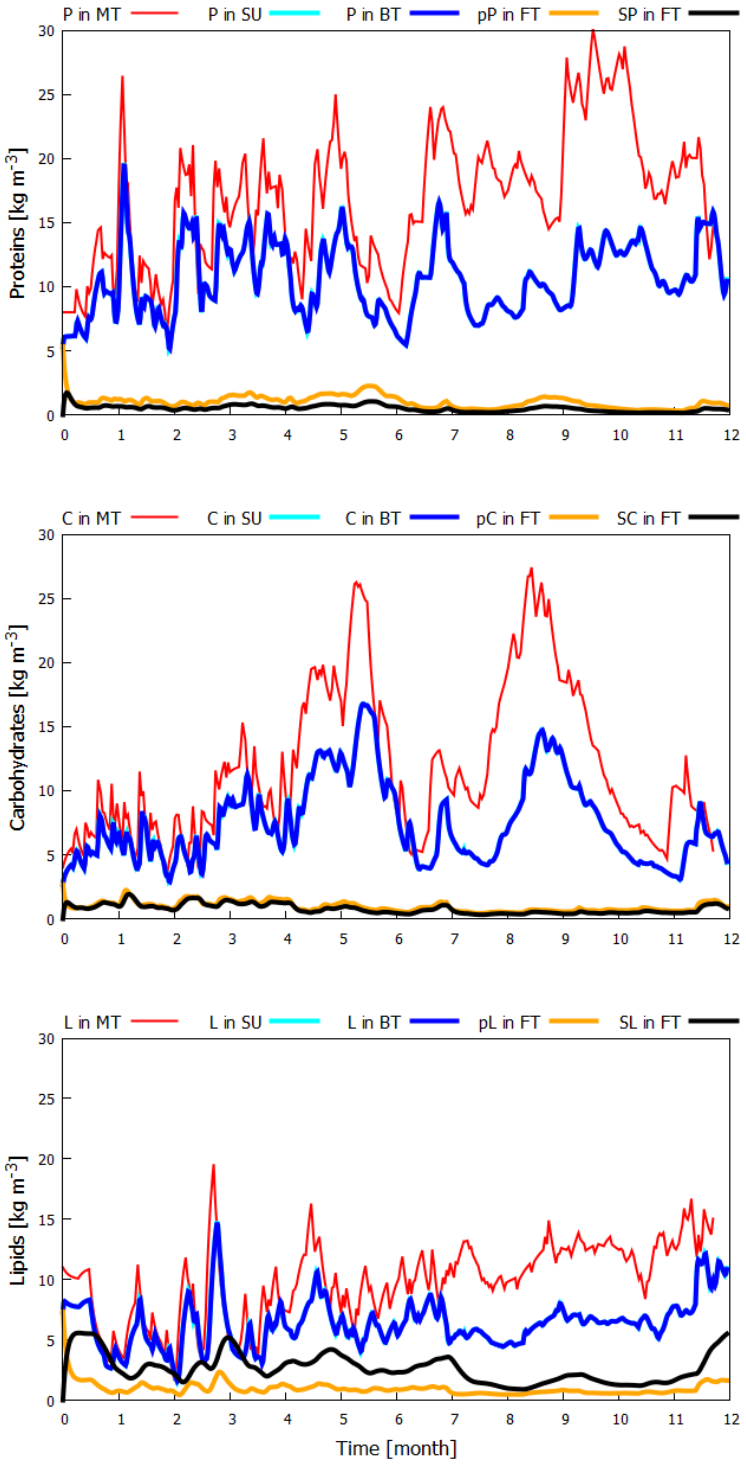

Figure 6-27: Simulations of the concentration dynamics of the digested proteins (P), carbohydrates (C) and lipids (L) through the tanks cascade: MT – mixing tank, SU – sanitation unit, BT – buffer tank, FT – fermenter, P, C and L - proteins, carbohydrates and lipids, respectively; pP, pC, pL – primary proteins, carbohydrates and lipids, respectively; SP, SC, SL – accessible proteins, carbohydrates and lipids, respectively

Figure 6-28 shows the simulated concentration of VFA which was changing from $9.5 \cdot 10^{-3}$ mol m^{-3} to $1.2 \cdot 10^{-1}$ mol m^{-3}. During a year two considerable peaks and two small at the end of simulation were observed. In the beginning of the first month the highest peak reached 1.07 mol m^{-3}. The second high peak was detected in the beginning of March and was equaled $7.73 \cdot 10^{-1}$ mol m^{-3}.

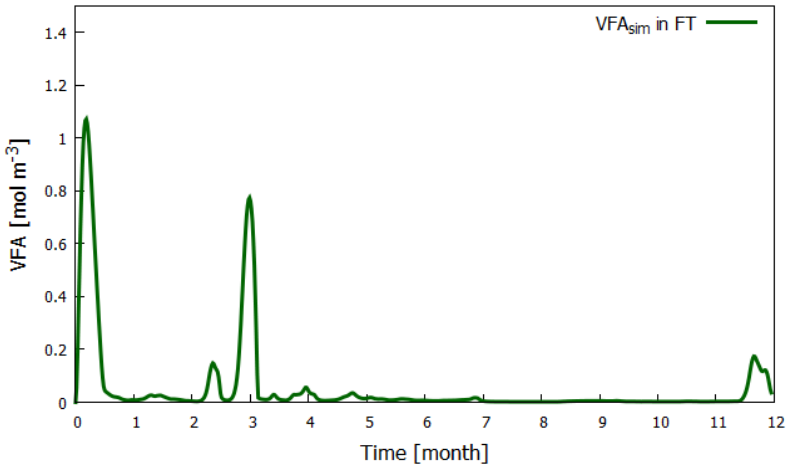

Figure 6-28: Simulations of the concentration dynamics of VFA

The calculated mixture of the master substrates, finally, predicted the following dynamics of the volumetric concentrations of methane and carbon dioxide and production of biogas which are shown in the Figure 6-29. Generally, throughout the fermentation the concentration of methane was maintained at the mean value of 70.2 Vol.-%. Annual concentration of CH_4 was not undergone any considerable deviations. However, after the first month there was a drop to 62 Vol.-% and back increase within the following two weeks. The second drop from 70 to 64 Vol.-% of CH_4 was observed at the end of February. The model could predict the second decrease of the concentration. The simulated biogas volume reached $2.09 \cdot 10^5$ m^3 while the measured biogas yielded $2.26 \cdot 10^5$ m^3.

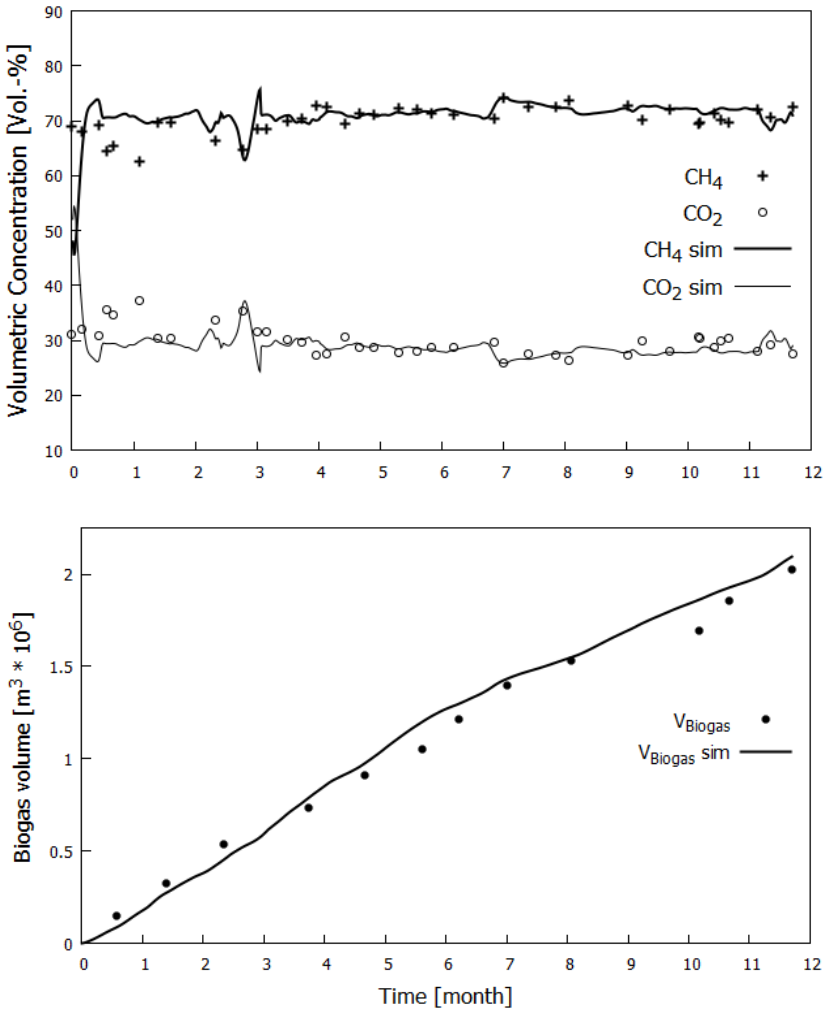

Figure 6-29: Prediction of the volumetric concentration of CH_4 and CO_2 (Vol.-%) in the biogas fermenter and generation of the volume of biogas in the biogas fermenter are shown here. The measured data is presented by dots and simulated dynamics is given in lines.

6.6 Sensitivity analysis of the parameters

For the sensitivity analysis the kinetics parameters ($k_{hyd\,X}$, K_{X_s}, μ_X^{max}, Y_{XX} and U_X, where X is a master-substrate) were ranging at ± 40%, ± 60% and ± 80% from the reference value. As a reference the estimated values for parameters were applied (see Table 6-2). The applied variations of the kinetic parameters for carbohydrates, proteins and lipids are shown in Tables 6-9, 6-10 and 6-11, respectively. Only one parameter had been changed per one simulation. Variations of the volume of biogas generation dependent on changes of parameters are shown in Figures 6-30 - 6-33.

Table 6-9: Deviations of $k_{hyd\,C}$, K_{X_C}, μ_C^{max}, Y_{XC} and U_C used for the sensitivity analysis

	$k_{hyd\,C}$	K_{C_s}	μ_C^{max}	Y_{XC}	U_C
-80%	$1.58 \cdot 10^{-6}$	1.3	$8.40 \cdot 10^{-7}$	0.044	0.126
-60%	$3.16 \cdot 10^{-6}$	2.6	$1.68 \cdot 10^{-6}$	0.088	0.252
-40%	$4.74 \cdot 10^{-6}$	3.9	$2.52 \cdot 10^{-6}$	0.132	0.378
+40%	$8.69 \cdot 10^{-6}$	9.1	$5.88 \cdot 10^{-6}$	0.308	0.882
+60%	$1.26 \cdot 10^{-5}$	10.4	$6.72 \cdot 10^{-6}$	0.352	1.01
+80%	$1.42 \cdot 10^{-5}$	11.7	$7.56 \cdot 10^{-6}$	0.396	1.13
Reference	**$7.90 \cdot 10^{-6}$**	**3.9**	**$4.20 \cdot 10^{-6}$**	**0.220**	**0.63**

Table 6-10: Deviations of $k_{hyd\,P}$, K_{X_P}, μ_P^{max}, Y_{XP} and U_P used for the sensitivity analysis

	$k_{hyd\,P}$	K_{C_P}	μ_P^{max}	Y_{XP}	U_P
-80%	$1.02 \cdot 10^{-6}$	1.0	-	0.1	0.13
-60%	$2.04 \cdot 10^{-6}$	2.0	$1.32 \cdot 10^{-6}$	0.2	0.26
-40%	$3.06 \cdot 10^{-6}$	3.0	$1.98 \cdot 10^{-6}$	0.3	0.39
+40%	$7.14 \cdot 10^{-6}$	7.0	$4.62 \cdot 10^{-6}$	0.7	0.91
+60%	$8.16 \cdot 10^{-6}$	8.0	$5.28 \cdot 10^{-6}$	0.8	1.04
+80%	$9.18 \cdot 10^{-6}$	9.0	$5.94 \cdot 10^{-6}$	0.9	1.17
Reference	**$5.10 \cdot 10^{-6}$**	**5.0**	**$3.30 \cdot 10^{-6}$**	**0.5**	**0.65**

Table 6-11: Deviations of $k_{hyd\,L}$, K_{X_L}, μ_L^{max}, Y_{XL} and U_L used for the sensitivity analysis

	$k_{hyd\,L}$	K_{C_L}	μ_L^{max}	Y_{XL}	U_L
-80%	$^{-7}$	0.64	-	0.11	0.192
-60%	-	1.28	-	0.22	0.384
-40%	$2.74 \cdot 10^{-6}$	1.92	$3.36 \cdot 10^{-6}$	0.33	0.576
+40%	$6.38 \cdot 10^{-6}$	4.48	$7.84 \cdot 10^{-6}$	0.77	1.34
+60%	$7.30 \cdot 10^{-6}$	5.12	$8.96 \cdot 10^{-6}$	0.88	1.54
+80%	$8.21 \cdot 10^{-6}$	5.76	$1.01 \cdot 10^{-5}$	0.99	1.73
Reference	**$4.56 \cdot 10^{-6}$**	**3.20**	**$5.60 \cdot 10^{-6}$**	**0.55**	**0.96**

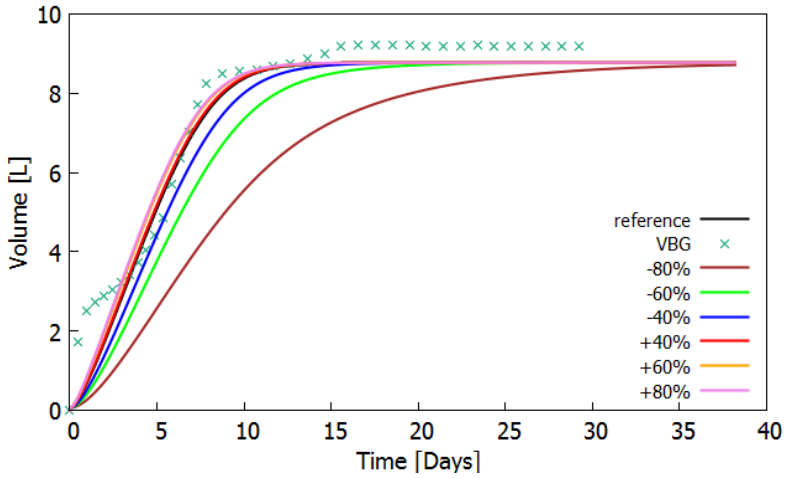

A.

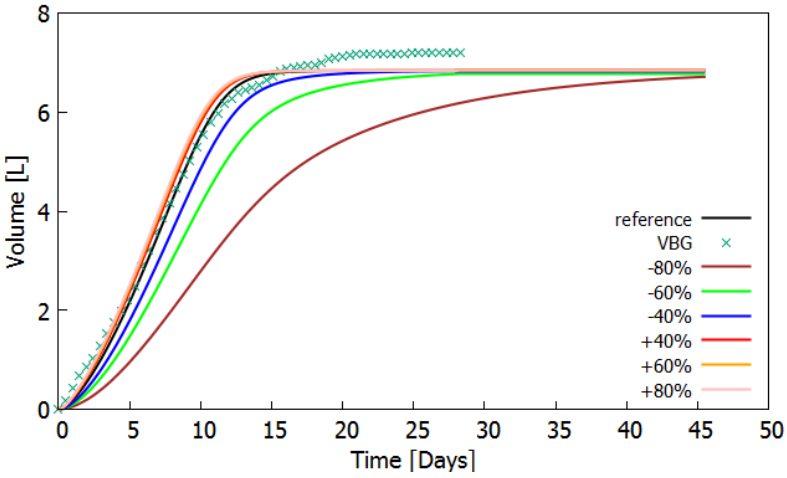

B.

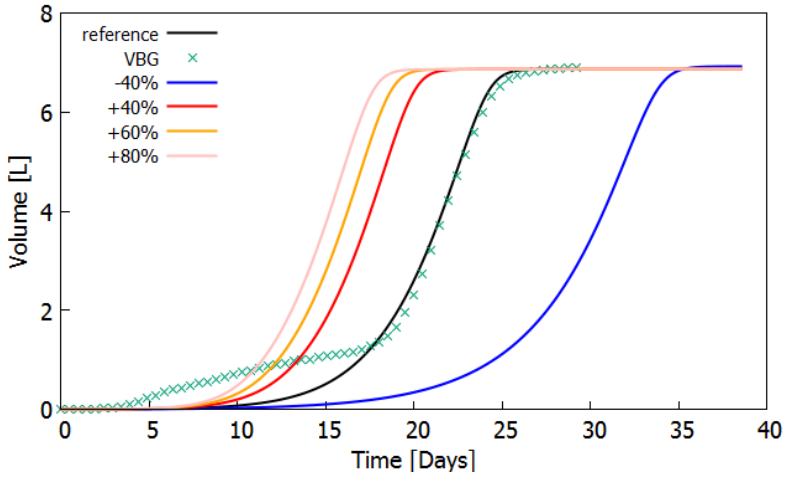

C.

Figure 6-30: Effect of the changes of $k_{hyd\,C}$ - A, $k_{hyd\,P}$ - B and $k_{hyd\,L}$ - C on the biogas production. VBG - the volume of biogas

The output results of the volume of biogas became almost unchanged when $k_{hyd\,C}$ and $k_{hyd\,P}$ were increased on 80% as compared to measured data (Figure 6-30A and B). It is found that a 80% decrease of the hydrolysis constants for proteins and carbohydrates resulted in 33% and 44% drop in the VBG on the day 12, respectively (Figure 6-30A and B). When $k_{hyd\,L}$ was incresed on 80% the maximum of the volume of biogas (VBG) was reached on five days earlier as compared to reference data (Figure 6-30C). As a reference the best simulated fit to the experimental data was used. With decrease on 40% the maximum VBG was achieved ten days later as compared to the reference data.

Figure 6-31A and Figure 6-32A show that ±80% fluctuations of K_{C_S} and K_{C_P} resulted in ±7.5% ranging in VBG. Ranging of K_{C_L} at ± 80% led to fluctuations of VBG ±12% from the reference curve (Figure 6-33A).

Figure 6-31B and Figure 6-32B show that increase of μ_C^{max} and μ_P^{max} led to 13% and 7% increase, respectevely. With decrease of the maximum uptake rates on 60% the output of VBG dropped on 14% for sucrose and on 23% for gelatine. Increase of μ_L^{max} on 80% resulted in right-sided shift and generation of the maximum VBG one week yealier comparing with the reference curve (Figure 6-33B). Right-sided shift and 6 days delay of the maximum VBG followed after decrease of μ_L^{max} by 40% . The influence on the final VBG yield of ranging of the yield factor for primary carbohydrates, proteins and lipids degradation (Y_{XC}, Y_{XP} and Y_{XL}) and the yield factor for VFA production from carbohydrates, proteins and lipids (U_C, U_P and U_L) are summed up in Table 6-12. As a reference values the simulated yield of biogas for each master substrate were applied.

Table 6-12: Effect of Y_{XC} and U_C , Y_{XP} and U_P, Y_{XL} and U_L on the final volume of biogas

	Y_{XC}	U_C	Y_{XP}	U_P	Y_{XL}	U_L
-80%	+20%	-18%	+80%	-12%	+97%	-17%
-60%	+14%	-15%	+60%	-9%	+73%	-13%
-40%	+9%	-12%	+40%	-6%	+49%	-8%
Reference [L]	**8.72**	**8.72**	**6.83**	**6.83**	**6.9**	**6.9**
+40%	-13%	+4%	-40%	+6%	-49%	+8%
+60%	-18%	+7%	-60%	+9%	-73%	+13%
+80%	-24%	+9%	-80%	+12%	-97%	+17%

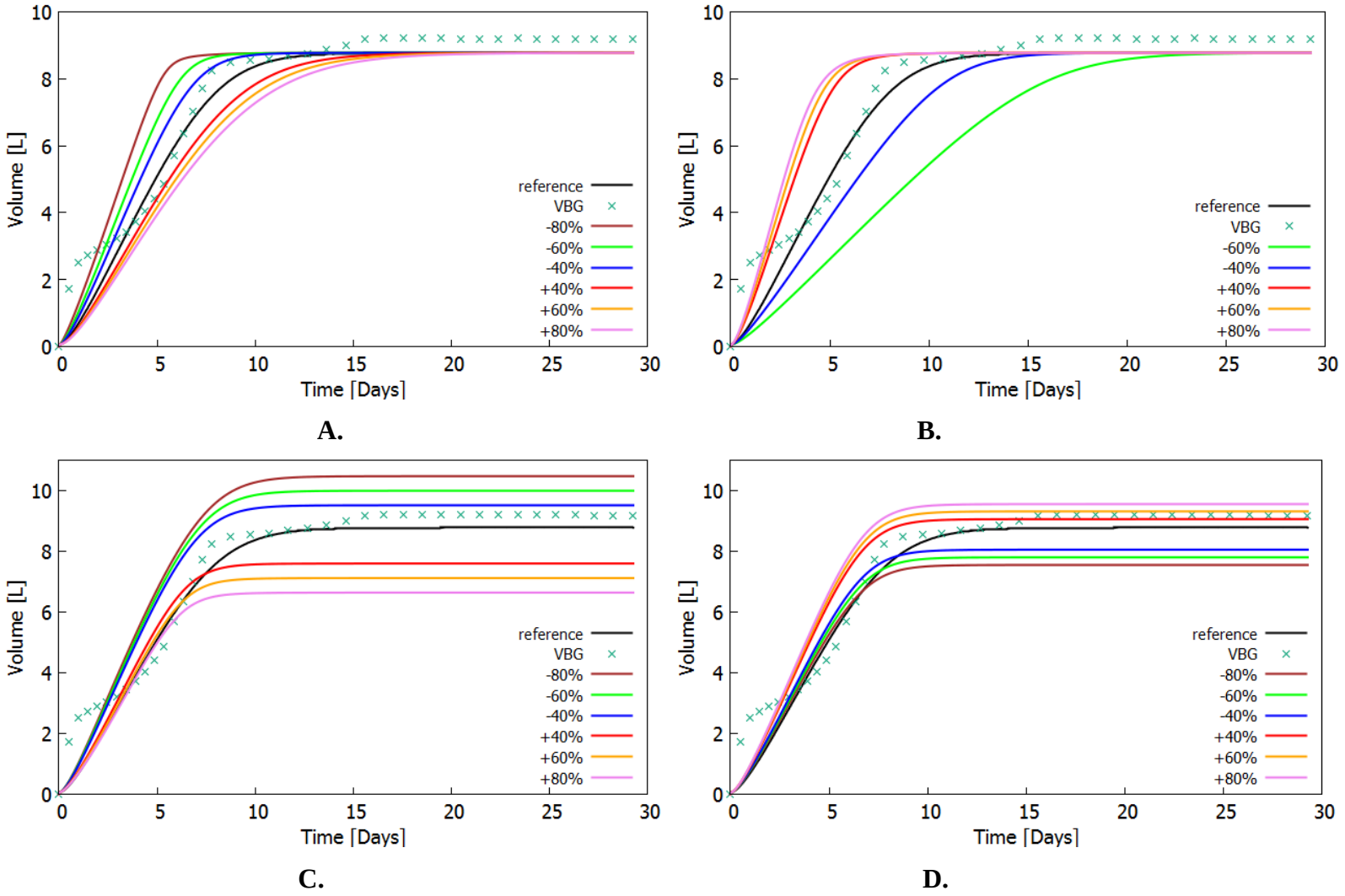

Figure 6-31: Effect of the changes of K_{C_s} - **A**, μ_C^{max} - **B**, Y_{XC} - **C** and U_C - **D** on the biogas production. VBG - the volume of biogas

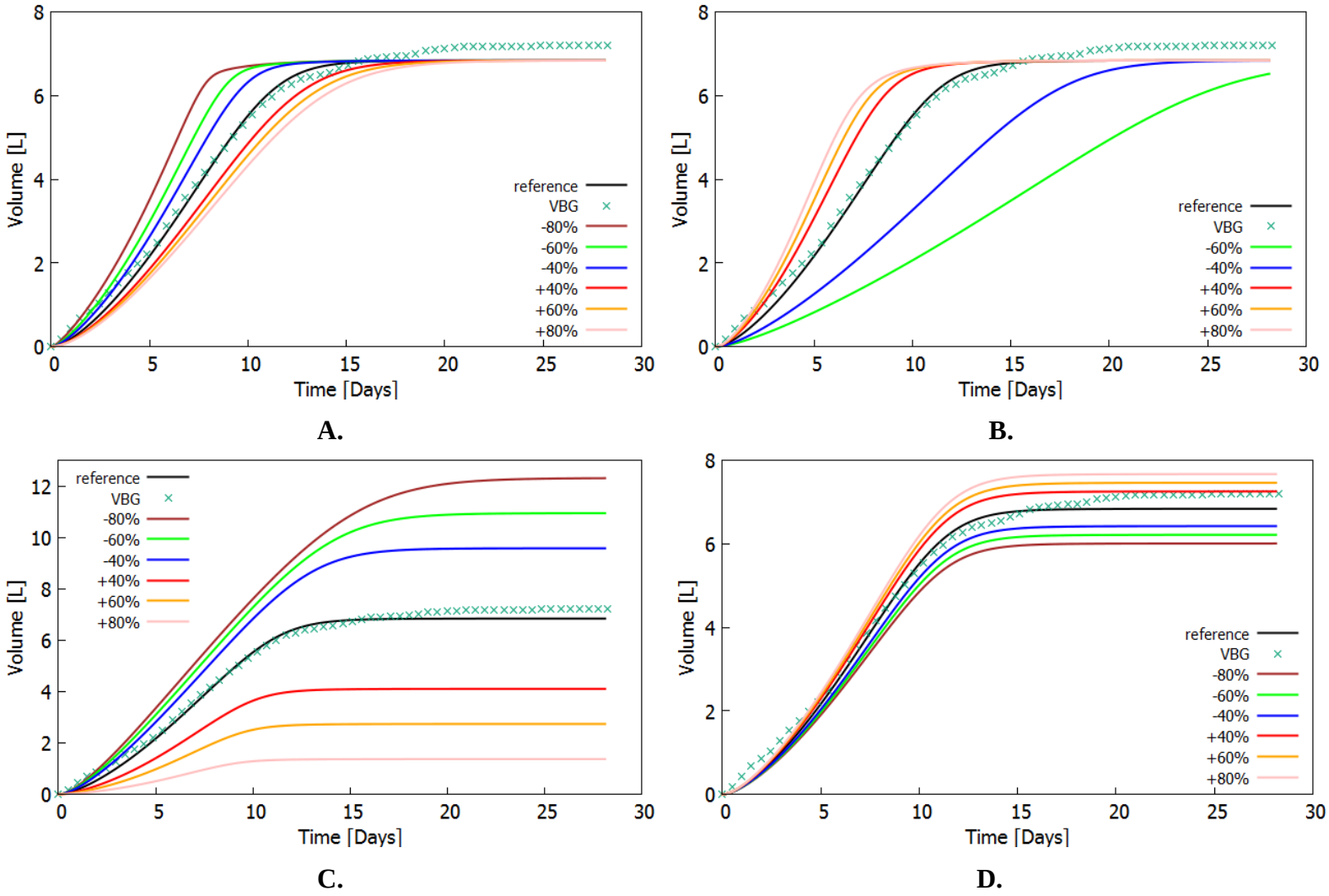

Figure 6-32: Effect of the changes of K_{C_P} - **A**, μ_P^{max} - **B**, Y_{XP} - **C** and U_P - **D** on the biogas production. VBG - the volume of biogas

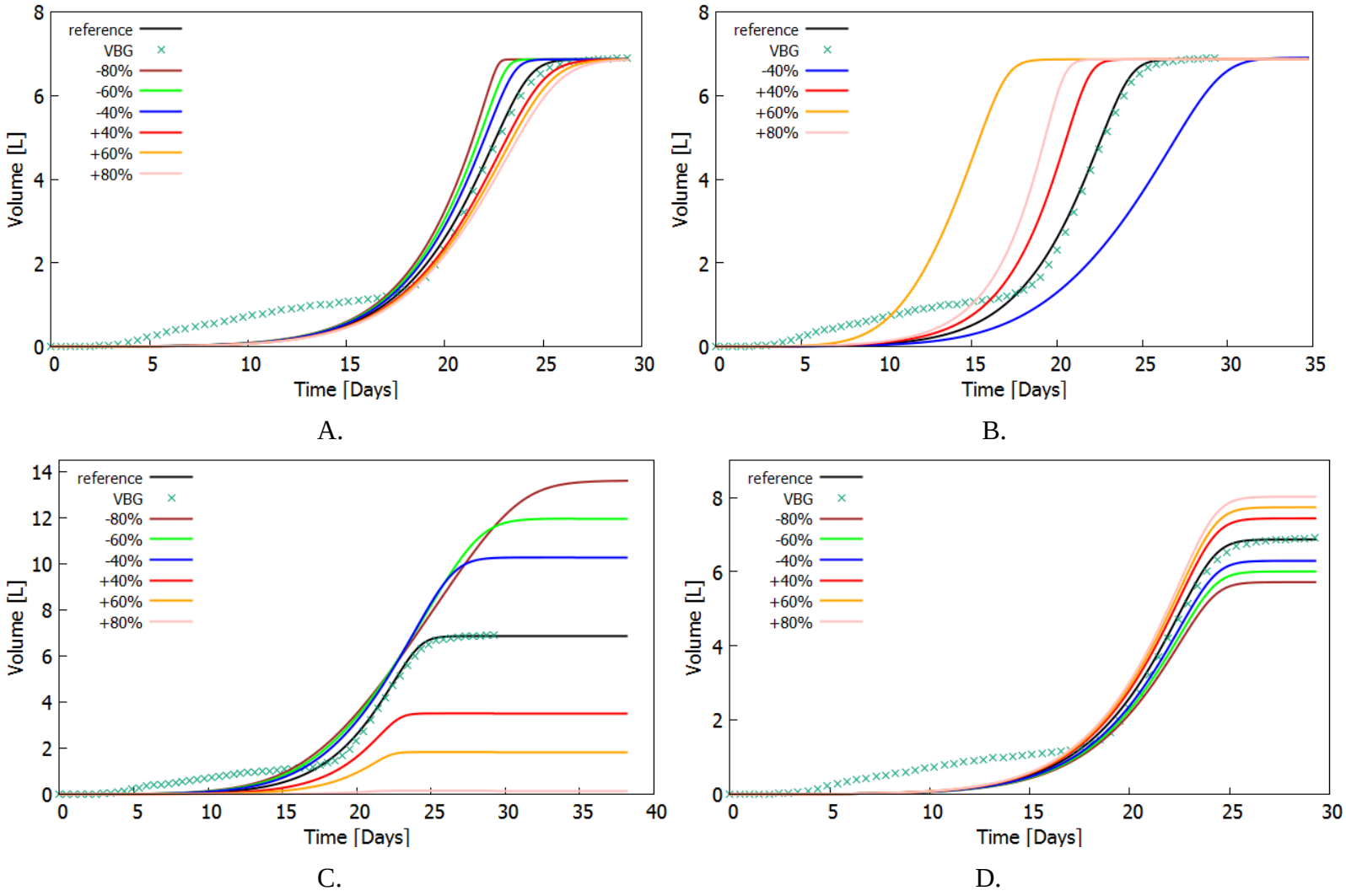

Figure 6-33: Effect of the changes of $\boldsymbol{K_{C_L}}$ - **A**, μ_L^{max}- **B** $\boldsymbol{Y_{XL}}$, - **C** and $\boldsymbol{U_L}$ - **D** on the biogas production. VBG - the volume of biogas

6.7 Sensitivity analysis of the process variables

In order to examine the dependence of the substrate concentration on the process variables several scenarios were developed. The effect of various input compositions on biogas generation in batch was studied. A percent amount of carbohydrates, proteins and lipids was varied in mixture of those. In order to maintain the substrate/inoculum ratio, the total mass of the mixture was kept constant at 14 g L^{-1}. That means, if mass of a certain substrate was increased on 50%, a mass of two rest substrates was decreased by the 25% for each. And vice versa, with decrease by 50%, the amount of others was increased by 25% each. Concentrations of the master-substrates in mixture were used as reference values. All numbers applied for the simulation scenarios are listed in Table 6-13. The chosen concentrations were applied for simulations of VBG simulations which are shown on Figure 6-34. The simulations showed that fluctuations of sucrose and rape seed oil in ±50% resulted in ±5 % and 2.5% fluctuations in VBG. Both increase and decrease of gelatine by 50% led to decrease in VBG by -2% and -6%, respectively. The simulated curves "- 50% Gelatine" and "+ 50% Rape seed oil" were overlapping each other in Figure 6-34.

In addition, the effect of increase of master-substrates on the volume generation of biogas in continuous mode was studied. For the simulations the feed concentrations of three master-substrates from the biogas process production (EWE Biogas GmbH in Surwold, Germany) were used as a basis (see Section 6.5). The amount of each master-substrates of choice was increased by 33% per one simulation.

Table 6-13: Full set of six scenarios

	Sucrose [g L^{-1}]	**Gelatine [g L^{-1}]**	**Raps [g L^{-1}]**
- 50% Sucrose	2.5	7.25	4.25
- 50% Gelatine	6.5	3	4.5
- 50% Rape seed oil	5.75	6.75	1.5
+ 50% Sucrose	7.5	4.75	1.75
+ 50% Gelatine	3.5	9	1.5
+ 50% Rape seed oil	4.25	5.25	4.5
Reference	**5.0**	**6.0**	**3.0**

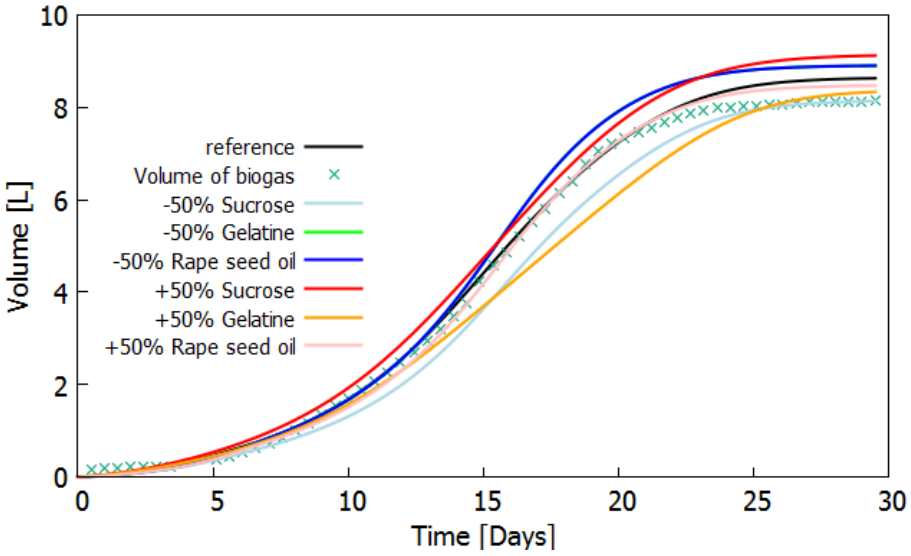

Figure 6-34: Effect of the changes of the substrates concentrations on the volume of biogas

The influence of changes of the feed concentrations of carbohydrates, proteins and lipids on the volumetric concentration of CH_4 and generation of the volume of biogas is shown in Figure 6-35. The predicted volumetric concentration of CH_4 in the biogas fermenter and generation of the volume of biogas were used as reference curves (see Figure 6-25).

Increase of lipids and decrease of carbohydrates on 33% resulted in increase of the volumetric concentration of methane in a range of 0.5-12.5% (Figure 6-35A and B). And vice versa, increase of carbohydrates lipids and decrease of lipids in 33% resulted in decrease of the CH_4 concentration in a range of 0.5-2.5%. Fluctuation of the feed concentration of proteins on ± 33 resulted in insignificant changes in the CH_4 concentration.

Figures 6-35C and D show that increase and decrease of carbohydrates on 33% resulted in increase of the final volume of biogas on 16% and drop in 20% as compared to the reference curve. The lowest fluctuation in VBG was observed in the case of ranging of the feed concentration of lipids.

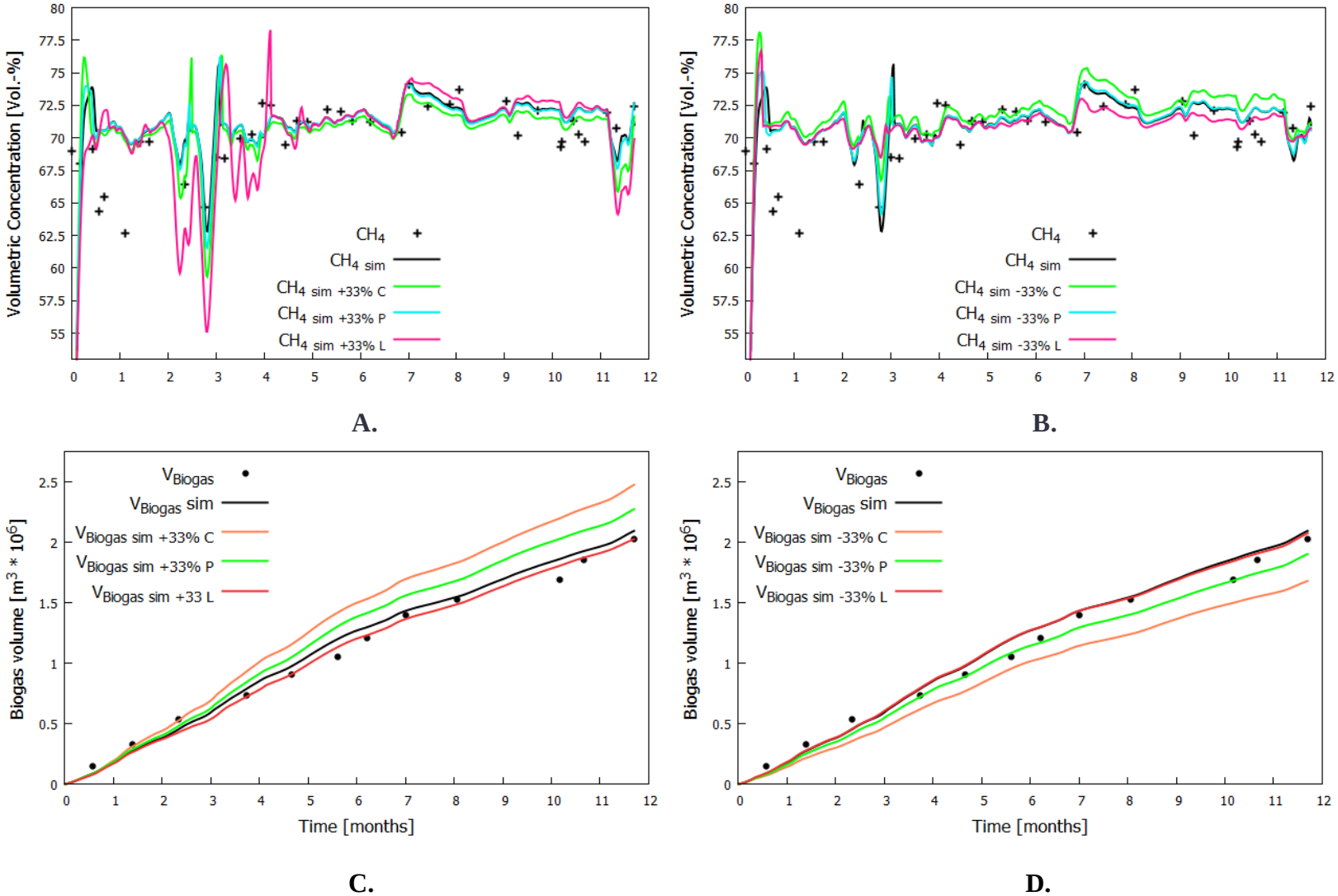

Figure 6-35: Simulated volumetric concentration of CH_4 [Vol.-%] (A-B) and the volume of biogas [$m3 \cdot 10^6$] (C-D)

DISCUSSION

Anaerobic digestion of biomass has become increasingly demandable, basically, due to strong support by European and national funding and remuneration schemes (see Section 1.1). Furthermore, the applicability of the AD processes is justified by reliable and economically feasible technology. The process of biogas production is quite complex implying the simultaneous performance of physical, chemical and biological reactions catalyzed by a consortium of various bacteria and additionally influenced by seasonal changes and daily feeding (see Section 1.3). The AD production process depends mainly on the digestion stability, which, in turn, is influenced by the chemical composition of the feedstock (see Section 1.5). In operating biogas plants, the organic waste undergoes high fluctuations in quantity and chemical content. In consequence, it affects bacterial growth and overall performance of the AD process. Successful feedstock combinations require a method to foresee the process outcome when new input waste material is introduced into the system.

Dynamic simulation models represent a quite attractive method for studying and improving the biogas process dynamics (Wolf et al., 2009) (see Section 2.3). From the literature overview it is known that the AD process has to deal with a huge variety of substrates (see Section 1.5). Many biogas models simulate the AD dynamics for a concrete type of waste which consumes a lot of effort and time. In this study we set a task to find a simple approach to map the variety of organic waste. Since the structures of substrates conversion models had a lot in common (see Section 2.6 - 2.9), in this study a relatively simple model (see Section 5.2 – 5.4) was formulated based on the general features of already existing models and on the previous experience with ADSIM model (Korjik, 2010; see Section 2-8). The proposed biogas model was used for testing of the substrate linearity hypothesis (see Section 3.2) and for the prediction of the effect of deviation of waste content and amount on the AD process and final CH_4 yield.

Within the scope of this work the following questions were clarified:

- Can a biogas model represent any mixture of organic waste as three master substrates?

- Can a biogas model be applied for both batch and continuous fermentations?

- Can a biogas model be applied for laboratory-scale and industrial-scale fermenter?

- To what extent the proportion of master substrates influence on the CH_4 yield and stability of the AD?

Below the experimental results, the model parameterization and verification are discussed. The following application of the biogas model for simulation of the continuous AD with PWW and starch is discussed. Finally, the simulation studies of the dynamics of the waste composition through the tanks cascade system was discussed.

7.1 Experimental results of the batch experiments

For the model parameterization batch experiments with sucrose, gelatine and rapeseed oil were carried out. The calibrated model was verified by experimental data from batch fermentation of those substrates mixture. Besides, we allowed several assumptions of the digestion: constant temperature, constant digester volume, perfect mixing, and complete digestion of the organic input, products of the digestion only include CO_2 and CH_4 and bacterial biomass. These process assumptions are the demanding prerequisites of the biogas model.

For more precise estimation of the model parameters the generation and consumption of VFA had to be measured during batch fermentation. In order to measure the dynamics of the intermediate substrate – VFA, the input concentration of substrates was changed by doubling the ratio oTS substrate/oTS inoculum (S/I) as compared to VDI 4630 protocol (see Section 4.1.1; German Engineers Association, 2006). The reason of the S/I ratio increase was in that the digested substrates were easily degradable and VFA´s were consumed by methanogenic bacteria immediately, right after the generation. The concentration of VFA were not measured due to technical reasons. Because of the change of the S/I ratio as compared to the recommended experimental procedure by VDI, it can

potentially lead to variation in the CH_4 yield. From other studies the doubling of the S/I ratio does not lead to the dramatic difference in the CH_4 yield. Yoon et al. (2014) found that the methane yields varied slightly over the range used, with an average of 0.084 by ± 0.007 Nm^3 / kg-blood, 0.141 ± 0.01 Nm^3 / kg- intestine residues and 0.101 ± 0.012 Nm^3 / kg- digestive tract content using three S/I ratios (0.5, 1.0 and 1.5). In addition, Raposo et al. (2006) carried out batch tests with maize at S/I ratios 3, 2, 1.5 and 1. The methane yielded little variation with an average value of 211 ± 6 ml CH_4 at standard temperature and pressure (STP) conditions per g VS added.

Batch fermentation with sucrose In previous studies it has been shown that the methane yield produced from the AD of sucrose varied in range of 240 - 360 ml CH_4 /g VS (Hansen et al., 2004, Matsakas et al., 2014). Kyazze et al. (2007) investigated the performance of a mesophilic two-stage system generating hydrogen and methane continuously from sucrose. As a result, 10 g L^{-1} sucrose yielded of 323 ml CH_4/g COD added which is nearly the same as in this study - 330 ml CH_4/g COD added (see Figure 6-16). Blesgen (2009) carried the batch experiment with sucrose which resulted in 210 ml biogas /g sucrose added. The present mean CH_4 yield matches the published results and equaled 301 ml CH_4 /g VS added (see Figure 6-14).

Batch fermentation with gelatine BMP tests with gelatine were carried out by Hansen et al. (2004) and 100-150 ml CH_4 /g VS were produced which is lower as compared to 244 ml CH_4 /g VS obtained in this work (see Figure 6-14). Blesgen (2009) carried out the batch experiment with gelatine which resulted in 420 ml biogas /g gelatine added. This yield is close to the measurements in the present study - 0.45 ml biogas /g gelatine added (see Figure 6-15). In addition, Nistor (2015) reported about the BMP experiments with generated 403 ± 7 Nml CH_4 /g VS added. According to the experimental studies from Raposo et al. (2011) the average volume of methane from gelatine was 380 ± 42 CH4 g^{-1} VS added.

Batch fermentation with rapeseed oil Kougias et al. (2013) reported that biochemical methane potential (BMP) tests of rapeseed oil yielded in 704±13 ml CH_4 /g VS added. The results of Hansen et al. (2004) corresponded to a higher production of 800-900 ml

CH_4 /g VS added. Figure 6-14 shows the produced volume of methane in the present study per g of organic 390 ml CH_4/g VS added which is lower as compared to the founding of others. Blesgen (2009) carried out a batch experiment with rapeseed oil which resulted in 470 ml biogas /g rapeseed oil added. Present experiments resulted in 850 ml biogas /g rapeseed oil added, which is nearly two times more.

Inhibition by LCFA's From Figure 6-8 the inhibition caused by LCFA was observed during the first five days of rapeseed oil digestion. As compared to other fermented substrates rapeseed oil yielded the highest amount of methane per VS added. However, the digestion of lipid matter caused some problems. In anaerobic environments lipids are hydrolyzed by lipases to glycerol and long-chain fatty acids (LCFA). Many researches consider LCFA degradation as a ‘‘limiting step’’ for a number of reasons: formation of floating scum which causes limiting bioavailability and becomes toxic for acidogenic and methanogenic bacteria (Nielsen and Angelidaki, 2003; Chen, 2008). Bacterial degradation of LCFAs begins with adsorption of LCFA by the cell and this can be inhibiting depending on type of bacteria, size of LCFA, whether the LCFA is saturated or unsaturated, and concentration of LCFAs (Salminen and Rintala, 2002). The inhibition on acetogenic and methanogenic activity is a non-competitive process and the biogas degeneration is usually resumed as soon as the amount of lipids becomes favorable for the bacterial growth (Angelidaki et al., 1999). Similarly, it can be assumed for this study that after the day 5, the concentration of LCFA's became favorable for the bacterial growth and, consequently, for the biogas production.

Batch fermentation with mixture Initially, the biogas generation was presumably inhibited by LCFA. The generation of volumes was resumed after the day 4. The final yield of CH_4 and biogas was less as compared to the theoretical estimations (Figure 6-3, see Section 6.1.5). The obtained results was difficult to compare with other studies. The calculations of theoretical CH_4 and biogas were necessary for the verification of the experimental reproducibility. There might be several reasons why the measured biogas was less than the theoretical potential: the bacterial population of the inoculum was not initially diverse as compared to the sludge used for the mono - fermentations. The second reason might be that more organic material was consumed to build up the bacterial

biomass (about 5-10% of substrate). Another reason can be that some part of the substrate was not accessible for the microorganisms.

7.2 Simulation results of the batch experiments

Initially, we had to answer two questions:

- Does the formulated model reproduce the anaerobic mono-fermentations of gelatine, sucrose and rapeseed oil in batch?
- Can the model predict the anaerobic digestion of the substrates mixture in batch?

Assigning individual model parameters to the master substrates In order to find the best agreement between simulated and experimental data, an appropriate criterion for the optimal solution of the model parameter identification must be selected. The unknown parameters were identified by applying the least squares procedure (see Section 4.3) which is wide-spread applicable method accordingly to other studies (Donoso-Bravo et al., 2010; Donoso-Bravo et al., 2011; Haugen et al., 2013). The hydrolytic unknowns were initially estimated by the least squares technique and, finally, relied on the previous studies (see Section 2.4, Table 2-3). Literature data usually assists a lot in estimation of unknowns and specify the boundaries for the estimated parameters.

Comparing the estimated hydrolysis constants from this study with the literature data, k_{hyd} for sucrose ($7.9 \cdot 10^{-6}$ s^{-1}) are in the range with the foundlings of Gujer and Zehnder (1983) (Table 2-3). Garcia-Heras (2003) and Batstone et al. (2002) proposed the range for k_{hyd} for lipids ($4.56 \cdot 10^{-6}$ s^{-1}) and proteins ($5.1 \cdot 10^{-6}$ s^{-1}) similar to the estimated numbers in this study. In addition, k_{hyd} for gelatine is defined in the middle of the values proposed for gelatine by Raposo et al. (2011) and Flotats et al. (2006) (Table 2-3).

From previous studies made by Simenov et al. (1996) and Hill and Barth (1977) the maximum uptake rate for carbohydrates equaled to $4.62 \cdot 10^{-6}$ s^{-1} at mesophilic conditions which is nearly the same in this study - $4.2 \cdot 10^{-6}$ s^{-1}. Accordingly to Siegrist et al. (1993) μ^{max} of biodegradable soluble organics was $6.36 \cdot 10^{-6}$ s^{-1}, which is, in principle, close to the present uptake rates of gelatine and rapeseed oil - $3.3 \cdot 10^{-6}$ and $5.6 \cdot 10^{-6}$ s^{-1}, respectively. (Noykova et al., 2001). Angelidaki et al. (1993) estimated

μ_{VFA}^{max} (7.0 10 $^{-6}$ s^{-1}) which was slightly less as compared to the current μ_{VFA}^{max} (8.20 · 10 $^{-6}$ s^{-1}).

The half - saturation constants for lipids in this study was higher (3.2 g L^{-1}) as compared to the literature data where K_L was varying between 0.2 - 2.0 g L^{-1}. Accordingly to calculations of Hill and Barth (1977) the half-saturation constant of VFA's was 0.025 [g L^{-1}]. Simenov et al. (1996) found that K_{VFA} was 0.00082 [g L^{-1}] (Noykova et al., 2001). Within the frames of this study K_{VFA} equaled to 0.01 [g L^{-1}]. The yield factors of the substrates degradation and generation of VFA from substrates of choice were estimated by minimization function.

The inhibition by LCFA which caused the delay in biogas and CH_4 production was described by non-competitive function (see Section 2.6). In earlier studies it was shown in batch experiments that LCFA can inhibit even at low concentrations (Angelidaki and Ahring, 1992; Batstone, 2002). Therefore, in this study for the digestion of lipids the Monod kinetics was assumed with Haldane type substrate inhibition by LCFA´s. From the previous studies the inhibition constant for Haldane kinetics was 0.040 g L^{-1} (Hansen, 1996) which is close enough to the estimated IpL_S in this study - 0.045 g L^{-1}.

Calibration of the model using the data set of the batch fermentations with sucrose, gelatine and rapeseed oil Development and calibration of the model were based on the accuracy of the prediction, simplicity in parameterization and explanation of the discovered phenomenon. Generally observed from the Figures 6-4 - 6-7, the simulations found a good agreement between the simulated and measured data except some discrepancies. In a whole, the mismatch was observed for the volumetric concentrations of CH_4 and CO_2 for three master substrates (Figures 6-4 - 6-9). The prediction capabilities of the biogas and methane was ranging at 0.4 - 7% as compared to the simulated dynamics (Figure 6-13, see Section 6.2.6).

Simulation of batch fermentation with mixture The prediction goodness of the calibrated mathematical model compared to the observed experimental data was 94.2 % for the volume of biogas and 93% for the volume of CH_4. The prediction of the biogas flow rate and COD $_{Tot}$ had the best agreement with experimental observations suggesting

that the model has a potential for the AD process forecast. Blesgen (2009) carried out the predictive simulations for the digestion of 42.8 g sucrose, 1.1 g gelatine and 24.1 g rapeseed oil in a batch. The volumetric concentrations of CH_4 and CO_2, biogas flow rate and volume of biogas were predicted by the model during 200 h. There was a slight deviation for the CH_4 and CO_2 concentrations and at some extent for the flow rate (Blesgen, 2009).

7.3 Experimental results of the continuous experiments and simulation

Cross - verification of the calibrated model was necessary in order to give answers on the following questions:

- Can the model simulate the AD process both in batch and continuous fermentations?
- Verification of the substrate linearity hypothesis: can the formulated model predict the methane volumetric concentrations and the biogas volume of the AD of other wastes (potato waste water (PWW) and starch)?
- How does the model react on the changes of the waste input in terms of the volumetric concentration of CH_4 and CO_2 and biogas volume?

Figures 6-17 and 6-18 show the prediction for the methane content and biogas volume production during 100 days of the AD. The only one parameter which was changed - the yield factor for VFA production from protein, U_P - was increased from 0.68 to 0.88. Difference of the U_P changes is shown in Figures 6-19 and 6-20. This might be explained by higher amount of VFA in the broth produced from the PWW comparing to the gelatine. It is obvious that the experimental and simulated curves are similar with a slight difference only. The main issue of this study was to check the capability of the model to mimic the independent set of data in continuous mode what in a fact it was possible with the proposed model. The overall cross-validation shows that sufficient agreement between simulated and measured data was achieved. Ideal prediction is hard to achieve because with the scaling up of the biogas fermenter the operator can meet with some difficulties like as low degree of instrumentation, accuracy of process measurements and

additional internal disturbances. Therefore, there must be a balance between applicability and accuracy.

Compared to other continuous experiments with potato waste (Parawira et al., 2004) the methane content was in a range of 65% - 80%. In earlier studies with potato juice as an effluent of the starch production, the methane content was 71% - 77 % and the carbon dioxide content was 19%-26%. The fermentation was carried out in an upflow reactor with a volume of 800 m^3 (van Bellegem, 1980). The experiments with potato pulp, potato peel pulp and potato fruit water resulted in the methane concentration ranging between 50.8 Vol.-% -59.2 Vol.- %, what is considerably less than obtained in this study (Kryvoruchko et al., 2009). Linke (2006) studied AD of solid potato wastes in CSTR at 55°C, with increased organic loading rate and its effect on the biogas yield. Both methane and biogas volume decreased with the increase of organic loading and other way around, however refers to a continuously fed fermenter. The methane range concentration was in a range of 58% - 50%.

7.4 Simulation results of the dynamics of the organic waste through the tanks cascade and within the biogas fermenter

The main question to answer in this part of the study was:

- Can the model predict the volumetric concentration of methane and the volume of biogas for a big-scale biogas plant?

For the simulation of the substrates dynamics for an industrial scale biogas plant, the model structure was adapted to the tanks cascade system and scaled-up. The substrate concentration and its amount flowing into the biogas fermenter was changing from day to day within the given HRT which results in growth rate changes of organisms as well as it influences the CH_4 production. The concentration of substrate also affects the catalytic properties of microorganisms (inhibitory or excitatory). Due to relatively reduced information on the experimental measurements, the dynamical changes in the substrates concentration can be only assumed and calculated theoretically.

From the dynamics of the substrates it is seen that the protein-rich substrates prevailed during the AD (Figure 6-27). Usually domination of proteins leads to the accumulation of ammonia and H_2S in the fermenter (see Section 1.5.1; Deublein and Steinhauser, 2008). Due to the tanks cascade system the raw materials are thoroughly mixed before the hygienisation process which, in principle, ensures maximal gas yield from the system in the biogas fermenter. The sanitation tank serves for the disinfection of the substrates for avoiding some undesirable pathogens. Additionally, the buffer tank take a role to damp down potential disturbances (the high oscillation) which might occur during the continuous process. Thus, the annual concentration of CH_4 was not undergone any possible inhibition effect or other possible disturbances. However, after 3 months of digestion there was a drop to 63 Vol.-%. The information about this drop and recovery from it is missing. It was proved that the model shows consistent results at the analysis of the substrates dynamics through the tanks cascade with the biogas formation in the final reactor.

7.5 Sensitivity analysis

The generated volume of biogas from three master-substrates was chosen in calculating the baseline scenario's for the sensitivity analysis. Initially, the influence of five kinetics parameters on the VBG generation in batch were investigated individually. Analysis of simulations helped to find out which parameters are important to choose correctly due to their effect on the final result. Simulations showed that the hydrolysis constant was the most sensitive to be decreased, especially, for the VBG from lipids (Figure 6-30). The yield factors for primary lipids and proteins degradation (Y_{XL} and Y_{XP}) were the most sensitive by changing and showed variations in ±97 and ± 80, respectively. Fluctuations in the maximum uptake rate for lipids showed the maximum variation of production of biogas between the different scenarios (Figure 6-33).

Biogas model predictions are dependent on the variations of the waste composition (Figure 6-35). The volumetric concentration of CH_4 produced after increase of the lipids and decrease of carbohydrates by 33% showed variations up to 12.5% and 2.5%, respectively (Figures 6-35A and B).

CONCLUSION and OUTLOOK

In this study, a three-step mathematical model was formulated based on fundamental principle of conservation of mass. The model was developed in a way to make the estimation of model parameters (model calibration) from experimental data easy to handle. The three-step mathematical model was calibrated based on mono-batch fermentations of easily degradable substrates: sucrose, gelatine and rapeseed oil. The representatives of proteins, carbohydrate and lipids in any organic matter: gelatine, sucrose and rapeseed oil, respectively. During the fermentation of lipids acidogenic and methanogenic microorganisms were inhibited by LCFA. A Haldane-type inhibition leads to a decrease of the hydrolysis rate and a slower biogas production. The model was verified by prediction of the fermentation of three substrates for the volume of biogas and methane, the volumetric flow rate of biogas, the volumetric concentration of methane and the total chemical oxygen demand. This caused a decrease of hydrolysis rate and slower biogas production that was accurately described by the model (Schneider et al., 2015). The simplifications in the model have shown to function amply well for the simulation of the biogas process production and it fulfills the basic model´s properties: causality, forecasting and simplicity

Three main expectations of scientific outcome of the study were fulfilled:

1. The calibrated model predicts the biogas dynamics only by adjustment of three master substrates, which proves the substrate linearity hypothesis. We managed to forecast the AD process for:

   - industrial potato waste water and starch in CSTR (the volumetric concentrations of methane and carbon dioxide and the volume of biogas)
   - agro-waste, food-waste and manure for a pilot-scale biogas fermenter with a system of tanks cascade (the volumetric concentration of methane and the volume of biogas)

2. The model has a good potential to predict the biogas process dynamics for laboratory-scale, both batch and continuous, and big-scale industrial level

3. Study of the influence of the proportion of master substrates in organic waste and their quantity on the final product and stability of the AD in long-term dynamics

- In spite of the limited amount we arranged to predict the volumetric concentration of methane and the volume of biogas by adjustment only three master substrates: proteins, carbohydrates and lipids
- The proposed model shows the smoothing of the substrates concentration through the tanks cascade, most probably; this is one of the reasons of the stable biogas production.

OUTLOOK

- With the further application of the model and simulations using new empirical results, a data base with the simulations for a certain mixtures and substrates can be created.
- Further simulations can be applied for creation of a data base using new empirical data of AD of other substrates.
- The model may be validated in future for instability cases, like organic overloading or variation of environmental conditions, and other configurations of biogas fermenters
- The model may be useful to verify the dynamics of VFA.
- Further investigation of the degradation process in various configurations of biogas fermenters and other substrates would be prospective.
- The proposed model is flexible to be adjusted according to operator’s needs.
- Moreover, the model can be extended and adapted to certain plant types for the instruction and training of the working personnel.

List of Figures

List of Tables

REFERENCES

Abbasi, T., Tauseef, S., Abbasi, S. (2012), Anaerobic digestion for global warming control and energy generation - An overview, *Renewable and Sustainable Energy Reviews*, **16**(5), 3228-42.

Agency for Renewable Resources (2013), Biogas, an introduction, pp. 4-25, https://mediathek.fnr.de

Ahring, B. K. (2003), Perspectives for Anaerobic digestion, *Advances in Biochemical Engineering/Biotechnology*, **81**, 1-30. Springer, Berlin and Heidelberg.

Al Seadi, T. (2001), Good practice in quality management of AD residues in biogas production: Task 24 og AEA Technology Environment, UK.

Amon, T., Amon, B., Kryvoruchko, V., Machmüller, A., Hopfner-Sixt, K., Bodiroza, V., Hrbek, R., Friedel, J., Pötsch, E., Wagentristl, H., Schreiner, M., Zollitsch, W. (2007a), Methane production through anaerobic digestion of various energy crops grown in sustainable crop rotations, *Bioresource Technol*, **98**, 3204-3212.

Amon, T., Amon, B., Kryvoruchko, V., Zollitsch, W., Mayer, K., Gruber, L. (2007b), Biogas production from maize and dairy cattle manure – influence of nutrient composition on methane yield, *Agr Ecosyst Environ*, **118**(1-4), 173-182.

Andrews, J.F. (1968), A mathematical model for the continuous culture of microorganisms utilizing inhibitory substance, *Biotechnology and Bioengineering*, **10**, 707–723

Agelidaki, I., and Ahring, B. K. (1992), Effects of free long chain fatty acids on thermophilic anaerobic digestion, Appl. *Microbiol Biotechnol*, **37**, 808-82.

Angelidaki, I., Ellegard, L., Ahring, B.K., (1993), A mathematical model for dynamic simulation of anaerobic digestion of complex substrates: focusing on ammonia inhibition, *Biotechnol Bioeng* **42**, 159-166.

Angelidaki, I., Ahring, B. K. (1994), Anaerobic thermophilic digestion of manure at different ammonia loads: Effect of temperature, *Water research*, **28**, 727-731.

Angelidaki, I., Ellegard, L., Ahring, B.K., (1999), A comprehensive model of anaerobic bioconversion of complex substrates to biogas, *Biotechnology and Bioengineering* **63**(3), 363-372.

Angelidaki, I., Ellegard, L., Ahring, B.K., (2008), Applications of the anaerobic digestion process, *Advances in Biochemical Engineering/ Biotechnology*, 82, pp. 11-12.

REFERENCES

Asam, Z. U. Z., Poulsen, T. G., Nzami, A-S., Raxique, R., Kiely, G. and Murphy, J. D. (2011), How can we improve biomethane production per unit of feedstock in biogas plant, *Applied Energy*, **88**, 2013-2018.

Bailey, J. E., Ollis, D. (1986), *Biochemical Engineering Fundamentals*, Mc-Graw Hill, 2nd Edition, New York, pp. 408-420.

Bala, B. K., Satter, M. A. (1991), System dynamics modeling and simulation of biogas production systems, *Renew. Energ.*, **1** (5/6), 723-728.

Batstone, D. J. (2006), Mathematical Modelling of Anaerobic Reactors Treating Domestic Wastewater: Rational Criteria for Model Use, *Reviews in Environmental Science and Bio/Technology*, **5**(1), 57–71.

Batstone, D. J. and Keller, J. (2003), Industrial Applications of the IWA Anaerobic Digestion Model No. 1 (ADM1), *Water Sci. Technol.*, **47**(12), 199-206, 2003.

Batstone, D. J., Keller, J., Angelidaki, I., Kalyuzhnyi, S.V., Pavlostathis, S.G., Rozzi, A., Sanders, W. T. M., Siegrist, H., Vavilin, V. A. (2002), *The IWA Anaerobic Digestion Model No 1 (ADM1)*, IWA publishing, London, U.K.

Bernard, O., Hadj-Sadok, Z., Dochain, D., Genovesi, A., Steyer, J.-P. (2001), Dynamical model development and parameter identification for an anaerobic wastewater treatment process, *Biotechnol. Bioeng*. **75**(4), 424-438.

Bilitewski, B., Härdtle, G., Marek, K. (1997), *Waste Management*, Springer, Berlin, pp. 259-338.

Birol, G., Kirdar, B. and Onsan Z. I. (2002), A simple structured model for biomass and extracellular enzyme production with recombinant *Saccharomyces cerevisiae* YPB-G, *J. of Industrial Microbiology & Biotechnology*, **29**(3), 111–116.

Blesgen, A. (2009), *Entwicklung und Einsatz eines interaktiven Biogas – Echtzeit-Simulators*, Ph. D. Thesis, Faculty of Chemistry and Biology, University of Bremen, Bremen, Germany.

Blesgen, A. and Hass, V. C. (2010), Efficient biogas production through process simulation, *Energy and Fuels*, **24**(9), 4721-4727.

Bolte, J. P., Hill, D. T. (1990), A Monod-based model of attached-growth anaerobic fermenters, *Biol. Wastes*. **31**(4), 275 - 289.

Bouallagui, H., Touhami, Y., Cheikh, R. B. and Hamdi, M. (2005), Bioreactor performance in anaerobic digestion of fruit and vegetable wastes, *Process Biochemistry*, **40**(3-4), 989-995.

REFERENCES

Boyle, W. C. (1976), *Energy recovery from sanitary landfills - a review*, In Seminar on Microbial Energy Conversion, Göttingen, Germany, Proceedings. Edited by Schlegel, H.G. and Barnea, J., New York, Academic Press, pp. 119-138.

Budhijanto, W., Purnomo, C. W., Siregar, N. C. (2012), Simplified mathematical model for quantitative analysis of biogas production rate in a continuous digester, *Engineering Journal*, **16**(5), http://engj.org/index.php/ej/article/view/267/259.

Buswell, A. M. and Mueller H. F. (1952), Mechanism of methane fermentation. *Industrial and Engineering Chemistry*, **44(**3), 550-552.

Chang, F., Otten, L., LePaige E., and van Opstal, B. (2004), *Is 100% diversion from a landfill an achievable goal?* A Report to the Toronto, Canada, New and Emerging Technologies, Policies and Practices Advisory Group.

Chawla, O. P. (1986), Methane fermentation technology. *Advances in Biogas Technology*, Indian Council of Agricultural Research, New Delhi p.144.

Chen, Y., Cheng, J. J., Creamer, K. S. (2008), Inhibition of anaerobic digestion process: a review, *Bioresource Technology*, **99**(10), 4044-4064.

Cheng, J. (2010), *Biomass to renewable energy processes*, Taylor and Francis Group, LLC, p. 135-150.

Christ, O., Wilderer, P. A., Angerhofer, R., Faulstich, M., (2000), Mathematical modeling of the hydrolysis of anaerobic processes, *Water Science and Technology*, **41**, 61-65.

Chynoweth, D. P., Owens, J. M., Legrand, R. (2001), Renewable methane from anaerobic digestion of biomass, *Renewable Energy*, **22**(1-3), 1–8.

Cirne, D. G., Paloumet. X., Björnsson, L., Alves, M. M., Mattiasson, B. (2007), Anaerobic digestion of lipid-rich waste — Effects of lipid concentration, *Renewable Energy*, **32,** 965–975.

Graef, S. P., Andrews, J. F. (1974), Dynamic modeling and simulation of the anaerobic digestion process, *Advances in Chemistry Series*, **105**, 126–162.

Demetriades, P. (2008), *Thermal pre-treatment of cellulose rich biomass for biogas production*, Master thesis, Swedish University of Agricultural Sciences, Uppsala.

Demirel, B. and Yenigun, O. (2002), Two Phase Anaerobic Digestion Processes: A Review. *Journal of Chemical Technology and Biotechnology*, **77**, 743-755. http://dx.doi.org/10.1002/jctb.630

Derbal, K., Behcheikh-Iehocine, M., Cecchi, F., Meniani, A.-H., Pavan, P. (2009), Application of the IWA ADM1 model to simulate anaerobic co-digestion of

organic waste with activated sludge in mesophilic condition. *Bioresource Technol.* **100**, 1539-1543.

Deublein, D. and Steinhauser, A. (2008), *Biogas from waste and renewable resources*, Wiley-VCH, Germany, pp. 1-30, 50-113, 225-239.

Divya, D., Gopinath, L. R., Christy, P. C. (2015), A review on current aspects and diverse procpects for enhancing biogas production in sustainable means, *Renewable and Sustainable Energy Reviews*, **42**, 690-699.

Dochain, D., and Vanrolleghem, P. A. (2001), Dynamic modeling and estimation in wastewater treatment process, Published by IWA, London, UK, pp. 28-34, 73-78, 339-356.

Donoso-Bravo, A., Perez-Elvira, S., Fdz-Polanco, F., (2010), Application of simplified models for anaerobic biodegradability tests. Evaluation of pre-treatment processes. *Chemical Engineering Journal*, **160**, pp. 607-614.

Donoso-Bravo, A., Mailier, J., Martin, C., Rodríguez, J., Aceves-Lara, CA., Wouwer A. V. (2011), Model selection, identification and validation in anaerobic digestion: A review, *Water Research* **45**(17), 5347-5364.

Duncan, M., Nigel, J. H. (2003), *Handbook of water and Wastewater Microbiology*, Academic press, London, UK, pp. 393-396.

Edwards, V.H. (1970), The influence of high substrate concentrations on microbial kinetics, *Biotechnology and Bioengineering*, **12**, 679–712.

Erickson, L. E., Fayet, E., Kakumanu, B. K., Davis, L. C. (2004), Anaerobic digestion. In: Carcass Disposal: A comprehensive review, National Agricultural Biosecurity Center, Kansas State University, Manhattan, Kansas, Chapter 7. pp. 1-19.

European Parliament and Council (2009), *Directive 2009/28/EC on the promotion of the use of energy from renewable sources*, Official Journal of the European Communities, **L 283/33**.

European Parliament and Council (2010), *Report from the commission to the council and the European Parliament on sustainability requirements for the use of solid and gaseous biomass sources in electricity, heating and cooling*.

Fachverband Biogas e.V., 2013. *Biogas Segment Statistics 2013: Development of the number of biogas plants and the total installed electric output in megawatt [MW] (as of 6/2012)* [online]. Available from: http://www.biogas.org/edcom/webfvb.nsf/id/DE_Branchenzahlen/$file/12-06-12_Biogas%20Branchenzahlen%202011_eng.pdf [Accessed July 2014].

Falk, H. M. (2011), *Monitoring the anaerobic digestion process*, PhD Thesis, Jacobs University Bremen, Germany.

Flotats, X., Palatsi, J., Fernández, B., Colomer, M. A., Illa, J. (2010), Identifying anaerobic digestion models using simultaneous batch experiments, *Environ Eng and Manag J*, **9**(3), pp. 313-318.

Franke-Whittle, I. H., Walter, A., Ebner, C., Insam, H. (2014), Investigation into the effect of high concentrations of volatile fatty acids in anaerobic digestion on methanogenic communities, *Waste management*, **34**, 2080-2089.

Fredrickson, A. G., McGee, R. D. I. and Tsuchiya, A. M. (1970), Mathematical models in fermentation processes. *Adv in Applied Microbiology*, **23**, 419.

Garcia-Heras, J. (2003), Reactor sizing, process kinetics and modelling of anaerobic digestion of complex wastes, In: Mata-Alvarez, J. (Ed.), Biomethanization of the organic Fraction of Municipal Organic Solid waters, *Water Sci Technol*, **40**, pp. 339-346.

Gavala, H. N., Angelidaki, I. and Ahring, B. K., (2003), Kinetics and modeling of anaerobic digestion process, *Advances in Biochemical Engineering/ Biotehnology*, **81**, 57-93.

Gerardi, M. (2003), *The microbiology of anaerobic digesters*, John Wiley& Sons Inc, Hoboken, New Jersey.

Gerber, M. (2008), *An Analysis of Available Mathematical Models for Anaerobic Digestion of Organic Substances for Production of Biogas*, International gas union research conference, Paris.

German Engineers Association (2006), *VDI 4630: Fermentation of organic materials - Characterization of the substrate, sampling, collection of material data, fermentation tests*, VDI Handbook Energietech. Berlin: Beuth Verlag GmbH.

Gonzales-Fernandez, C. and Garcia-Encina, P.A. (2009), Impact of substrate to inoculum ratio in anaerobic digestion of swine slurry, *Biomass Bioener*, **33**, 1065-1069.

Gujer, W. and Zehnder, A. J. B. (1983), Conversion processes in anaerobic digestion, *Water Sci Technol*, **15**(8). pp. 127–167.

Gunaseelan, V.N. (1997), Anaerobic Digestion of Biomass for Methane Production: A Review, *Biomass and Bioenergy*, **13,** 83-144. http://dx.doi.org/10.1016/S0961-9534(97)00020-2.

Hansen, J.A (1996), *Management of urban biodegradable wastes: collection, occupation, health, biological treatment product quality criteria and end user demand*, James & James, Copenhagen, pp.144-152.

Hansen, T.L., Schmidt, J. E., Angelidaki, I., Marca, E., Jansen, J. C., Mosbæk, H., Christensen, T. H. (2004), Measurement of methane potentials of solid organic waste, *Waste Manag*, **24**, 393–400.

Haugen, F., Bakke, R., Bernt, L. (2013), Adapting dznamic mathematical models to a pilot anaerobic digestion reactor, *Modeling, Identification and Control*, **34**(2) pp. 35–54.

Henze, M., van Loosdrecht M., Ekama, G., Brdjanovic, D. (2008), *Biological waste water treatment: principles, modelling and design*, IWA Publishing, London, UK.

Hill, D. T., Barth, C. L. (1977), A dynamical model for simulation of animal waste digestion, *J Water Pollution Control Federation*, **49**(10), 2129-2143.

Husain, A. (1998), Mathematical models of the kinetics of anaerobic digestion – a selected review, *Biomass and Bioenergy*, **14**, 561-571.

Issazadeh, K., Nejati, P., Zare, F., Laczai, O. (2013), Diversity of methanogenic bacteria in ecological niches, *Ann Biol Res*, **4**, 36-42.

James, F. (2006), *Statistical methods in experimental physics*, 2nd Ed. World Scientific, London, pp. 127-139.

Jayathilakan, K., Sultana, K., Radhakrishna, K., Bawa, A. S. (2012), Utilization of byproducts and waste materials from meat, poultry and fish processing industries: a review, *J Food Sci Technol*, **49**(3), 278-293.

Kabara, J. J., Vrable, R., Lie Ken Jie, M. S. F., (1977), Antimicrobial lipids: natural and synthetic fatty acids and monoglycerides, *Lipids*, **12**(9), 753–759.

Kalfas, H., Skiadas, I. V., Gavala, H. N., Stamatelatou, K., Lyberatos, G. (2006), Application of ADM1 for the simulation of anaerobic digestion of oilve pulp under mesophilic and thermophilic conditions, *Water Sci Technol*, **54**(4), 149 -156.

Kerroum, D., Bencheikh-Lehocine Mossaab, B. – L., Abdessalam Hassen, M. (2010), Use of ADM1 model to simulate the anaerobic digestion process used for sludge waste treatment in thermophilic conditions, *Turkish J Eng Env Sci*, **34**, 121-129.

Khalid, A., Archad, M., Anjum, M., Mahmood, T., Dawson, L. (2011), The anaerobic digestion of solid organic waste, *Waste Management*, **31**(8), 1737-44.

Kitzing, I., Mitchell, C., Morthorst, P. E., (2012), Renewable energy policies in Europe: Converging or diverging? *Energy Policy*, **51**, 192-201.

Kleerebezem, R. and van Loosdrecht, M. C. M. (2006), Waste characterization for implementation in ADM1, *Water Sci and Technol*, **54**, 167-174.

Kleinstreuer, C. and Poweigha, T. (1982), Dynamic simulator for anaerobic digestion process, *Biotechnology and Bioengineering*, **24,** 1941-1951.

Koch, K., Lübken, M., Gehring, T., Wichern, M., Horn, H. (2010), Biogas from grass silage - measurments and modeling with ADM1, *Bioresour Technol*, **101**(21), 8158 -8165.

Korjik, A. (2010), *Model based optimization of the substrate dynamics during anaerobic digestion*, Master Thesis, Jacobs University Bremen, Germany pp. 39-51.

Kougias, P. G., Boe, K., Tsapekos, P., Angelidaki, I. (2013), Foam suppression in overloaded manure-based biogas reactors using antifoaming agents, *Bioresour Technol*, **153**, 198-205.

Kryvoruchko, V., Machmuller, A., Bodiroza, V., Amon, B., Amon, T. (2009), Anaerobic digestion of by-products of sugar beet and starch potato processing, *Biomass and Bioenergy*, **33**(4), 620-7.

Kumar, K. V., Sridevi, V., Rani, K., Sakunthala, M., Kumar, S. C. (2013), A review on production of biogas, fundamentals, application and its recent enhancing techniques, *Chemical Engineering*, **57**, 14073-14079.

Kyazze, G., Dinsdale, R., Guwy, A. J., Hawkes, F. R., Premier, G. C., Hawkes, D. L. (2007), Performance characteristics of a two-stage dark fermentative system producing hydrogen and methane continuously, *Biotechnol Bioeng.* **97**(4), 759-70.

Kythreotou, N., Florides, G., Tassou, S. A. (2014), A review of simple to scientific models for anaerobic digestion, *Renewable Energy*, **71**, 701-714.

Labatut, R. A. and Gooch, C. A. (2012), *Monitoring of anaerobic digestion process to optimize performance and prevent system failure*, Proceedings of Got Manure Tradeshow and Conference, Enhancing Environmental and Economic Sustainability, pp. 209-225.

Lauwers, J., Appels, L., Thompson, I. P., Degrève, J., van Impe, J. F., Dewil, R. (2013), Mathematical modelling of anaerobic digestion of biomass and waste: power and limitations, *Progress in Energy and Combustion Science*, **39**(4), 383–402.

Layokun, S.K., Umoh, E.F., Solomon, B.O. (1987), A kinetic model for the degradation of dodecane by P. fluorescens isolated from the oil polluted area, Warri in Nigeria, *Journal of NSChE*, **16**, 48–52.

Liu, J., Olsson, G., Mattiasson, B. (2004), Control of an anaerobic reactor towards maximum biogas production, *Water Sci Technol*, **50**(11), 189-198.

Liu, J. Z., Weng, L. P., Zhang, Q. L., Xu, H., Ji, L. N. (2003), A mathematical model for glucolic acid fermentation by *Aspergillus niger*, *Biochem Eng J*, **14**: 137-41.

Lyberatos, G., Skiads, I. V. (1999), Modeling of anaerobic digestion- a review. *Global Nest: the Int J*, **1**(2), 63-76.

Linke, B. (2006), Kinetic study of thermophilic anaerobic digestion of solid wastes from potato processing, *Biomass and Bioenergy*, **30**(10), 892-6.

Lissens, G., Vandevivere, P., de Baere, L., Biey, E. M., Verstraete, W. (2001), Solid waste digesters: process performance and practice for municipal solid waste digestion, *Water Sci Technol*, **44**(8), 91–102.

Marchaim, U. (1992), *Biogas process for sustainable development*, Chapter eight, MIGAL Galilee Technological Centre Kiryat Shmona, Israel, Available from: http://www.fao.org/

Masse, L., Masse, D. I., Kennedy, K. J., Chou, S. P., (2002), Neutral fat hydrolysis and long-chain fatty acid oxidation during anaerobic digestion of slaughterhouse wastewater, *Biotechnology and Bioengineering*, **79**, 43-52.

Mata-Alvarez, J. (2003), *Biomethanization of the organic fraction of municipal solid wastes*, IWA Publishing, Department of Chemical Engineering, University of Barcelona, Spain, pp. 1-18, 91-105.

Matsakas, L., Rova, U. and Christakopoulos, P. (2014), Evaluation of dried sweet sorghum stalks as raw material for methane production, *BioMed Res Int.* Available: http://www.hindawi.com/journals/bmri/2014/731731/abs/.

Mendes, C., Esquerre, K., Matos Queiroz, L. (2015), Application of Anaerobic Digestion Model No. 1 for simulating anaerobic mesophilic sludge digestion, *Waste Manag*, **35**, 89-95.

Méndez-Acosta, H.O., Campos-Delgado, D. U., Femat, R. and González-Alvarez, V. (2005), A robust feed forward/ feedback control for an anaerobic digester, *Computers and Chemical Engineering*, **29**(7), 1613–1623.

Merlin Christy, P., Gopinath, L. R., Divya, D. (2014), A review on anaerobic decomposition and enhancement of biogas production through enzymes and microorganisms, *Renewable and Sustainable Energy Reviews*, **34**, 167-173.

Miyamoto, K. (1997), *Renewable biological systems for alternative sustainable energy production*, Chapter 4: Methane production, Available: http://www.fao.org/docrep/w7241e/w7241e0f.htm.

Modhoo, A (2012), *Biogas production: pretreatment methods in anaerobic digestion*, John Wiley and Sons, New Jersey, pp. 159-162.

Moletta, R., Verrier, D. and Albagnac, G. (1986), Dynamic modelling of anaerobic digestion, *Wat Res*, **20**, 427-434.

Monod, J. (1942), The Growth of Bacterial Cultures. *Annual Reviews of Microbiology***, 3**, 371 – 394.

Montgomery, L. and Bochmann, G. (2014), *Pretreatment of feedstock for enhanced biogas production, Technical Brochure,* 24, EA Bioenergy, ISBN: 978-1-910154-05-2.

Moosbrugger, R. E., Wentzel, M. C., Ekama, G. A. and Marais, G. V. R. (1993), A 5 pH point titration method for determining the carbonate and SCFA weak acid/bases in anaerobic systems. *Water Sci and Technol*, **28**(2), 237-245.

Moser, H. (1958), *The dynamics of bacterial populations in the chemostat*, Bd. 614. Washington : Carnegie Inst. Publication.

Najafpour, G. (2015), *Biochemical Engineering and Biotechnology*, Ed. 2nd, Elsevier, pp.173-180.

Nistor, M. (2015), *Monitoring and process control of anaerobic digestion plants*, Bioprocess Control, Optimization tools for biogas research and operation of full-scale plants, oral presentation, March 18, Leipzig, Germany.

Nizami, A-S., Murphy, J. D. (2010), What type of digesters configurations should be employed to produce biomethane from grass silage? *Renewable and Sustainable Energy Reviews*, **14**, 1558-1568.

Nopens, I., Batstone, D. J., Copp, J. B., Jeppsson, U., Volcke, E., Alex, J., Vanrolleghem P A. (2009), An ASM/ADM model interface for dynamic plant-wide simulation, *Water Res*, **43(7)**,1913-1923.

Noykova, N., Mueller, T. G., Gyllenber, M., Timmer, J. (2001), Quantitave analyses of anaerobic wastewater treatment processes: identifiability anad parameter estimation, *Biotechnology and Bioengineering*, **78**(1), 93-103.

Ostrem, K. (2004), *Greening waste: anaerobic digestion for treating the organic fraction of municipal solid wastes*, Master thesis, Earth Engineering Center Columbia University, US.

Parawira, W., Murto, M., Zvauya, R., Mattiasson, B. (2004F), Anaerobic batch digestion of solid potato waste alone and in combination with sugar beet leaves, *Renewable Energy*, **29**(11), 1811-23.

Patzwahl, S., Thomas, N., Frense, D., Beckmann, D., Kramer, K.-D., Tautz, T., Vollmer, G.-R. (2001), *Microcontroller-Based Fuzzy system to optimize the anaerobic digestion in biogas reactors*, Computational Intelligence theory and applications: International Conference, 7th Fuzzy days, Dortmund, Germany, pp. 2-10.

Pavlostathis, S. G. and Giraldo-Gomez, E. (1991), Kinetics of Anaerobic Treatment, *Water Sci and Technology*, **25**(8), 35–59.

Petzold, L. R. (1982), *A description of DASSL: a differential/ algebraic system solver*, *SOND82-8637*, Sandia national Laboratory, Albuquerque, NM.

Ploit, M., Estaben, M., Labat, P. (2002), A fuzzy model for an anaerobic digester, comparison with experimental results, *Engineer Appl and Artif Intelligence*, **15** (5), 385 – 390.

Processing, https://processing.org/ Accessed 3 February 2014

Product specification. Fat greaves, http://eyeqeye.nl/media/pdf/25110.pdf, Accessed 10 July 2010

Qdais, A. H., Bani Hani, K., Shatnawi, N. (2010), Modeling and optimization of biogas production from a waste digester using artificial neural network and generic algorithm, *Resources Conservation and Recycling,* **54**(6), 359 – 363.

Ramsay, I. R., and Pullammanappallil, P. C. (2001), Protein degradation during anaerobic wastewater treatment: derivation of stoichiometry, *Biodegradation*, **12**(4), 247–257.

Raposo, F., Banks, C. J., Siegert, I., Heaven, S., Borja, R. (2006), Influence of inoculum to substrate ratio on the biochemical methane potential of maize in batch tests, *Proc. Biochem*. **41**, 1444-1450.

Raposo, F., Fernandez-Cegri, V., De la Rubia, M. A., Borja, R., Béline, F., Cavinato, C., Demirer, G., Fernández, B., Fernández-Polanco, M., Frigon, J. C., Ganesh, R., Kaparaju, P., Koubova, J., Méndez, R., Menin, G., Peene, A., Scherer, P., Torrijos, M., Uellendahl, H., Wierinckm, I., De Wilde, V. (2011), Biochemical methane potential (BMP) of solid organic substrates: evaluation of anaerobic biodegradability using data from an international interlaboratory study, *J Chem Technol Biotechno,* **86**(8), 1088–1098.

Report from the commission to the European parliament the council, the European economic and social committee and the committee of the regions. Renewable energy progress report /* COM/2013/0175 final */ http://eur-lex.europa.eu/legal-content/EN/TXT/?uri=celex:52013DC0175

Tafdrup, S. (1995), Viable energy production and waste recycling from anaerobic digestion of manure and other biomass materials, *Biomass Bioenergy*, **9**(1), 303–14.

Thorin, E., Nordlander, E., Lindmark, J., Dahlquist, E., Yan, J., Fdhila, R. B. (2015), *Modeling of the biogas production process – a review*, International Conference on Applied Energy ICAE 2012, Jul 5-8 Suzhou, China.

Tomei, M.C., Braguglia, C.M., Cento, G. and Mininni, G., (2009), Modeling of Anaerobic Digestion of Sludge. *Critical Reviews in Environmental Science and Technology*, **39**(12), 1003–1051.

Trojanowski, J, Kharazipour, A., Mayer, F., Huttermann, A. (2006), Verwendung von Kartoffelpulpe und Kartoffelfruchtwasser als Nährmedium zur Anzucht von Laccase produzierenden Pilzen, *Starch/starke*, **47**(3), 116-118.

Salminen, E. and Rintala, J. (2002), Anaerobic digestion of organic solid poultry slaughterhouse waste – a review, *Bioresour Technol*, **83**(1), 13-26.

Sanders, W.T.M. (2001), *Anaerobic hydrolysis during digestion of complex substrates*, Ph.D. thesis. Wageningen University, the Netherlands.

Schink, B. (1997), Energetics of syntrophic cooperation in methanogenic degradation. *Microbiology and Molecular Biology Reviews*, **61**(2), 262-280.

Schneider, A., Barbot, Y., Kuhnen, F., Benz, R., Hass, V. C. (2015), Dynamic modeling of anaerobic degradation in batch operation for gelatine, sucrose, rapeseed oil and their mixture, *Inter J of Engineering and Technical Res*, **3**(7), 267-275.

Schön, M. (2009), *Numerical modeling of anaerobic digestion processes in agricultural biogas plants*, Ph. D. Thesis University of Insbruck, Insbruck, Germany.

Schnürer, A. and Jarvis, Å. (2010), *Microbial handbook for biogas plants*, Swedish Waste Management U2009:03, Swedish gas centre report 207.

Shang, Y., Johnson, B. R., Sieger, R. (2005), Application of the IWA anaerobic digestion aanerobic digestion model (ADM1) for simulating full-scale anaerobic sewage sludge digestion, *Water Sci Technol*, **52**(1-2), 487-92.

Shimizu, T., Kudo, K., Nasu, Y., (1993), Anaerobic waste-activated sludge-digestion - a bioconversion mechanism and kinetic-model, *Biotechnology and Bioengineering*, **41**, 1082-1091.

Simenov, I., Momchev, V., Grancharov, D. (1996), Dynamic modelling of mesophilic anaerobic digestion of animal waste, *Wat Res*. **30**, 1087 – 1094.

Smith, P. H., Bordeaux, F. M., Goto, M., Shiralipour, A., Wilke, A., Andrews, J. F., and Barnett, M. W. (1988), *Biological production of methane from biomass*, In Smith, W. H. and Frank, J. R. (Eds.), Methane from biomass - A treatment approach. Elsevier, London, pp. 291-334.

Strik, D. P. B. T. B., Domnanich, A. M., Zani, L., Braun, R., Holubar, P. (2005), Prediction of trace compounds in biogas from anaerobic digestion using the MATLAB neural network Toolbox, *Environ Model and Software,* **20**, 803 – 810.

Sung, S., Liu, T. (2003), Ammonia inhibition on thermophilic anaerobic digestion, *Chemosphere*, **53**, 43-52.

van Bellegem, T. M. (1980), Methane production from the effluent of the potato starch industry, *Biotechnol Letters*, **2**(5), 219-224.

Vargas, A. and Moreno, I. A. (2015), *On-line maximization of biogas production in an anaerobic reactor using a pseudo-super-twisting controller*, 9th International Symposium on Advanced Control of Chemical Processes, June 7-10, 2015, Whistler, British Columbia, Canada.

Vavilin, V.A., Lokshina, L., Y., Rytov S.V., Kotsyurbenko, O. R., Nozhevnikova A. N. (2000), Description of two-step kinetics in methane formation during psychrophilic H_2/CO_2 and mesophilic glucose conversions, *Bioresource Technol*. **71**(3), 195 - 209.

Vavilin, V.A., Fernandez, B., Palatsi, J., Flotats, X. (2008), Hydrolysis kinetics in anaerobic degradation of particulate organic material: An overview, Waste Management, **28**, 939-951.

Verma, S., (2002), Anaerobic digestion of biodegradable organics in municipal solid wastes, Fu Foundation School of Engineering and Applied Science Columbia University, US.

Walker, M., Zhang, Y., Heaven, S., Banks, C. (2009), Potential errors in the quantitative evaluation of biogas production in anaerobic digestion process, *Bioresource Technol*, **100**, 6339-6346.

Wang, L., Fan, D., Chen, W., Terentjev, E. M (2015), Bacterial growth, detachment and cell size control on polyethylene terephthalate surfaces, *Scientific Report*, **5**,15159.

Wang, Y., Zhang, Y., Wang, J., Meng, L. (2009), Effects of volatile fatty acid concentrations on methane yield and methanogenic bacteria, *Biomass Bioenergy*, **33**, 848–853.

Weiland, P. (2010), Biogas production: current state and perspectives. *Appl. Microbiol Biotechnol*. **85** (4), 849-60.

Wolf, C., McLoone, S., Bongards, M. (2009), Biogas plant control and optimization using computational intelligence methods, *Automatisierungstechnik*, **57**, 638- 650.

Wolfsberger, A. and Holubar, P., (2006), WP7 Biokinetic Data, Modelling and Control 2nd Year CROPGEN meeting, Vienne.

Yadvika, A., Santosh, A., Sreekrishan, T. R., Rana, V. (2004), Enhancement of biogas production from solid substrates using different techniques – a review, *Bioresour Technol*, **95**(1), 1-10.

Yen, H. W. and Brune, D. E. (2007), Anaerobic co-digestion of algal sludge and waste paper to produce methane, *Bioresource Technology*, **98**, 130-134.

Yoon, Y.-M., Kim, S-H., Shin, K- S., Kim C-H., (2014) Effects of Substrate to Inoculum Ratio on the Biochemical Methane Potential of Piggery Slaughterhouse Wastes, *Asian Australas. J. Anim. Sci.*, **27**(4) 600-607.

Yu, H. Q., Fang, H. H. P. (2002), Acidogenesis of dairy wastewater at various pH levels, *Water Sci Technol*, **45**(10), 201-206.

REFERENCES

Yu, L., Wensel, P. C., Ma, J., Chen, S. (2013), Mathematical modeling in anaerobic digestion, *J Bioremed Biodeg*, S4 http://dx.doi.org/10.4172/2155-6199.S4-003.

Zaher, U., Rodriguez, J., Franco, A., Vanrolleghem, P.A. (2003), *Application of the IWA ADM1 model to simulate anaerobic digester dynamics using a concise set of practical measurements*, IWA Conference on Environ. Biotech, Kuala Lumpur, Malaysia.

Appendix 1

Table 7-1: List of initial values which are located in the feed files

Initial Value	Definition	Units
C_p^0	initial concentrations of proteins	[kg·m^{-3}]
P_p^0	initial concentrations of carbohydrates	[kg·m^{-3}]
L_p^0	initial concentrations of lipids	[kg·m^{-3}]
$\dot{q}_C^0$	inflow rate of proteins	[kg·m^{-3}·s^{-1}]
$\dot{q}_P^0$	inflow rate of carbohydrates	[kg·m^{-3}·s^{-1}]
$\dot{q}_L^0$	inflow rate of lipids	[kg·m^{-3}·s^{-1}]
X_{Aci}^0	initial concentrations of acidogenic	[kg·m^{-3}]
X_{Meth}^0	initial concentrations of methanogenic bacteria	[kg·m^{-3}]
$\dot{q}_{ino}^0$	inflow of inoculum into the digester	[kg·m^{-3}·s^{-1}]

Table 7-2: Dynamic state variables

State variable	Definition	Units
X_{aci}	Concentration of the acidogenic bacteria	[kg·m^{-3}]
X_{meth}	Concentrations of the methanogenic bacteria	[kg·m^{-3}]
C_P	Concentration of the primary carbohydrates	[kg·m^{-3}]
P_P	Concentration of the primary proteins concentration	[kg·m^{-3}]
L_P	Concentration of the primary lipids concentration	[kg·m^{-3}]
C_S	Concentration of the simple carbohydrates	[kg·m^{-3}]
P_S	Concentration of the simple proteins	[kg·m^{-3}]
L_S	Concentration of the simple lipids	[kg·m^{-3}]
VFA	Concentration of the volatile fatty acids	[mol·m^{-3}]
V_{BG}	Volume of biogas	[m^3]
V_{CH_4}	Dynamics of methane volume	[m^3]
V_{liq}	Dynamics of the reactor volume	[m^3]
V_K	Volume in the head space	[m^3]
xCH_4	Volumetric concentration of methane	[Vol.-%]
xCO_2	Volumetric concentration of carbon dioxide	[Vol.-%]
$\dot{q}_{out}Ga$	Biogas flow rate	[m^3·s^{-1}]
$\dot{q}_{out}CH_4$	Methane flow rate	[m^3·s^{-1}]
CODtot	Total chemical oxygen demand	[kg COD·m^{-3}]

Table7-3: Model parameters

Parameter	Definition	Units
$k_{hyd\ C}$	Hydrolysis constant for carbohydrates	[s^{-1}]
μ_C^{max}	Maximum uptake rate for carbohydrates	[s^{-1}]
K_{C_s}	Half-saturation constant carbohydrates	[$kg \cdot m^{-3}$]
Y_{XC}	Yield factor for primary carbohydrates degradation	[$kg \cdot kg^{-1}$]
U_C	Yield factor for VFA production from carbohydrates	[$kg \cdot kg^{-1}$]
$k_{hyd\ P}$	Hydrolysis constant for proteins	[s^{-1}]
μ_P^{max}	Maximum uptake rate for proteins	[s^{-1}]
K_{P_s}	Half-saturation constant proteins	[$kg \cdot m^{-3}$]
Y_{XP}	Yield factor for primary proteins degradation	[$kg \cdot kg^{-1}$]
U_P	Yield factor for VFA production from protein	[$kg \cdot kg^{-1}$]
$k_{hyd\ L}$	Hydrolysis constant for lipids	[s^{-1}]
μ_L^{max}	Maximum uptake e rate for lipids	[s^{-1}]
K_{L_s}	Half-saturation constant lipids	[$kg \cdot m^{-3}$]
Y_{XL}	Yield factor primary lipids degradation	[$kg \cdot kg^{-1}$]
U_L	Yield factor VFA production from lipids	[$kg \cdot kg^{-1}$]
μ_{VFA}^{max}	Maximum uptake rate for VFA	[s^{-1}]
K_{VFA}	Half-saturation constant VFA	[$kg \cdot m^{-3}$]
Y_{XVFA}	Yield factor VFA degradation	[$kg \cdot kg^{-1}$]
v_{VFA}	Yield factor for CH_4 production from VFA	[$mol \cdot kg^{-1}$]
IpL_S	Inhibition coefficient	[$mol \cdot kg^{-1}$]
VR	Volume of the reactor	[m^3]
TR	Temperature in the reactor	[K]

Appendix 2

Biogas Model code

```
#include"SimTool/SimUtils.h"
#include"SimTool/SimException.h"
#include"ADSIM12.h"
#include"nTools/BasicFunctions.h"
#include<iostream>
#ifdef DEBUG
#include"SimTool/ErrorLogger.h"
#endif
#include<cmath>
// default constructor
ADSIM12::ADSIM12()
    :
      SimModel() {
// do nothing special
}
// copy constructor
ADSIM12::ADSIM12(const ADSIM12 &Src)
    :
      SimModel(Src)
// eventually list additional initializations below (comma separated)
{
// routine here
  RefreshParameters();
}
// destructor
ADSIM12::~ADSIM12() {
// perform the necessary operations of mem release etc
}
//  clone  functionality  returns  shared  pointer  to  the  object
(modification not necessary)
SimModel::Pointer ADSIM12::clone() const {
return SimModel::Pointer(new ADSIM12(*this));
}
int ADSIM12::Equation(SIMFORMAT t, const array1d &y, array1d &dydt) {
#ifdef DEBUG
  ErrorLogger eL;
#endif
// association of states to local variables
SIMFORMAT CXaci   = y(1);
SIMFORMAT CXmeth  = y(2);
SIMFORMAT CSM     = y(3);
SIMFORMAT CpC     = y(4);
SIMFORMAT CpP     = y(5);
SIMFORMAT CpL     = y(6);
SIMFORMAT CSC     = y(7);
SIMFORMAT CSP     = y(8);
SIMFORMAT CSL     = y(9);
SIMFORMAT CVFA    = y(10);
SIMFORMAT VBG     = y(11);
```

```
SIMFORMAT VCH4    = y(12);
SIMFORMAT Vliq    = y(13);
// some xtra stuff to arrange order of associations
  SIMFORMAT VK      = VR - Vliq;
// disintegration rate
const SIMFORMAT rD = kD * CSM;
// hydrolysis rates
const SIMFORMAT rhydC = khydC * CpC;
const SIMFORMAT rhydP = khydP * CpP;
const SIMFORMAT rhydL = khydL * CpL;
// inhibition by LCFA
const SIMFORMAT inhibL = IpL / (IpL + CpL);
// compute acitogenetic rates
const SIMFORMAT rXC = rMaxXC * CSC * CXaci  / (KsC + CSC);
const SIMFORMAT rXP = rMaxXP * CSP * CXaci / (KsP + CSP);
//const SIMFORMAT rXL = rMaxXL * CSL * CXaci / (KsL + CSL);
const SIMFORMAT rXL = rMaxXL * CSL * CXaci * inhibL / (KsL + CSL);
// compute methanogenetic rate
//const SIMFORMAT rVFA = rMaxVFA * CVFA * CXmeth / (KVFA + CVFA);
const SIMFORMAT rVFA = rMaxVFA * CVFA * CXmeth * inhibL/ (KVFA + CVFA);
#ifdef DEBUG
  eL.Log("ADSIM12::Equation(...): rVFA = %12.4e", rVFA);
#endif
// compute concentration changes of compounds
const SIMFORMAT q0tot  = q0CpC + q0CpP + q0CpL + q0Ino;
const SIMFORMAT qoutTo = qout + qoutsa;
// concentration of acidogenic bacteria (CXaci)
  dydt[0] = (q0Ino * C0Xaci - CXaci * q0tot)/Vliq + yXC * rXC + yXP *
rXP + yXL * rXL;
// concentration of methanogenics (CXmeth);
  dydt[1] = (q0Ino * C0Xmeth - CXmeth * q0tot)/Vliq + yXVFA * rVFA;
// substrates mixture (CSM)
  dydt[2] = -rD;
// disintegration of carbo hydrate  (CpC)
  dydt[3] = (q0CpC * C0CpC - CpC * q0tot)/Vliq + fC * rD - rhydC;
// disintegration of protein (CpP)
  dydt[4] = (q0CpP * C0CpP - CpP * q0tot)/Vliq + fP * rD - rhydP;
// disintegration of lipid (CpL)
  dydt[5] = (q0CpL * C0CpL - CpL * q0tot)/Vliq + fL * rD - rhydL;
//  hydrolysis of carbohydrate (CSC)
  dydt[6] = -(CSC * q0tot)/Vliq + rhydC - rXC;
// hydrolysis of  protein (CSP)
  dydt[7] = -(CSP * q0tot)/Vliq + rhydP - rXP;
// hydrolysis of lipid (CSL)
  dydt[8] = -(CSL * q0tot)/Vliq + rhydL - rXL;
// volatile fatty acid  (CVFA)
  dydt[9] = -(CVFA * q0tot)/Vliq + (1.0 - yXC) * uC * rXC + (1.0 - yXP)
* uP * rXP + (1.0 - yXL) * uL * rXL - rVFA;
// inorganic carbon (CTIC)
const SIMFORMAT rTIC = (1.0 - yXC) * (1.0 - uC) * rXC + (1.0 - yXP) *
(1.0 - uP) * rXP + (1.0 - yXL) * (1.0 - uL) * rXL + (1.0 - yXVFA) *
(1.0 - vVFA) * rVFA;
// methane(Me)
const SIMFORMAT rMet = (1.0 - yXVFA) * vVFA * rVFA;
#ifdef DEBUG
  eL.Log("ADSIM12::Equation:rMet = %12.4e", rMet);
#endif
```

```
// molar release of carbon dioxide
const SIMFORMAT MWCO2   = 0.04401E+00;
const SIMFORMAT nDotCO2 = rTIC / MWCO2 * Vliq;
// molar release of methane
const SIMFORMAT MWCH4   = 0.01604E+00;
const SIMFORMAT nDotCH4 = rMet / MWCH4 * Vliq;
// output of carbon dioxide and methane mole fractions and volume flow
const SIMFORMAT constant_R = 8.314E+00;
const SIMFORMAT constant_p = 1.000E+05;
  xCO2   = (nDotCO2 / (nDotCO2 + nDotCH4));
  xCH4   = (1.00E+00 - xCO2);
// molar wt is given in kg/mol
  qoutGa = (nDotCO2 + nDotCH4) * constant_R * TR / constant_p;
  SIMFORMAT dVBGdt = qoutGa;
  dydt[10] = dVBGdt;
  qoutCH4 = nDotCH4 * constant_R * TR / constant_p;
  SIMFORMAT dVCH4dt = qoutCH4;
  dydt[11] = dVCH4dt;
  dydt[12] = q0tot - qoutTo;
return 0;
}

// just define the names of the state quantities y
SpecificationList ADSIM12::GetStateSpecifications() const {
  SpecificationList Specs;
// this appends a name to the end of the Specs vector
  Specs.append("CXaci");  //  0
  Specs.append("CXmeth"); //  1
  Specs.append("CSM");    //  2
  Specs.append("CpC");    //  3
  Specs.append("CpP");    //  4
  Specs.append("CpL");    //  5
  Specs.append("CSC");    //  6
  Specs.append("CSP");    //  7
  Specs.append("CSL");    //  8
  Specs.append("CVFA");   //  9
  Specs.append("VBG");    // 10
  Specs.append("VCH4");   // 11
  Specs.append("Vliq");   // 12
// return the complete list
return Specs;
}
// define the names of the parameters
SpecificationList ADSIM12::GetParameterSpecifications() const {
  SpecificationList Names;
  Names.append("kD");
  Names.append("khydC");
  Names.append("khydP");
  Names.append("khydL");
  Names.append("KsC");
  Names.append("KsP");
  Names.append("KsL");
  Names.append("KVFA");
  Names.append("IpL");
  Names.append("rMaxXC");
  Names.append("rMaxXP");
  Names.append("rMaxXL");
```

```
  Names.append("rMaxVFA");
  Names.append("yXC");
  Names.append("yXP");
  Names.append("yXL");
  Names.append("yXVFA");
  Names.append("fC");
  Names.append("fP");
  Names.append("fL");
  Names.append("uC");
  Names.append("uP");
  Names.append("uL");
  Names.append("vVFA");
  Names.append("VR");
  Names.append("TR");
return Names;
}
// this method will be automatically called when the parameters are
set. if you want
// to copy the parameters to member variables for performance reasons,
you must do this
// in this routine. just use m_Parameters.GetQuant(name) to access the
parameter value
// this routine can be empty. then you must access the parameters in
the Equation
// via m_Parameters.GetQuant(name)
void ADSIM12::RefreshParameters() {
  kD          = m_Parameters.GetQuant("kD");
  khydC       = m_Parameters.GetQuant("khydC");
  khydP       = m_Parameters.GetQuant("khydP");
  khydL       = m_Parameters.GetQuant("khydL");
  KsC         = m_Parameters.GetQuant("KsC");
  KsP         = m_Parameters.GetQuant("KsP");
  KsL         = m_Parameters.GetQuant("KsL");
  KVFA        = m_Parameters.GetQuant("KVFA");
  IpL         = m_Parameters.GetQuant("IpL");
  rMaxXC      = m_Parameters.GetQuant("rMaxXC");
  rMaxXP      = m_Parameters.GetQuant("rMaxXP");
  rMaxXL      = m_Parameters.GetQuant("rMaxXL");
  rMaxVFA     = m_Parameters.GetQuant("rMaxVFA");
  yXC         = m_Parameters.GetQuant("yXC");
  yXP         = m_Parameters.GetQuant("yXP");
  yXL         = m_Parameters.GetQuant("yXL");
  yXVFA       = m_Parameters.GetQuant("yXVFA");
  fC          = m_Parameters.GetQuant("fC");
  fP          = m_Parameters.GetQuant("fP");
  fL          = m_Parameters.GetQuant("fL");
  uC          = m_Parameters.GetQuant("uC");
  uP          = m_Parameters.GetQuant("uP");
  uL          = m_Parameters.GetQuant("uL");
  vVFA        = m_Parameters.GetQuant("vVFA");
  VR          = m_Parameters.GetQuant("VR");
  TR          = m_Parameters.GetQuant("TR");
};
// define the m_Parameters.GetQuant( names of intermediates.
SpecificationList ADSIM12::GetIntermediateSpecifications() const {
  SpecificationList Names;
// this appends a name to the end of the names vector
```

```
  Names.append("xCH4");
  Names.append("xCO2");
  Names.append("qoutGa");
  Names.append("CODtot");
  Names.append("CODloss");
  Names.append("BiomassTotal");
  Names.append("qoutCH4");
  Names.append("XCH4accum");
// return the complete list
return Names;
}
// evaluate potential intermediate quantities from control, state, rate
of change of state
// and from time
// prerequisites:
//   for   each   quantity   used,   a   name   must   be   defined   in
GetIntermediateNames()
void  ADSIM12::GetIntermediates(SIMFORMAT  t,  const  array1d  &control,
const array1d &y, const array1d &dydt, array1d &intermed) const {
// do the computations and store the results in intermed
  intermed[0] = xCH4;
  intermed[1] = xCO2;
  intermed[2] = qoutGa;
// total COD in solution
  {
const SIMFORMAT CXaci   = y[0];
const SIMFORMAT CXmeth  = y[1];
const SIMFORMAT CSM     = y[2];
const SIMFORMAT CpC     = y[3];
const SIMFORMAT CpP     = y[4];
const SIMFORMAT CpL     = y[5];
const SIMFORMAT CSC     = y[6];
const SIMFORMAT CSP     = y[7];
const SIMFORMAT CSL     = y[8];
const SIMFORMAT CVFA    = y[9];
      const SIMFORMAT VBG     = y[10];
      const SIMFORMAT VCH4    = y[11];
    intermed[3] = CpC + CpP + CpL + CSC + CSP + CSL + CVFA; //CXaci +
CXmeth + CSM +
    intermed[5] = CXaci + CXmeth;
      intermed[6] = qoutCH4;
      if ((VBG > 0.0) && (VCH4>0.0)){
            intermed[7] = VCH4/VBG;
      } else {
            intermed[7] = 0.0;
      }
  }
// total COD loss one mole methane is oxidized by 2 moles of o2
  {
const SIMFORMAT nCH4 = y[14];
    intermed[4] = 64.0 * nCH4;
}
}
// return the names of scalar data. if there are some scalar data that
should
// be stored after simulation, define its names here
SpecificationList ADSIM12::GetScalarSpecifications() const {
```

```
  SpecificationList names;
// todo: call names.push_back("name") for each name of a scalar date
return names;
}
// fill the scalar data into the appropriate location
void ADSIM12::GetScalars(array1d &scalars) const {
// todo: if there is scalar data of the simulation (e.g. generated by
the methods
//       PreEvaluate or PostEvaluate) fill it into scalar
//
// example:
// --------
// scalar[0] = MemberVariableForScalarInformation_0;
// ...
// scalar[n] = MemberVariableForScalarInformation_n;
// for each name, defined in GetScalarNames() there will be one element
in the
// scalar array1d.
}
// define the names of control quantities
SpecificationList ADSIM12::GetControlQuantitySpecifications() const {
  SpecificationList Names;
// this appends a name to the end of the names vector
// return the complete list
      Names.append("C0Xaci");
      Names.append("C0Xmeth");
      Names.append("q0Ino");
      Names.append("q0CpC");
      Names.append("q0CpP");
      Names.append("q0CpL");
      Names.append("C0CpC");
      Names.append("C0CpP");
      Names.append("C0CpL");
      Names.append("qout");
      Names.append("qoutsa");
return Names;
}
void    ADSIM12::SetControlQuantities(SIMFORMAT    t,    const    array1d
&control,const array1d &y) {
// route the information in control to appropriate member variables
      C0Xaci       = control( 1);
      C0Xmeth      = control( 2);
      q0Ino        = control( 3);
      q0CpC        = control( 4);
      q0CpP        = control( 5);
      q0CpL        = control( 6);
      C0CpC        = control( 7);
      C0CpP        = control( 8);
      C0CpL        = control( 9);
      qout         = control( 10);
      qoutsa       = control( 11);
}
void ADSIM12::PreEvaluate(SIMFORMAT t, array1d &y) {
```

Configuration file for validation of the model using experimental data with mixture of gelatin, sucrose and rapeseed oil

tInitial:	0.000000e+000
tFinal:	2.550000e+006
Steps:	720
Solvertype:	Dassl
Optitype:	Nelder
AbsTol:	1.000000e-006
RelTol:	1.000000e-006
khydC:	7.9e-06
khydP:	5.1e-06
khydL:	4.56E-06
KsC:	6.5
KsP:	5.0
KsL:	3.20
KVFA:	0.01
IpL:	0.045
rMaxXC:	4.2e-06
rMaxXP:	3.3e-06
rMaxXL:	5.6e-06
rMaxVFA:	8.2e-06
yXC:	0.22
yXP:	0.50
yXL:	0.55
yXVFA:	0.35
uC:	0.65
uP:	0.68
uL:	0.96
vVFA:	0.552
VR:	1.1e-003
TR:	3.11e+002
CXaci:	0.6073
CXmeth:	3.588
CpC:	5.0
CpP:	6.0
CpL:	3.0
CSC:	0.0
CSP:	0.0
CSL:	0.0
CVFA:	0.03
Vliq:	1.0e-003
dVK:	5.0e-004
VBG:	0.0
VCH4:	0.0

Appendix 3

Modification of the model for a tank cascade system

```
  SIMFORMAT VM      = y(1);
  SIMFORMAT V       = y(2);
  SIMFORMAT cs1     = y(3);
  SIMFORMAT cs2     = y(4);
  SIMFORMAT cs3     = y(5);
  SIMFORMAT VS      = y(6);
  SIMFORMAT cs1s    = y(7);
  SIMFORMAT cs2s    = y(8);
  SIMFORMAT cs3s    = y(9);
  SIMFORMAT cM      = y(10);
  SIMFORMAT VB      = y(11);
  SIMFORMAT cs1sb   = y(12);
  SIMFORMAT cs2sb   = y(13);
  SIMFORMAT cs3sb   = y(14);
  SIMFORMAT VF      = y(15);
  SIMFORMAT CXaci   = y(16);
  SIMFORMAT CXmeth  = y(17);
  SIMFORMAT CSM     = y(18);
  SIMFORMAT CpC     = y(19);
  SIMFORMAT CpP     = y(20);
  SIMFORMAT CpL     = y(21);
  SIMFORMAT CSC     = y(22);
  SIMFORMAT CSP     = y(23);
  SIMFORMAT CSL     = y(24);
  SIMFORMAT CVFA    = y(25);
  SIMFORMAT VBG     = y(26);
  SIMFORMAT VCH4    = y(27);
// disintegration rate
const SIMFORMAT rD = kD * CSM;
// hydrolysis rates
const SIMFORMAT rhydC = khydC * CpC;
const SIMFORMAT rhydP = khydP * CpP;
const SIMFORMAT rhydL = khydL * CpL;
// inhibition by LCFA
const SIMFORMAT inhibL = IpL / (IpL + CpL);
// compute acitogenetic rates
const SIMFORMAT rXC = rMaxXC * CSC * CXaci  / (KsC + CSC);
const SIMFORMAT rXP = rMaxXP * CSP * CXaci / (KsP + CSP);
const SIMFORMAT rXL = rMaxXL * CSL * CXaci * inhibL / (KsL + CSL);
// compute methanogenetic rate
const SIMFORMAT rVFA = rMaxVFA * CVFA * CXmeth * inhibL/ (KVFA + CVFA);
  dydt[0]   = FMin  - FMout; // VM
  dydt[1]   = Fin - Fout;           // V
// concentration of proteins, carbo and lipids and manure in mixing
tank
  dydt[2] = (cs10 * Fin - cs1 * Fout)/V - (cs1/V)*dydt[1];
  dydt[3] = (cs20 * Fin - cs2 * Fout)/V - (cs2/V)*dydt[1];
  dydt[4] = (cs30 * Fin - cs3 * Fout)/V - (cs3/V)*dydt[1];
  dydt[9] = (cM0  * FMin- cM * FMout)/VM - (cM/VM)*dydt[0];
  dydt[5]   = (FMout + Fout) - Fsout;
```

```
  dydt[6] = ((cs1 * Fout + 1.0/3.0 * cM * FMout) - cs1s * Fsout)/VS -
(cs1s/VS)*dydt[5];
  dydt[7] = ((cs2 * Fout + 1.0/3.0 * cM * FMout) - cs2s * Fsout)/VS -
(cs2s/VS)*dydt[5];
  dydt[8] = ((cs3 * Fout + 1.0/3.0 * cM * FMout) - cs3s * Fsout)/VS -
(cs3s/VS)*dydt[5];
// volume in Buffer Tank
  dydt[10]  = Fsout - Fbout ;
// concentration of proteins, carbo and lipids in buffer tank
  dydt[11] = (cs1s * Fsout  - cs1sb*Fbout)/VB - (cs1sb/VB)*dydt[10];
  dydt[12] = (cs2s * Fsout  - cs2sb*Fbout)/VB - (cs2sb/VB)*dydt[10];
  dydt[13] = (cs3s * Fsout  - cs3sb*Fbout)/VB - (cs3sb/VB)*dydt[10];
//dydt[14] = (cMs  * Fsout  - cMsb  * Fbout)/VB - (cMsb/VB)*dydt[10];
// volume in Fermenter
  dydt[14] = Fbout - Ffout ;
// concentration of acidogenic bacteria (CXaci)
  dydt[15] = ( C0Xaci * Fbout - CXaci * Ffout)/VF + yXC * rXC + yXP *
rXP + yXL * rXL;
// concentration of methanogenics (CXmeth);
  dydt[16] = ( C0Xmeth * Fbout - CXmeth * Ffout)/VF + yXVFA * rVFA;
// substrates mixture (CSM)
  dydt[17] = -rD;
// disintegration of carbo hydrate  (CpC)
  dydt[18] = ( cs1sb * Fbout - CpC * Ffout)/VF + fC * rD - rhydC;
// disintegration of protein (CpP)
  dydt[19] = ( cs2sb * Fbout - CpP * Ffout)/VF  + fP * rD - rhydP;
// disintegration of lipid (CpL)
  dydt[20] = ( cs3sb * Fbout - CpL * Ffout)/VF  + fL * rD - rhydL;
//  hydrolysis of carbohydrate (CSC)
  dydt[21] = -(CSC * Ffout)/VF + rhydC - rXC;
// hydrolysis of  protein (CSP)
  dydt[22] = -(CSP * Ffout)/VF + rhydP - rXP;
// hydrolysis of lipid (CSL)
  dydt[23] = -(CSL * Ffout)/VF + rhydL - rXL;
// volatile fatty acid  (CVFA)
  dydt[24] = -(CVFA * Ffout)/VF + (1.0 - yXC) * uC * rXC + (1.0 - yXP)
* uP * rXP + (1.0 - yXL) * uL * rXL - rVFA;
// inorganic carbon (CTIC)
const SIMFORMAT rTIC = (1.0 - yXC) * (1.0 - uC) * rXC + (1.0 - yXP) *
(1.0 - uP) * rXP + (1.0 - yXL) * (1.0 - uL) * rXL + (1.0 - yXVFA) *
(1.0 - vVFA) * rVFA;
// methane(Me)
const SIMFORMAT rMet = (1.0 - yXVFA) * vVFA * rVFA;
// molar release of carbon dioxide
const SIMFORMAT MWCO2   = 0.04401E+00;
const SIMFORMAT nDotCO2 = rTIC / MWCO2 * VF;
// molar release of methane
const SIMFORMAT MWCH4   = 0.01604E+00;
const SIMFORMAT nDotCH4 = rMet / MWCH4 * VF;
// output of carbon dioxide and methane mole fractions and volume flow
const SIMFORMAT constant_R = 8.314E+00;
const SIMFORMAT constant_p = 1.000E+05;
  xCO2    = (nDotCO2 / (nDotCO2 + nDotCH4));
  xCH4    = (1.00E+00 - xCO2);
// molar wt is given in kg/mol
  qoutGa = (nDotCO2 + nDotCH4) * constant_R * TR / constant_p;
  SIMFORMAT dVBGdt = qoutGa;
```

```
dydt[25] = dVBGdt;
qoutCH4 = nDotCH4 * constant_R * TR / constant_p;
SIMFORMAT dVCH4dt = qoutCH4;
dydt[26] = dVCH4dt;
```

Configuration file for the prediction of the AD process of the biogas plant in EWE Biogas GmbH in Surwold, Germany

		V:	633.0
khydC:	7.9e-06		
khydP:	5.1e-06	cs1:	8.0
khydL:	4.56E-06	cs2:	4.0
		cs3:	11.0
KsC:	6.5	cM:	1.0
KsP:	5.0		
KsL:	3.20	VS:	61.0
KVFA:	0.01	cs1s:	5.33
		cs2s:	2.67
IpL:	0.045	cs3s:	7.33
rMaxXC:	4.2e-06	VB:	22.0
rMaxXP:	3.3e-06	cs1sb:	5.33
rMaxXL:	5.6e-06	cs2sb:	2.67
rMaxVFA:	25.2e-06	cs3sb:	7.33
yXC:	0.22	VF:	2500.0
yXP:	0.50	CXaci:	9.80
yXL:	0.55	CXmeth:	8.3
yXVFA:	0.35		
		CpC:	2.67
		CpP:	5.33
uC:	0.65	CpL:	7.33
uP:	0.68		
uL:	0.96	CSC:	0.0
vVFA:	0.8	CSP:	0.0
		CSL:	0.0
TR:	3.11e+002	CVFA:	7.15e-005
		VBG:	0.0
VM:	633.0	VCH4:	0.0

Feed file of the proteins concentration

Time [s]	Conc. [kg·m^3]	Time [s]	Conc. [kg·m^3]	Time [s]	Conc. [kg·m^3]	Time [s]	Conc. [kg·m^3]
0.0	8	5788800	22	11577600	39	17712000	12
345600	8	5875200	9	11750400	25	17798400	15
518400	15	5961600	34	11836800	7	17884800	16
604800	7	6307200	26	11923200	11	17971200	20
691200	7	6393600	12	12009600	8	18057600	9
950400	7	6480000	12	12096000	27	18230400	19
1036800	17	6566400	9	12441600	22	18316800	4
1123200	8	6652800	11	12528000	31	18403200	1
1209600	11	6912000	38	12614400	37	18489600	7
1296000	16	6998400	27	12700800	10	18662400	
1555200	17	7084800	11	12960000	25	18748800	20
1641600	15	7171200	24	13046400	23	18835200	12
1728000	5	7257600	13	13132800	16	18921600	25
1814400	14	7516800	21	13219200	3	19008000	12
1900800	12	7603200	9	13305600	9	19094400	38
2160000	13	7689600	13	13564800	16	19353600	16
2332800	10	7776000	18	13651200	4	19440000	17
2419200	17	8208000	22	13737600	8	19526400	29
2505600	37	8294400	25	13824000	11	19612800	29
2764800	10	8380800	22	14083200	4	19699200	
2851200	7	8467200	7	14169600	14	19785600	11
2937600	17	8726400	8	14256000	31	19872000	10
3024000	7	8812800	18	14342400	11	19958400	9
3110400	6	8899200	25	14688000	7	20044800	18
3369600	7	8985600	14	14774400	8	20131200	9
3456000	23	9072000	27	15120000	6	20217600	16
3542400	4	9331200	10	15206400	8	20304000	17
3628800	17	9417600	11	15292800	7	20390400	9
3715200	11	9504000	25	15638400	15	20563200	21
3974400	7	9590400	13	15724800	19	20649600	
4060800	3	9676800	18	15811200	18	20736000	27
4147200	13	9936000	10	16070400	27	20995200	22
4233600	15	10022400	28	16156800	16	21081600	16
4320000	7	10108800	15	16243200	11	21168000	34
4579200	10	10195200	7	16329600	16	21254400	13
4665600	5	10540800	16	16416000	15	21340800	15
4838400	13	10627200	9	16761600	32	21686400	15
5097600	37	10713600	18	17020800	32	21772800	25
5184000	21	10800000	9	17107200	16	21859200	15
5270400	11	10886400	4	17193600	4	21945600	11
5356800	36	11145600	25	17280000	29	22032000	15
5443200	17	11232000	32	17539200	33	22291200	7
5702400	19	11318400	8	17625600	26	22377600	11

Time [s]	Conc. [kg·m^3]	Time [s]	Conc. [kg·m^3]	Time [s]	Conc. [kg·m^3]	Time [s]	Conc. [kg·m^3]
		24969600	14	27388800	9	29721600	9
22464000	10	25228800	37	27561600	17	29808000	15
22550400	10	25315200	27	27648000	21	29894400	5
22636800	17	25401600	14	27734400	17	30153600	17
22982400	16	25488000	24	27820800	20	30240000	22
23068800	12	25574400	37	27907200	13	30326400	19
23155200	38	25920000	23	27993600	10	30412800	29
23241600	59	26006400	15	28080000	27	30499200	10
23500800	11	26092800	54	28166400	27	30585600	28
23587200	13	26179200	10	28425600	14	30758400	12
23673600	15	26265600	16	28512000	11	30844800	11
23760000	37	26438400	11	28598400	19	30931200	18
24019200	13	26524800	14	28684800	27	31017600	13
24105600	2	26611200	11	28944000	10	31104000	8
24192000	18	26870400	19	29030400	24	31363200	15
24278400	11	26956800	12	29116800	21	31449600	8
24364800	54	27043200	4	29203200	19	31536000	10
24624000	49	27129600	22	29289600	20	31622400	15
24710400	20	27216000	27	29548800	29	31708800	4
24796800	15	27302400	15	29635200	17		

Feed file of the carbohydrates concentration

Time [s]	Conc. [kg·m^3]	Time [s]	Conc. [kg·m^3]	Time [s]	Conc. [kg·m^3]	Time [s]	Conc. [kg·m^3]
0.0	6	5788800	12	11750400	15	19008000	7
345600	4	5875200	6	11836800	24	19094400	7
432000		5961600	18	11923200	17	19353600	24
11		6307200	9	12009600	24	19440000	5
518400	8	6393600	19	12096000	14	19526400	14
604800	4	6480000	8	12441600	23	19612800	22
691200	4	6566400	6	12528000	30	19785600	38
950400	15	6652800	7	12614400	14	19872000	34
1036800	6	6912000	4	12960000	4	19958400	20
1123200	4	6998400	28	13046400	28	20044800	12
1209600	8	7084800	8	13132800	25	20131200	20
1296000	6	7171200	8	13219200	33	20217600	34
1555200	24	7257600	14	13564800	27	20304000	25
1641600	8	7516800	7	13651200	24	20563200	28
1728000	4	7603200	16	13737600	27	20736000	34
1814400	8	7689600	9	13824000	23	20995200	15
1900800	6	7776000	12	14083200	24	21081600	9
2160000	21	8208000	19	14169600	7	21168000	20
2332800	7	8294400	22	14342400	8	21254400	25
2419200	13	8380800	11	14688000	34	21340800	39
2505600	4	8467200	4	14774400	13	21686400	27
2764800	18	8726400	18	15120000	5	21772800	34
2851200	4	8812800	23	15292800	4	21859200	11
2937600	9	8899200	4	15638400	29	21945600	8
3024000	4	8985600	8	15724800	7	22032000	34
3110400	3	9072000	7	16156800	4	22291200	15
3369600	7	9331200	9	16243200	8	22377600	9
3456000	29	9417600	8	16329600	5	22464000	23
3542400	4	9504000	14	16416000	5	22550400	38
3628800	11	9590400	11	16761600	9	22636800	11
3715200	2	9676800	4	17020800	29	22982400	13
3974400	17	9936000	6	17107200	24	23068800	8
4060800	3	10022400	13	17193600	14	23155200	18
4147200	9	10108800	24	17539200	4	23500800	29
4233600	8	10195200	4	17625600	3	23587200	9
4320000	4	10540800	24	17712000	4	23673600	3
4665600	5	10627200	29	17798400	5	23760000	24
4838400	7	10713600	8	17971200	7	24019200	2
5097600	15	10886400	24	18230400	30	24105600	16
5184000	9	11145600	19	18316800	17	24192000	8
5270400	8	11232000	11	18489600	4	24278400	8
5356800	3	11318400	25	18748800	12	24364800	4
5443200	4	11577600	20	18921600	4	24624000	7

Time [s]	Conc. [kg·m^3]	Time [s]	Conc. [kg·m^3]	Time [s]	Conc. [kg·m^3]	Time [s]	Conc. [kg·m^3]
24710400	12	26438400	8	27993600	2	30153600	4
24796800	11	26524800	6	28166400	27	30240000	1
24969600	3	26611200	8	28425600	11	30326400	7
25228800	7	26956800	8	28512000	11	30499200	7
25315200	2	27043200	3	28598400	9	30758400	3
25401600	4	27129600	7	28944000	26	30844800	8
25488000	14	27216000	4	29030400	4	30931200	8
25574400	4	27302400	4	29116800	4	31017600	11
25920000	2	27561600	4	29289600	8	31363200	3
26006400	8	27648000	4	29635200	11	31449600	8
26092800	4	27734400	4	29721600	8	31536000	1
26179200	7	27820800	6	29808000	11	31622400	1
26265600	4	27907200	4	29894400	4	31708800	4

Feed file of the carbohydrates concentration

Time [s]	Conc. [kg·m^3]	Time [s]	Conc. [kg·m^3]	Time [s]	Conc. [kg·m^3]	Time [s]	Conc. [kg·m^3]
0.0	10	8812800	4	16070400	17	21772800	4
691200	11	8899200	4	16156800	2	21859200	17
1209600	4	9072000	15	16243200	15	21945600	14
1728000	4	9331200	5	16329600	11	22377600	24
1900800	3	9417600	3	16416000	15	22464000	7
2160000	6	9504000	12	16761600	5	22550400	34
2246400	11	9590400	6	17020800	15	22636800	4
2332800	3	9676800	14	17107200	26	22982400	19
2764800	3	9936000	2	17193600	4	23068800	13
2851200	9	10022400	4	17280000	2	23155200	17
3369600	17	10108800	7	17539200	26	23241600	12
3456000	4	10540800	12	17712000	2	23500800	15
3542400	3	10627200	15	17798400	27	23587200	5
3628800	3	10713600	10	17884800	4	23673600	20
3715200	5	10800000	12	17971200	26	24019200	6
3974400	3	10886400	15	18057600	2	24105600	10
4060800	14	11145600	14	18230400	29	24192000	11
4147200	4	11232000	12	18316800	10	24278400	4
4579200	2	11318400	23	18403200	20	24364800	14
4665600	4	11577600	2	18662400	13	24624000	14
4752000	11	11750400	16	18748800	14	24710400	4
5184000	7	11923200	4	18835200	4	24796800	18
5270400	15	12441600	19	18921600	14	24969600	12
5702400	5	12528000	10	19008000	3	25228800	17
5788800	7	12614400	17	19094400	7	25315200	16
5875200	2	12700800	2	19353600	2	25401600	16
5961600	16	12960000	17	19440000	2	25488000	4
6307200	2	13046400	2	19526400	12	25574400	11
6393600	5	13132800	18	19612800	4	25920000	14
6480000	5	13219200	3	19699200	11	26006400	10
6566400	15	13305600	2	19785600	4	26092800	4
6652800	25	13564800	19	19872000	12	26179200	7
6998400	5	13651200	4	19958400	2	26265600	14
7084800	7	13737600	17	20044800	16	26438400	17
7171200	2	13824000	15	20131200	13	26524800	8
7257600	4	14083200	4	20217600	14	26611200	4
7516800	5	14256000	11	20304000	12	26870400	14
7689600	5	14342400	4	20390400	2	26956800	1
7776000	4	14688000	12	20563200	17	27129600	24
8208000	7	15206400	12	20649600	11	27216000	11
8294400	10	15638400	17	20736000	11	27302400	19
8380800	15	15724800	16	21168000	17	27388800	22
8726400	6	15811200	4	21254400	13	27561600	12

Time [s]	Conc. [kg·m^3]	Time [s]	Conc. [kg·m^3]	Time [s]	Conc. [kg·m^3]	Time [s]	Conc. [kg·m^3]
27648000	22	28684800	22	29894400	12	31017600	12
27734400	17	28944000	12	30153600		31104000	2
27820800	12	29030400	14	30240000	21	31363200	5
27907200	16	29116800	18	30326400	16	31449600	18
27993600	4	29203200	22	30412800	2	31536000	10
28080000	2	29289600	6	30499200	14	31622400	15
28166400	17	29548800	22	30585600	2	31708800	14
28425600	7	29635200	6	30758400	5		
28512000	11	29721600	18	30844800	18		
28598400	16	29808000	27	30931200	18		

Influent flow of organic waste

Time	**Conc.**
[s]	**[kg·m^3· s^{-1}]**
0.0	0.002228
2678400.00	0.002207
5097600.00	0.002016
7776000.00	0.001868
10368000.00	0.001229
13046400.00	0.001268
15638400.00	0.001257
17500000.00	0.000514
18316800.00	0.000514
20995200.00	0.000738
23587200.00	0.000512
26265600.00	0.000718
28857600.00	0.001506

Influent flow of manure

Time	**Conc.**
[s]	**[kg·m^3· s^{-1}]**
0.0	0.000742
2678400.00	0.000700
5097600.00	0.000626
7776000.00	0.000684
10368000.00	0.000661
13046400.00	0.000765
15638400.00	0.000566
18316800.00	0.000781
20995200.00	0.000673
23587200.00	0.000580
26265600.00	0.000625
28857600.00	0.000554